Consejo **S**uperior de **I**nvestigaciones **C**ientíficas
Instituto de **C**iencia de **M**ateriales de **M**adrid

Departamento de **F**ísica de la **M**ateria **C**ondensada, y nanotecnología
Universidad **A**utónoma de **M**adrid

Single and biphase magnetic microwires: Microwave behavior and temperature dependence.

Rhimou EL KAMMOUNI

Supervisor: Prof. Manuel Vázquez Villalabeitia

Tutor: Dr. Miguel Ángel Ramos Ruiz,

Thesis manuscript submitted to reach the degree of Doctor in Physical Sciences

March 2015

Abstract

This work is has been devoted to the study of single and biphase magnetic microwires, from fabrication to their magnetic characterization at low but particularly at microwave frequencies.

As single phase microwires we consider glass-coated amorphous microwires with very soft magnetic behavior (both, positive magnetostriction Fe-based and vanishing magnetostriction CoFe-based samples). In biphase microwires, we grow an external layer of polycrystalline character with either soft (FeNi) or medium-hard (CoNi) magnetic character so that, we consider soft/soft and soft/hard magnetic biphase systems.

Microwires have been fabricated by combined glass-coating rapid-solidification technique (the amorphous core) and sputtering/electrodeposition technique (the external shell). After their fabrication, the microwires were characterized from a geometry, composition and structure points of view. Quite a number of different samples were produced as a function of core and external shell magnetic phases as well as for different thickness of intermediate insulating Pyrex thickness and external layer. In addition, selected samples were selected for studies on the influence of thermal annealing at temperatures up to reaching first steps of crystallization at 600ºC.

A first magnetic characterization was performed at low-frequency magnetic fields in a Vibrating Sample Magnetometer, VSM, to determine the magnetization processes and main magnetic magnitudes as coercivity and remanence of each magnetic phase. This has been performed for all the series of samples mentioned above.

Studies have been extended to different measuring temperature particularly in the range up to 900ºC; where after partial crystallization significant deterioration of properties is confirmed. The study about the coercive field of individual and bimagnetic phase systems is analyzed in view of the relevance for technological applications of bimagnetic microwires. Also, the magnetic phase transitions (ferro to paramagnetic) of some individual phases are first identified.

The main part of the study has been devoted to the magnetic properties at high frequency, in the microwave regime. The ferromagnetic resonance (FMR) spectra have been determined for single and biphase samples with different geometry and compositional characteristics as indicated above. FMR experiments in wires can be

basically divided into two categories. The former is done by means of network analyzer up to around 15 GHz and as a function of applied magnetic field. The latter has been performed in a coaxial or microstrip microwave circuit making use of classical FMR spectrometers and waveguide microwave techniques.

A first study was focused on the influence of glass Pyrex on single and biphase microwires. For single-phase microwires, the increase of the Pyrex thickness results in a continuous strengthening of the circular magnetoelastic anisotropy of the CoFe-based core as deduced from FMR and confirmed by low-frequency measurements. For biphase microwires three absorption peaks are observed: two of them can be ascribed to each magnetic phase since FMR frequencies obey the Kittel condition for a thin film. A third absorption peak is observed at lower frequencies that does not follow such an equation and can be ascribed to a pure geometrical effect of these biphase microwires.

Then, the effect of annealing treatment at temperatures up to 700ºC on high frequency behavior was investigated. FMR behavior was analyzed by fitting to Kittel equation for annealed samples. The observed different absorption peaks are correlated with the presence of the soft core and the peaks presented at low frequency do not obey such Kittel condition. In this regards, it has been confirmed that the peaks observed at lower frequency corresponded to a capacitance effect.

Additional studies have been presented investigating the microwave absorption phenomena of single and biphase magnetic microwires with soft magnetic behavior using two alternative techniques: (i) absorption measurements in the temperature range of -271_25ºC using a spectrometer operating at X-band frequency, at 9.5GHz, and (ii) room temperature, RT, ferromagnetic resonance measurements in a network analyzer up to 15 GHz. For single phase CoFeSiB microwire, a single absorption is observed, whose DC field dependence of resonance frequency at RT fits to a Kittel law behavior for in-plane magnetized thin film. The temperature dependence behavior shows a monotonic increase in the resonance field, Hr, with temperature. For biphase,CoFeSiB/FeNi, microwires, the absorption phenomena at RT also follow the Kittel condition. The observed opposite evolution with temperature of resonance field, Hr, in two different thick FeNi samples is interpreted considering the opposite sign of magnetostriction of the respective FeNi layers.

Contents

Chapter 1

Introduction and state of art

1.1. Introduction

The magnetic behavior of various kinds of soft amorphous microwires has been the topic of many systematic studies and doctoral studies. This is because of the outstanding behavior from a fundamental research point of view but also, especially more recently, because of their applications as sensing elements in different families of magnetic sensor devices.

In this introductory section we collect some general information on the various aspects related to our original contributions. We review some general magnetic properties of soft magnetic materials and their hysteresis loops, and then we summarize relevant characteristics of amorphous materials and especially glass-coated amorphous microwires. We introduce comparative properties of single anf biphase microwires as it has been the topic of previous works in the research center where this study has been performed. Afterwards, we pay particular attention to the ferromagnetic resonance characteristics of this kind of samples which is the main part of the original work introduced in this manuscript. Finally, we describe some of the applications (i.e., sensors) where magnetic microwires have been employed.

1.2. General review of magnetic materials

1.2.1. Magnetism of materials:

Magnets play an important role in a modern life. In ancient times human beings experienced magnetic phenomena by utilizing natural iron minerals, especially magnetite Fe_3O_4. It was not until modern times that magnetic phenomena were appreciated from the standpoint of electromagnetics, to which many physicists such as Oersted and Faraday made a great contribution. In particular, Ampère explained magnetic materials in 1822, based on a small circular electric current. This was the first explanation of a molecular magnet. Furthermore, Ampère's circuital law introduced the concept of a magnetic moment or magnetic dipoles, similar to electric dipoles.

Initially it was believed that ferromagnetism could not exist in amorphous solids because of lack of atomic ordering. Gobanov et al. [1] theoretically predicted in 1960 that amorphous solids would be ferromagnetic. Later it was found that the 3d metal based amorphous alloys obtained by rapid-quenching of the melt are excellent soft

magnetic materials, i. e., they exhibit very low value of the coercive field and relatively high saturation magnetization [2]. Such magnetic softness originates from the absence of magnetocrystalline anisotropy in these alloys [2]. Most commercial and technological interest has been paid attention to soft amorphous magnetic materials.

1.2.2. Introducing amorphous magnetic materials

In earlier years, amorphous metallic materials were discovered and occupied an extremely important place among metallic materials due to their unique and favorable association of physical properties. The achievement of the energetically metastable amorphous state requires the use of preparation methods that allow rapid condensation of atoms or rapid solidification of liquid metallic melts in order to avoid crystallization. The formation of the amorphous state depends on the alloy composition as well as on the process conditions. There are presently known amorphous metallic materials obtained in the shapes of thin films[3], ribbons[4], wires[5], powders[6]. Amorphous metallic materials are used in applications based on their mechanical, electrical, magnetic, and chemical properties[7-10]. Some of the most important applications are based on their magnetic properties, profiting of their high permeability magnetic materials.

Typically, the magnetic properties [11] of materials are measured from the variation of magnetization with magnetic field, as shown in Fig. 1.1. Magnetic materials are broadly classified into two main groups with either hard or soft magnetic characteristics. Soft magnetic materials can be magnetized by relatively low-strength magnetic fields, and when the applied field is removed, they return to a state of relatively low residual magnetism. The magnetic properties of materials can be divided into two general categories: those that are structure sensitive and those that are structure insensitive.

- Structure insensitive refers to properties not markedly affected by changes in materials processing (heat treatment or mechanical deformation) or by small changes in composition, including small amounts of certain impurities. Structure-insensitive properties include the saturation magnetization, Curie

temperature and resistivity. These properties are largely dependent on the composition of the particular alloy and are not changed substantially in the process of manufacturing a component from the alloy.

- Structure-sensitive properties are those that are drastically affected by impurities. Small amounts of elements such as carbon, oxygen, nitrogen, and sulfur are commonly found in small quantities in magnetic materials. These elements tend to locate at interstitial sites in the crystalline lattice which can be severely strained. As a result small concentrations of these elements can have large effects on some of the magnetic properties of the materials. Permeability, coercivity, hysteresis loops, remanence, and magnetic stability are all considered to be structure sensitive. The structure sensitive properties are controlled through processing of the material including mechanical and thermal treatments.

In recent years the range of available soft magnetic materials has been significantly increased by the development of nanocrystalline magnetic materials earlier performed by Yoshizawa et al. [12]. The most widely investigated alloy is FeSiBNbCu, which is produced by rapid solidification and is then annealed above its crystallization temperature to produce the nanocrystalline structure. Development in these nanocrystalline materials have been described by Herzer [13].

Recent developments in soft magnetic materials have included what may be termed artificially structured materials in which the structure of *heterogenous materials*, consisting of nanocrystalline particles embedded in an amorphous matrix phase, is carefully controlled to produce the desired magnetic properties.

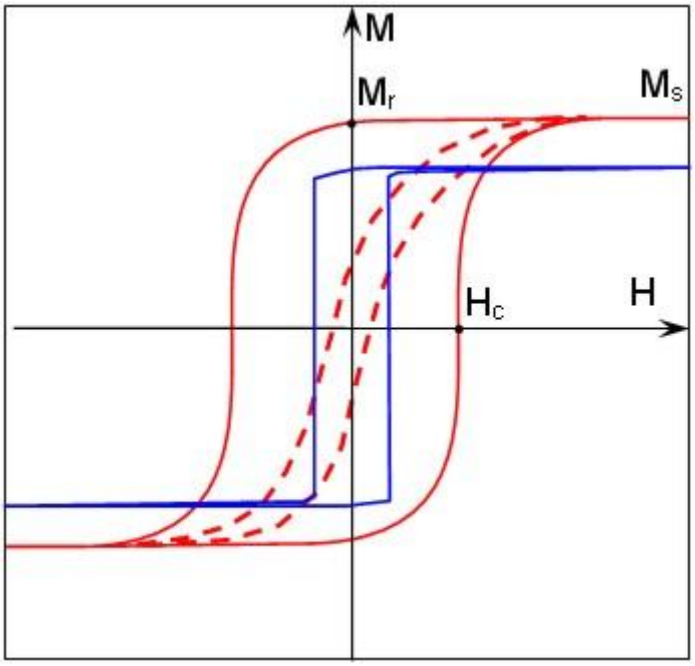

Figure 1.1 Typical hysteresis loops of ferromagnetic materials.

Soft magnetic alloys can be prepared in amorphous state are known as metallic glasses (ribbons).

In the preferred planar flow casting method of production, the metal is rapidly quenched from the melt onto cooled rotating drums to form long ribbons approximately 30-50 μm thick, which can be up to 1 cm wide. Those produced for soft magnetic materials are based on Fe, Co, and Ni alloys.

A relevant development in soft magnetic materials has been amorphous production of magnetic fibers or wires. These are produced by rapid solidification from the melt, and ejected in a jet from nozzle and quenched in a stream of liquid, usually water. The final product is a fiber or wire typically 50μm in diameter which has no long range crystalline structure. In this memory, we are interested to the amorphous glass-coated microwire, which is explained in more details in the following section.

1.2.3. State of the art: Glass-coated microwires

Glass-coated microwires, GCM, are composite materials that consist of metallic nucleus and glass coating (see Fig. 1.2) [14]. The diameter of metallic nucleus is from 100 nm up to 50 μm, whereas the glass-coating thickness is from 2 up to 20 μm [15]. Their biggest advantage is the simple and cheap method of preparation, efficiency (up to few kilometers of microwire can be produced from 1 g of master alloy); glass-coating that provides electrical insulation, small dimensions and circular symmetry [16, 14]. They are prepared by drawing and rapid quenching of molten master alloy [17]. It was firstly introduced by Taylor in 1924 in USA, according to whom this method is named [18]. Later, this method was improved by Ulitovski in 1950 in order to be able to produce large amount of such microwires [19]. In later years, studies have been published on its mechanical properties by Nixdorf from Germanys 1967[20], and Goto from Japan 1977[21]. Electromagnetic absorption properties of GCM in a wide range of micro-wave frequency attracted significant interest in the Soviet Union in the 70-ies of 20 century for their use as radar-absorbing filims in military vehicles.

Renewed interest appeared at the end of 20 century when amorphous glass-coated microwires became to be produced and studied in different countries when the main interest was focused to magnetic microwires with specific magnetic properties for sensing applications.

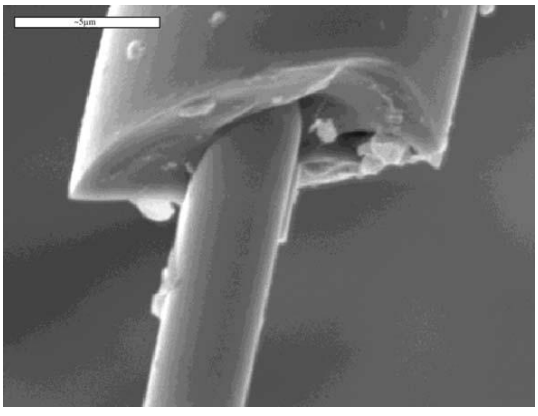

Figure 1.2 SEM photograph of an $(Fe_{30}Co_{70})_{72.5}Si_{12.5}B_{15}$ amorphous magnetic microwires with total diameter D = 12 μm and metal core diameter d_m = 12 μm [14].

In the 70s, several works were published on the magnetic properties by researchers from Eastern Europe (J. Schneider and L. kraus [22]). Investigation on this

material was developed in an independent manner by different laboratories in the Soviet Union (Kichinev, Moscow and Leningrad). In the 90s, the first works in occidental journals were reported by Chiriac from Romania and Vázquez from Spain through their contact with Larin and Torcunov of Moldova. The interest of the GCM lies in the fact of having similar properties as the amorphous wires manufactured by ultra-rapid solidification into water with the advantage of their reduced size due to their low diameter and insulating layer of glass (Pyrex) [17, 23].

From these preliminary studies, the Russian school research has been extended to many other groups that continue to work with these systems. Some of them are directed by M. Vazquez, A. Zhukov, A. Hernando, B. Hernando, C. Gomez-Polo, J. Gonzales, I. Iñiguez from Spain, H. Chiriac from Romania, R. Varga from Slovakia, N. A .Usov from Russian, R. Valenzuela from Mexico, M. Knobel from Brazil, and A. Yelon from Canada.

1.3. Magnetic behavior and properties relevant

In fact, studies of magnetic properties of amorphous glass coated microwires started even in the 1970s [25], but recently these tiny glass-coated ferromagnetic wires have been rediscovered mainly due to a number of unusual magnetic properties and their potential applications in sensor devices [24-28].

1.3.1 Amorphous glass-coated microwires: Single phase

Amorphous glass-coated microwires are characterized by a low anisotropy (since the most important crystalline anisotropy is missed). Hence, their magnetic properties are given mainly by magnetoelastic and shape anisotropy. The magnetoelastic anisotropy arises from the interaction of local magnetic moments with applied mechanical stress induced during microwires production by drawing, quenching as well as due to different thermal expansion coefficients of metallic nucleus and glass-coating. As it was shown in [29, 30, 31], axial tensile stress dominates in the center of metallic nucleus, whereas compressive axial and radial tensile stresses prevail just below the surface. Such a distribution of mechanical stresses is crucial to determined magnetic properties of amorphous glass-coated microwires.

Depending on the sign of magnetostriction, the glass-coated microwires are usually divided into the three groups.

a. Microwires with negative magnetostriction

There are mainly CoSiB-based microwires that are characterized by relatively high and negative magnetostriction. As a result of the stress distribution the easy axis in theses microwires will be circular. Hence, they are characterized by a domain structure that consists of circular domains (see Fig. 1.3(a)) [32]. Magnetization process in axial direction runs through reversible rotation of magnetic moments inside domains. The typical hysteresis loop of such microwires is unhysteretic and magnetization is proportional to the applied magnetic field, as presented in fig. 1.4. They are ideal for the construction where such hysteresis loop characteristics are profited of miniaturized sensors, transformers.

b. Microwires with low magnetostriction

There are usually CoFeSiB (3-5 at% of Fe) -based microwires that are characterized by very low, but negative magnetostriction. This results in small circular magnetoelastic anisotropy. The domain structure of such microwirers is characterized by circular domains below the surface of metallic nucleus and axial domain structure in the center of the wire (see Fig. 1.3(b)) [33]. The hysteresis of the loop of microwires with low magnetostriction is very reduced (see Fig.1.4 (a)) while coercivity is very small and initial permeability very high. Apart from the possibility to study the domain wall propagation theoretically [34], high sensitivity of initial susceptibility to external parameters (like temperature, magnetic field, mechanical stress, etc...) can be employed in construction of miniaturized very sensible sensors. Particularly, the microwires with low and negative magnetostriction are already employed in sensors of magnetic field based on the GMI effect [35] that is one of the most promising applications of glass-coated microwires.

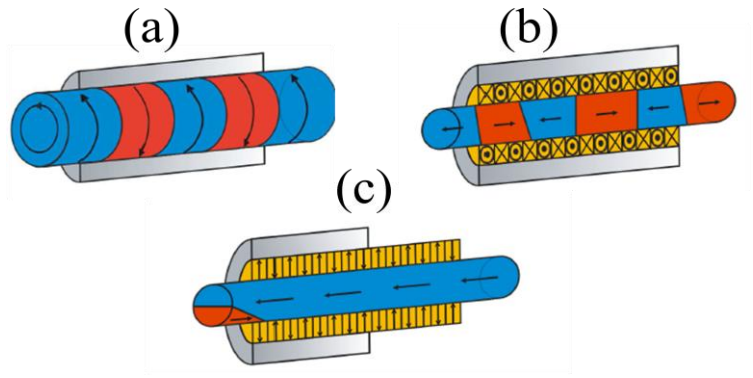

Figure 1.3 Schematic domain structure domain wall of glass-coated microwire with (a) negative, (b) nearly zero, and (c) positive magnetostriction.

c. Microwires with positive magnetostriction

The last group that has been intensively studied in last years is that of the glass-coated microwires with positive magnetostriction. Due to the magnetoelastic interaction of magnetic moments with stress distribution introduced during the microwire's production, their domain structure consists of large single domain in the core of metallic nucleus that is covered by a radial domain structure (see Fig. 1.3(c)) [36, 37]. Moreover, small closure domains appear at the ends of the wire in order to decrease the stray fields [38].

As a result of the peculiar domain structure, the magnetization process runs through the deepening of a domain wall from the closure domain and its subsequent propagation along entire microwire giving rise to a single large Barkhausen jump. Such a domain structure and magnetization process is ideal to study the single domain wall propagation on large distances (centimeters or even meters). On the other hand, the hysteresis loop of such microwire is perfectly rectangular (see Fig. 1.4(b)) and magnetization can have only two values $\pm M_s$ (where M_s is the saturation magnetization) parallel or antiparallel to the wire axis. The switching between the two magnetization values appears when external field exceeds the so-called switching field, H_{sw}.

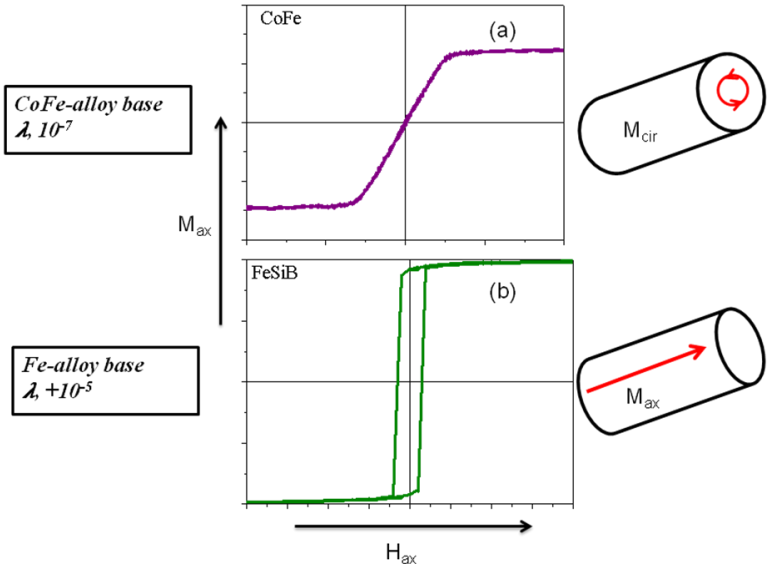

Figure 1.4 Hysteresis loops of FeBSi ($\lambda s > 0$), and CoFeSiB($\lambda s \approx 0$) microwires.

In these magnetic microwires with amorphous structure, the Pyrex cover insulates the core from electrical and corrosion viewpoints [14]. In addition, the magnetic core is subjected to strong stresses induced during the fabrication process that depend on the thickness of the Pyrex (more details will be presented in chapter. 3 section 3.2.1). These stress results in significant magnetoelastic anisotropy, where the corresponding anisotropy field, H_k, can be evaluated directly from its dependence on applied stress [39].

Whereas, single wires have been exhaustively investigated from many points of view at room temperature, only few data are available regarding their temperature behavior. In this regard, the influence of thermal treatments on the low-frequency magnetic behavior of amorphous alloys was systematically performed years ago. While treatments at moderate temperature result in relaxation of the amorphous structure, annealing at higher temperatures leads to the crystallization of the amorphous microstructure and to the growing of crystal phases with size in the nano and microscale that destroy the soft magnetic behavior [14, 40, 11] (more details will be indicated in chapter 3 section 3.2.2).

High temperature studies were mainly focused towards thermal treatments to achieve specific field-induced magnetic anisotropies or nanocrystalline structure with improved magnetic softness [41-43], and more recently to Hopkinson effect just below

Curie temperature [44]. Only few studies were reported on the temperature dependence in the low-temperature regime, magnetization reversal behavior or giant magnetoimpedance [45-47] (more details will be given in chapter 3 section 3.3).

1.3.2 Biphase microwires

In recent years, magnetic multilayer materials have attracted much interest, since the control of morphological properties allows the tailored modification of magnetic behavior.

The group of *Nanomagnetism and Magnetization Processes in Madrid* (ICMM-CSIC) was a pioneer in the manufacture and first studies comprehensively of magnetic properties of multilayer microwires. The starting point was the microwires with a multi-phase behavior introduced by K. Pirota in 2004 [48]: a glass-coated microwire on which a non-magnetic metal layer (Au) is deposited by sputtering, and then an external magnetic layer is grown by galvanostatic electrodeposition.

There are two main types of biphase systems: soft /soft and soft /hard. In these systems the hysteresis loops does not shift, as a consequence of any exchange interaction [49], since the Pyrex interlayer avoids that interaction. In turn, magnetoelastic interactions induced during the growth process of a tiny external layer can change the magnetic behavior of the core as shown in Figure 1.5. In the case of soft magnetic core with bistable behavior and a magnetically harder external shell, the low-frequency magnetic characteristics of the core are determined by the strength of the magnetoelastic coupling with the external shell that can even destroy the bistable behavior. In addition, the low-field hysteresis loops of the core may exhibit a shift as a consequence of the stray field generated by the external shell. Particularly, significant magnetostatic and magnetoelastic interactions have been systematically investigated in biphase microwires [50].

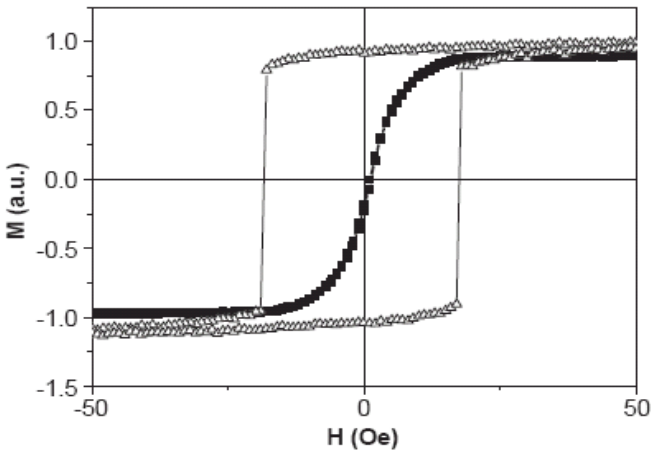

Figure 1.5 hysteresis loops of a CoFeNiSiB glass-coated microwires (8 and 30 metallic and total diameter, respectively) before (■) and after (Δ) sputtering a 100nm thick Ti nanolayer [48].

The biphase magnetic behaviors of multilayer microwires have been studied by Dr. Jacob Torrejon, who focused in his thesis in soft/hard systems, which consist of amorphous core with positive (Fe-based) and vanishing (CoFe-based) magnetostriction, and both of them are covered by a hard magnetic external layer (CoNi) [51] (see Figure 1.6). The external magnetic shell originates a non-homogeneous magnetic field on the inner wire, which is responsible for a displacement and a change of the width of the hysteresis curve of the wire. Moreover, different reversal modes occur at each branch of the hysteresis loop, which can be understood by analyzing the interaction magnetostatic field along the wire[52]. The magnetostatic interaction between magnetic layers is proved to give rise to an antiferromagnetic like coupling resulting in a magnetostatic bias in the hysteresis curves of the soft nucleus. This magnetostatic biasing effect is investigated in terms of the microwire geometry [53].

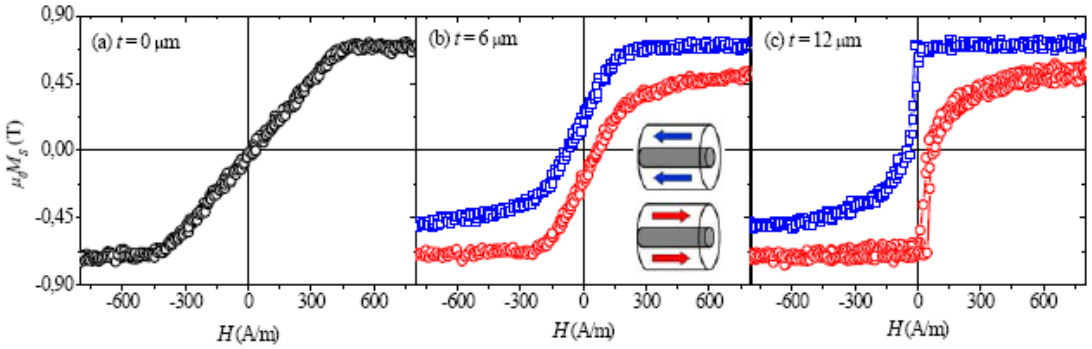

Figure 1.6 Hysteresis loops of a biphasic Microwire CoFe/CoNi measured at low field for different thicknesses of hard external shell (CoNi) [51].

Later Dr. German Infante, investigated the evolution of the magnetic bistability of Fe-based microwires in the presence of hard (CoNi) and soft (FeNi) magnetic external shell (see Figure 1.7).

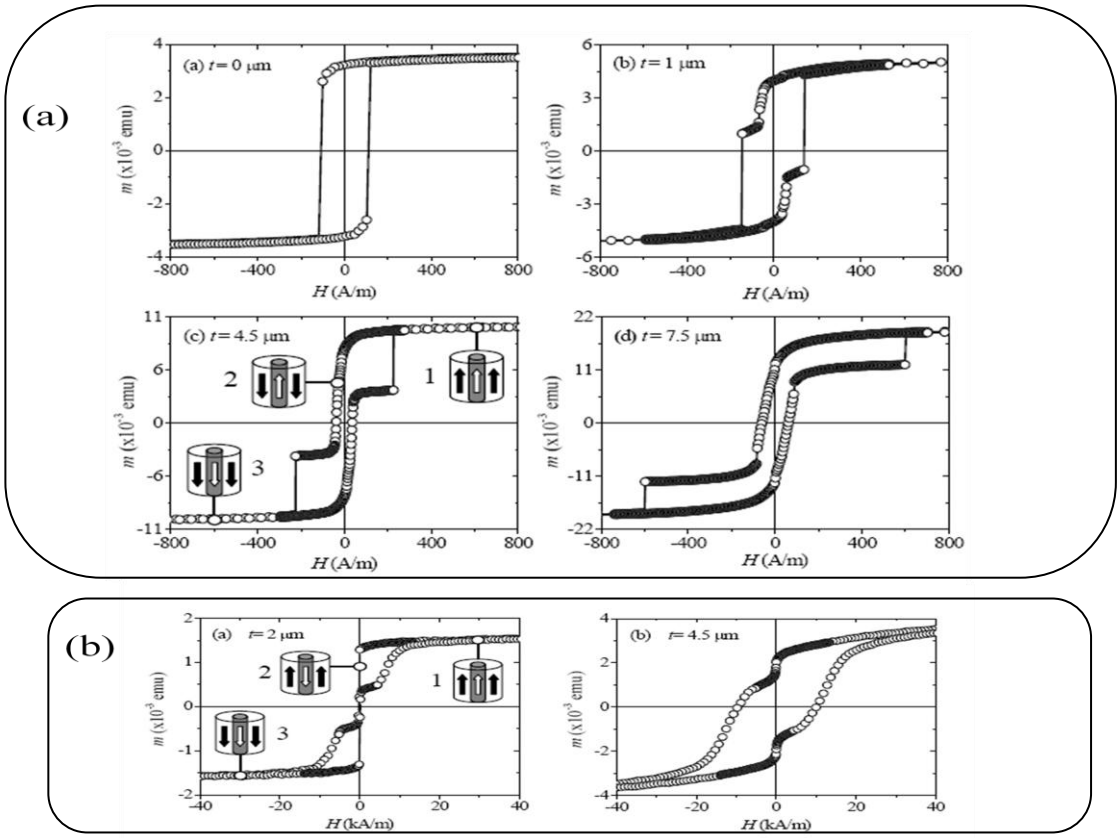

Figure1.7 Hysteresis loops of a biphasic Microwire Fe/FeNi (a) and Fe/CoNi (b) measured at high field for different thicknesses of hard external shell CoNi and FeNi [54].

Fig.1.7 presents the high field hysteresis loops measured at room temperature for two magnetic phases multilayer of selected systems: soft/soft and soft/hard, with different thickness of external shell FeNi (a) and CoNi (b).

As in the case of other magnetostatically coupled two-phase systems, the hysteresis loops are characterized by two well-defined Barkhausen jumps corresponding each one to the magnetization reversal of the individual phases, separated by a plateau. The strong dipolar interaction that leads to the appearance of the plateau was investigated in terms of the microwire geometry. It was shown that this sort of coupling is able of increasing up to one order of magnitude the switching field of the Fe-rich core [55]. Thus, the magnetic bistability can be effectively controlled in these kinds of composite wires. Dipolar coupling analysis was extended to other geometries such as three layer films by Dr. J. Torrejon [51].

1.3.4. Electromagnetic characterization

Until the early decades of the 1800's, experiments conducted to investigate electrical phenomena were completely separate from those focused on magnetic phenomena. Then, in 1820, *Hans Christian Oersted* was the first one who demonstrated that an electric current generates a magnetic field, establishing for the relationship between magnetism and electricity, and the electromagnetism phenomena.

The basic laws of electromagnetic are summarized in four elegant equations by Maxwell. These equations (1.1) and (1.2) describe the connection between electric and magnetic fields, and how they are influenced by the mater. Maxwell's Equations shows that separated charge (positive and negative) gives rise to an electric field and their movement to magnetic fields. Maxwell's Equations are critical in understanding all electromagnetic phenomena (*giant magneto-impedance GMI and ferromagnetic resonance, FMR).*

The study of the electric and magnetic fields in space occupied by material, Maxwell's equations have been carefully analyzed and described over a century [50]:

$$\nabla D = \rho \qquad \nabla \times E = -\frac{\partial B}{\partial t} \tag{1.1}$$

$$\nabla B = 0 \qquad \nabla \times B = J + \frac{\partial D}{\partial t} \tag{1.2}$$

Particularly, the electrodynamic response to electrical current of high frequency is strongly affected by the skin effect whose penetration depth is derived from the computation of eddy currents as:

$$\delta = \sqrt{\frac{2}{\mu_0 \mu' \sigma \omega}} \tag{1.3}$$

where σ is the conductivity of the metal, μ' is real relative permeability, and ω=2πf where *f* is the frequency of the current.

In this regards, the GMI effect, rediscovered in ultra soft amorphous materials in the beginning of the 1990s, has been accepted as being related to modifications of the skin depth at the presence of static fields or mechanical stresses for which the origin relates to classical electromagnetic.

Ferromagnetic resonance

Ferromagnetic resonance, FMR, absorption is the analog of paramagnetic and nuclear resonance absorption. The ferromagnetic effect was found originally by Griffiths [64] and further confirmation has been reported by Yager and Bozorth [6x].

The theory of FMR absorption previously developed and is extended to induce the effect of the shape of the specimens. Whereas, in a typical experimental arrangement the ferromagnetic specimen is the form of thin sheet or foil, which is employed as one wall of rectangular cavity terminating a wave guide fed by microwave generator. The ferromagnetic side of cavity is chosen so that the magnetic victor of the microwave field is constant in direction in the plan of the wall. A static magnetic field is applied (by means of electromagnet) also in the plan of the wall but perpendicular to the microwave magnetic field.

However, the new ferromagnetic semi- conductor materials offer unusual possibilities for working with specimens of a convenient size.

The magnetization M and angular momentum density J are related by:

$$M = \gamma \times J \tag{1.4}$$

Where γ is the gyromagnetic ratio and numerically is equal, γ/2π=2.8 megacycles/Oe.

The equation of motion referred to unit volume of materials:

$$\frac{dJ}{dt} = \gamma M \times H \tag{1.5}$$

Since the expression on the right is the torque acting on a unit volume. This equation may be written:

$$\frac{dM}{dt} = \gamma M \times H \tag{1.6}$$

The principal result of theory [65] is that resonance condition for a plan surface should be given by:

$$\omega_0 = \gamma (BH)^{\frac{1}{2}} \tag{1.7}$$

Instead of the Larmor condition $\omega_0 = \gamma H$ here ω_0 is the frequency, γ is geromagnetic ratio for an electron spin, H is strength of the static magnetic field, and B is the magnetic induction of the specimen. In the case of circular cylinder the resonance condition may be written:

$$\omega_0 = \gamma H_{eff} \tag{1.8}$$

where H_{eff} is H+2πM.

It is pointed out that two distinct resonance effects take place in ferrite samples at microwave frequencies, ferromagnetic resonance and an effect due to the shape of the specimen.

The latter effect is called Kittel resonance. Kittel's theory was based on small signal solution of equation of motion for the magnetization vector M.

$$\frac{dM}{dt} = -\gamma M \times H + a\ dissipative\ term \tag{1.9}$$

Generally, FMR occurs in samples submitted simultaneously to a longitudinal static field, H_0, which causes saturation on the sample and precession of the spin, and a perpendicular oscillating field H (t), which provides the energy to maintain the precession and produced the resonance.

The field in equation (1. 9) is the total effective field H_{eff} comprising, in the case of uniform motion, the applied steady and microwave field, the shape of demagnetization field, and crystalline anisotropy field.

$$H = H_{eff} + H(t) + H_{des} + H_{an} + H_{ex} \tag{1.10}$$

As an example of typical FMR spectra, Fig. 1.8 shows the real component of impedance, R, as a function of exciting frequency for a FeSiB magnetostrictive glass-coated microwire. Measurements were taken in a network analyzer with a transmission coaxial line under variable axial DC magnetic field [67].

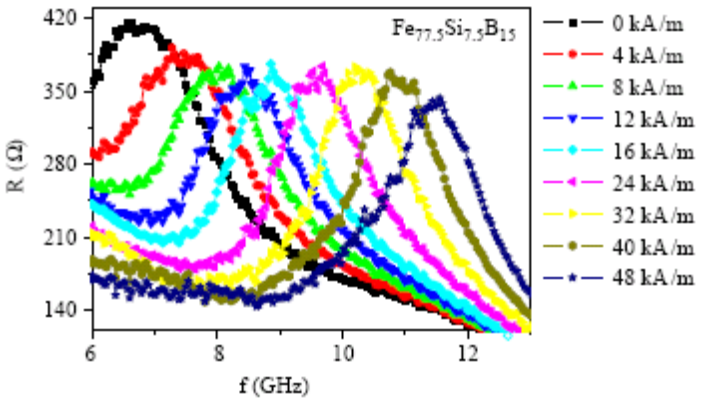

Figure 1.8 Real component of impedance for a FeSiB glass-coated microwire as a function of frequency for selected values of applied field [51].

More complex absorption behavior can be observed in the case of the biphase magnetic microwires. Real and imaginary components of impedance under 24kA/m axial DC applied field are depicted in Fig. 1.9 for a biphase microwire consisting of a soft CoFe-based non-magnetostrictive amorphous glass-coated core and a magnetically harder electroplated poly- crystalline CoNi outer shell.

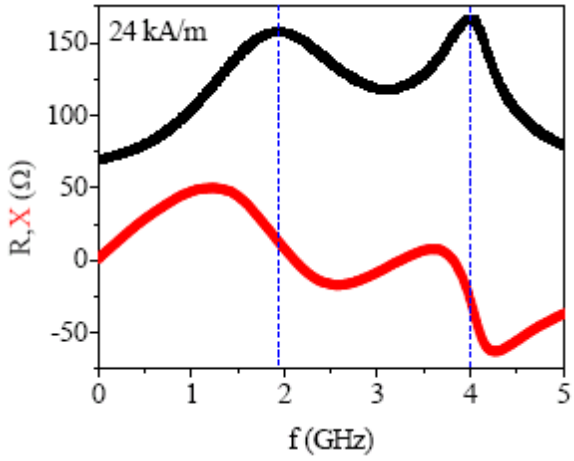

Figure 1.9 Real, R, and imaginary, X, components of impedance for soft/hard biphase microwire [51].

On the other hand, some interesting phenomena have been observed, correlating microwave absorption and magnetization reversal processes. Microwave absorption measurements at microwave cavities at a given frequency (GHz range) and applied magnetic field have been performed by several groups [68].

1.4. Applications interest

The investigation on the magnetic properties of single-phase microwires has been presented by their potential application. Depending of the nature of metallic core, the microwires properties are very different. In these applications the ferromagnetic microwires can be embedded in different matrices.

Aichi Steel has recently succeeded in the development of a magnetic sensor in which the GMI phenomenon was applied [69]. This company developed the magneto-impedance sensor (MI sensor) using amorphous wires with zero-magnetostrictive CoFe and CMOS IC sensor circuit [70].

Anti-shoplifting devices based on glass coated microwires, elements for security of products and documents authentication, or shielding against electromagnetic radiation was investigated by E. Manta et al. [71], who studied the conditions for obtaining composites reinforced with ferromagnetic microwires.

A recent application related to the frequency behavior of single-phase microwires is the absorption of microwave power. Researchers from the Institute of Magnetic Applied have patented adsorbent media based of microwires [72] and efforts are being made to obtain the absorption of microwaves on a wide bandwidth.

Microwires with nearly zero magnetostriction have been used in a broad range of devices: magnetic tips in scanning tunneling microscopes spin polarized (SP-STM) [14] and sensors for biomedical applications based on the GMI effect [73].

The microwires are also useful elements as magnetic field generators. The laboratory of optical nanomanipulation in the CNB-CSIC led by Dr. R. Arias Gonzalez used microwires polished by an electrochemical process for the realization of a magnetic intracellular manipulator: these researchers have managed to control the motion of magnetic nanoparticle in a tiny region of space by varying the polarity of arrangement 3 microwires forming a micro-electro-magnet.

There are many applications that have been patented or published in last years based on Fe-rich microwires. The magnetostrictive character of Fe-based microwires is very suitable for various magnetoelastic sensing applications. Few examples are mentioned in the following. Delay lines and sound velocity sensors using magnetostrictive Fe-based microwires have been proposed by Hristoforou [74] and Hristoforou and Niarchos [75]. A thermoelastic sensor makes use of differential thermal expansion coefficients of glass-coated microwires [76]. A novel viscometer is based on the field-induced rotation effect of magnetostrictive wires discussed above [77]. A magnetoelastic sensor for signature identification based on the magnetoelastic behavior of magnetostrictive microwires has also been proposed [78, 79]. As an example of its possibilities for signature identification and authentication, a schematic view of the sensor is shown in Fig. 1.10 (a). A typical magnetoelastic signature before digitalizing is depicted in Fig. 1.10 (b), where the voltage peaks, proportional to the mechanical stress are plotted as a function of time. An individual magnetoelastic signature is characterized by the number of peaks, their trend, and time intervals, while amplitude of peaks typically depends on the mood of the signatory.

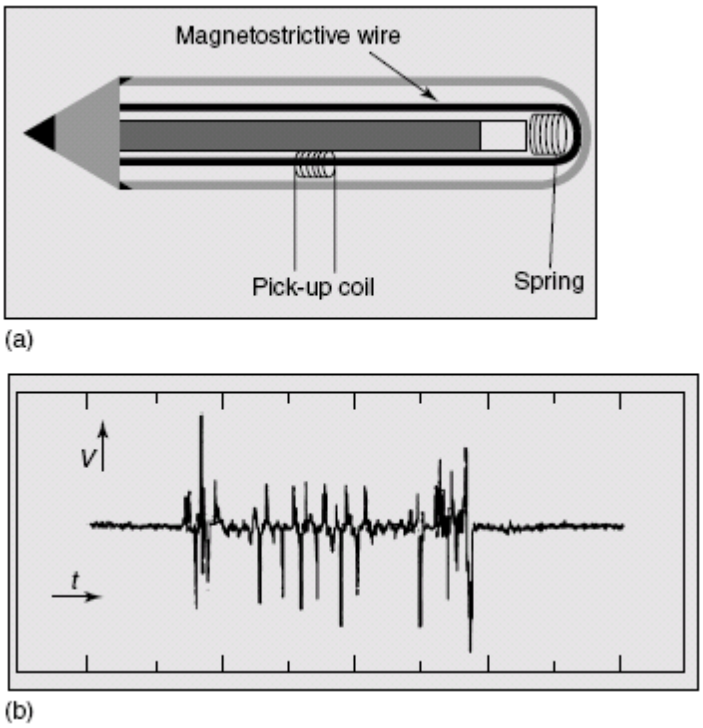

Figure 1. 10 Schematic view and principle of operation of the magnetoelastic sensor (a), and a typical magnetoelastic signature defined by a number of pulses with given serial time interval (b) [14].

For biphase microwires, with a specific geometry and magnetic properties of two magnetic phases, which coupled by magnetostatic and magneto-elastic provide great potential in technological applications. Recently a patent has been fitted on a multifunctional sensor (temperature, mechanical stress, magnetic field and position) based on biphase microwire with soft / hard system [80]: the sensor element is CoFe amorphous core, while the hard coating and controls CoNi optimizes its response. Moreover, the asymmetrical behavior of MI at these microwires is certainly useful as it allows to obtain a linear behavior around H = 0 without recourse to external agents such as an electric current [81] or a polarizing circuit [82].

1.5. Context and objectives of this work

Main objective of this work has been to study the microwave behavior and ferromagnetic resonance at high frequency of various systems of magnetic materials with micrometer scale. To do this series of specific objectives can be summarized in the following points:

- Samples preparation techniques using rapid solidification, sputtering and electrodeposition for getting single and biphase microwires.
- Magnetic characterization at low frequency: H- loops measurement using two techniques: (i) flux-meter (low field) and (ii) vibrating sample magnetometer (high field) at low (in the range of -175_25ºC) and high (25_900ºC) temperature.
- Study of microwave absorption phenomena using two alternative techniques: (i) absorption measurements in the temperature range of 4–300K using a spectrometer operating at X-band frequency, at 9.5GHz, and (ii) room-temperature, RT, ferromagnetic resonance measurements in a net work analyzer in the frequency range up to20 GHz.

1.6. Thesis outline and structure

This work deals with the development of glass-coated microwires obtained by rapid solidification technique and multilayer microwires by sputtering and electrodeposition. It is followed by the magnetic and electromagnetic characterization, in ICMM / CSIC, Madrid. Microwave characterization has been complementary performed in collaboration with Department of Electricity and Electronics from the University of the Basque Country, Bilbao, under the supervision of Dr. Galina Kurlyandskaya. Particular support in the interpretation of FMR data was given by Dr. Ludek Kraus from the Czek Academy of Sciences in Prag. Other collaborations included the preparation of external shell microwires under particular conditions of helical magnetic field to induce particular anisotropy with Dr, Mattia Butta from the Techinal University in Prag. Finally, experimental measurements at high temperature were performed at the Laboratory of Novel Magnetic Materials, from Innovation Park of Immanuel Kant Baltic Federal University, Kaliningrad Russia, under the supervision of Dr. Valeria Rodionova.

This work lies within one of the research lines of the Group Nanomagnetism and Magnetization Processes in the Department of Materials for Information Technologies, and can be considered as the continuation of the doctoral work of Drs. J. Torrejón and G. Infante in the laboratory of ICMM / CSIC in Madrid [51, 54].

Thus, the presentation of this work will be organized around four chapters:

The first chapter is devoted to ***the general review***, and we briefly describe the basics of magnetism, followed by state of the art for single and biphase systems of magnetic microwires and finally their magnetic and electromagnetic behavior of these systems.

The second chapter presents the different ***experimental techniques*** for fabrication and characterization methods used in this work. The first part describes the preparation of the samples was carried out independently in the ICMM-CSIC (Madrid) and combine different methods: ultrafast solidification, sputtering and electroplating. The second part describes the techniques used for the analysis of their magnetic and electromagnetic properties which have been done in different laboratory.

The third chapter presents the results of ***the static magnetic characterization*** of different families of single and biphase magnetic microwires. The M-H loops have been analyzed at low and high field. In this chapter we have presented three main objects. The first one described the influence of thicknesses of insulting glass Pyrex for single and biphase microwires of two different systems. The second objecive corresponds to the effects of annealing treatment on single and biphase microwires. The last objective consists of the high and low temperature dependence of single and biphase microwires of two different multilayer systems.

The fourth chapter will discuss the experimental results of ***Ferromagnetic resonance (FMR)*** obtained and their interpretations for single and biphase microwires. In this chapter, we also studied the influence of the thicknesses of insulting glass Pyrex and the effects of annealing treatments for single and biphase microwires. Then, we have investigated the temperature and angle dependence of microwave absorption phenomena at a constant frequency 9.5GHz in single and biphase microwires. The FMR was evaluated in the range of 10 MHz to 18 GHz using net work analyzer.

1.7. References

[1] Gobanov, A. I. Fizika 2: 502 (1960).
[2] Luborsky, F. E. In: F. Luborsky ed. Amorphous metallic alloys. Butterworth and CoPublishers Ltd (1983).
[3] Cahn, R. W., in Rapidly Solidified Alloys: Processes, Structures, Properties, Applications, ed. H. H. Liebermann. Marcel Dekker Inc., New York, 1993, Chap. 1, p.
[4] Shingu, P. H. and Ishihara, K. N., in Rapidly Solidified Alloys: Processes, Structures, Properties, Applications, ed. H. H. Liebermann. Marcel Dekker Inc., New York, 1993, Chap. 4, p. 103.
[5] Masumoto, T., Inoue, A. and Hagiwara, M., US Patent No. 4523626, 1985.
[6] Schwartz, R. B., in Rapidly Solidified Alloys: Processes, Structures, Properties, Applications. ed. H. H. Liebermann. Marcel Dekker Inc., New York, 1993, Chap. 7, p. 157.
[7] Kadir, W. M. S. B. W., Hayzelden, C. and Cantor, B., J. Mater. Sci. 15, 2663 (1980).
[8] Tsuei, C. C. and Duwez, P., J. Phys. E; Sci. Instrum**.** 4, 466 (1971).
[9] Konczos, G., Kisdi-Koszo, E. and Lovas, A., Physica Scripta T24, 42 (1988).
[10] Froes, F. H. and Carbonara, R. S., J. Metals 40, 20 (1988).
[11] H. Chiriac and T. A. Ovari, "Amorphous glass-covered magnetic wire: preparation, properties, application," Prog. Mater. Sci., vol. 40, p. 333, 1996.
[12] Yoshizawa Y, Oguma S. Yamauchi K. J Appl Phys 64;6044:1988.
[13] Herzer G. J Mag Mag Mater 157;133:1996.
[14] M. Vazquez, "Advanced Magnetic Microwires", in Handbook of Magnetism and Advanced Magnetic Materials, Ed. H. Kronmüller and S.S.P. Parkin (Wiley, Chichester, West Sussex, England, 2007), Vol. 4, p. 2193.
[15] H. Chiriac, T. A. Ovari: Progress Mater. Science 40 (1996) 333
[16] A. Zhukov, J. Gonzalez, M. Vazquez, V. Larin, A. Torcunov Nanocrystalline and amorphous magnetic microwires in: Encyclopedia of Nanoscience and Nanotechnology (American Scientific Publishers,2004)
[17] M. Vazquez: Physica B 299 (2001) 302
[18] G. F. Taylor: Phys. Rev. 23 (1924) 655
[19] A. V. Ulitovski Method of continuous fabrication of microwires coated by glass (authors certifications (USSR patent), No 128427, 1950)
[20] J. Nixdorf; Drah-Welt 53 (1967) 696.
[21] T. Goto; Bull. Japan Inst. Metals 15 (1977) 633.
[22] L. Kraus, J. Schneider, H. Wiesner, *Czech. J. Phys. B* 26 (1976) 601-602.

[23] M. Vázquez; J. Magn. Magn. Mat. 226-230 (2001) 693.

[24] M. Vázquez and A. P. Zhukov, J. Magn. Magn. Mater. 160, 223 (1996).
[25] L. Kraus, J. Schneider, and H. Wiesner, Czech. J. Phys. B 26, 601 (1976).
[26] H. Chiriac and T. A. Ovari, Progr. Mater. Sci. 40, 333 (1997).
[27] A. Zhukov, J. González, J. M. Blanco, M. Vázquez, and V. Larin, J. Mater. Res. 15, 2107 (2000).
[28] A. Zhukov, J. Magn. Magn. Mater. 242–245, 216 (2002).
[29] H. Chiriac, T. A. Ovari, G. Pop: Phys. Rev. B 52 (1995) 10104
[30] H. Chiriac, T. A. Ovari, S. Corodeanu, G. Ababei: Phys. Rev. B 76 (2007) 214433

[31] A. S. Antonov, V. T. Borisov, O. V. Borisov, A. F. Prokoshin, N. A. Usov: J. Phys. D: Appl. Phys. 33 (2000) 1161
[32] S. A. Gudishnikov, B. Y. Ljubimov, P. S. Pavlanov, Y. V. Prokhorova, V. S. Skomartovski, N. A. Usov, A. V. Torcunov: Phy. Stat. Solidi A 206 (2009) 625
[33] A. Chizhik, A. Zhukov, J. M. Blanco, J. Gonzalez: J. Magn. Magn. Mater. 249 (2002) 27
[34] J. Ziman, J. Onufer, M. Kladivova: Physica B 406 (2011) 3576
[35] L. V. Panina, K. Mohri: Appl. Phys.Lett. 65 (1994) 1189
[36] N. N. Orlova, A. S. Aronin, S. I. Bozhko, Yu. P. Kabanov, V. S. Gornakov: J. Appl. Phys. 111 (2012) 073906
[37] K. H. Liu, Z. C. Lu, T. C. Liu, D. R. Li: Chin. Phys.Lett. 30 (2013) 017501
[38] J. Ye, R. P. de Real, G. Infante, M. Vazquez: J. Appl. Phys. 113 (2013) 043904
[39] R. Valenzuela, A. Fessant, J. Gieraltwski, and C. Tannous, Sens. Actuators A 142, 533 (2008).
[40] A. Zhukov and V. Zhukova, Magnetic Properties and Applications of Ferromagnetic Microwires with Amorphous and Nanocrystalline Structure. Hauppauge, NY: Nova Science Publishers, Inc., 2009, vol. 162, p. 11788.
[41] J. Arcas, C. Gomez-Polo, A. Zhukov, and M. Vazquez, Nanostruct. Mater. 7, 823 (1996).
[42] H. Chiriac, T. A. Ovari, Gh. Pop, and F. Barariu, J. Appl. Phys. 81, 5817 (1997).
[43] A. Talaat, M. Ipatov, V. Zhukova, J. M. Blanco, M. Churyukanova, S. Kaloshkin, and A. Zhukov, Phys. Status Solidi C 11, 1120 (2014).
[44] V. Zhukova, M. Ipatov, A. Talaat, and A. Zhukov, Phys. Status Solidi C 11, 1130 (2014).
[45] H. Lluma, M. Vazquez, J. M. Hernandez, J. M. Ruiz, J. M. Garcia- Beneytez, A. Zhukov, J. Casta~no, X. X. Zhang, and J. Tejada, J. Magn. Magn. Mater. 196–197, 821 (1999).
[46] M. Vazquez, A. P. Zhukov, K. L. Garcia, and K. R. Pirota, Mater. Sci. Eng. A 375–377, 1145 (2004).
[47] A. A. Rakhmanov, N. Perov, P. Sheverdyaeva, A. Granovsky, and A. S. Antonov, Sens. Actuators, A 106, 240 (2003).
[48] K. R. Pirota, M. Hernández-Vélez, D. Navas, A. Zhukov, M. Vázquez, *Adv. Funct. Mater.* 14 (2004) 266-268
[49] W. H. Meiklejohn, C. P. Bean, *Phys. Rev.* 105 (1957) 904–913.
[50] S. Allende, J. Escrig, D. Altbir, E. Salcedo, M. Bahiana, *Nanotechnology* 20 (2009) 445707
[51] J. Torrejón, *"Estudio del acoplamiento magnetoelástico y magnetoestático en microsistemas multicapas bifásicos"*, Tesis Doctoral, Universidad Autónoma de Madrid (2008)
[52] J. Escrig, S. Allende, D. Altbir, M. Bahiana, J. Torrejón, G. Badini, M. Vázquez, *J. Appl. Phys.* 105 (2009) 023907
[53] S. Allende, J. Escrig, D. Altbir, E. Salcedo, M. Bahiana, *Nanotechnology* 20 (2009) 445707
[54] G. Infante, "*Propiedades magnéticas y de transporte de nuevos microhilos mono y bifásicos*", Tesis Doctoral, Universidad Autónoma de Madrid (2010)
[55] G. Infante, G. A. Badini-Confalonieri, R. P. del Real, and M. Vazquez, J. Phys. D 43, 345002 (2010).

[56] A. Yelon, D. Menard, M. Britel, P. Ciureanu, Appl. Phys. Lett. 69 (1996) 3084;
[57] D. Menard, M. Britel, P. Ciureanu, A. Yelon, J. Appl. Phys. 84 (2008) 2805.
[58] J. M. Barandiaran, A.Garcı´a-Arribas, D.deCos, J.Appl.Phys.99 (2006)103904.
[59] D.de Cos,A.Garcia-Arribas, J.M.Barandiara´ n, IEEETrans.Magn.41(2005) 3649.
[60] M. Britel, D. Menard, L. Melo, P. Ciureanu, A. Yelon, R. Cochrane ,M. Rouabhi, B. Cornut, Appl. Phys. Lett. 17 (2000) 2737.
[61] Landul and lifshitz E. Phys. R. zeitsch d. sowjetuniou 8, 153 (1935).
[62] C. Kittel, Phys. Rev. 71, 270 (1947).
[63] Van VLECK J. H. Phys. Rev. 78, 266 (1950).
[64] J. H. E. Griffiths, *Nature* 158 (1946) 670-671
[6x]W. A. Yagar and R.M. Bozorth, Phys. Rev. 72, 80 (1947).
[65] C. Kittel; Phys. Rev. 73 (2) (1948) 155.
[66] L. Kraus; Sens. Actuators A, 106 (2003) 187.
[67] J.Torrejon, G.Badini-Confalonieri,M.Vazquez, *J. Appl. Phys.* 106 (2009) 023913

[68] T.A.Ovari, H.Chiriac,M. Vazquez, A. Hernando, IEEE Trans.Magn.36(2000) 3445.

[69] Aichi Micro Intelligent Corporation: http//www.aichi-mi.com/

[70] K. Mohri, Y. Honkura, Sens. Lett. 5 (2007) 267-270

[71] E. MANTA, M. M. CODESCU, M. PETRESCU, U.P.B. Sci. Bull., Series B, Vol. 74, Iss. 4 (2012) 177-184.

[72] D. P. Belozorov, V. N. Derkach and S. I. Tarapov, Adv. Modern Radio Science, 12 (2002) 48.
[73] W. Wulfhekel, H. Ding, W. Lutzke, G. Steirl, M. Vázquez, P. Marín, A. Hernando, *Appl. Phys. A* 72 (2001) 463-470
[74] Hristoforou, E. (1997). Magnetostrictive delay lines and their applications. Sensors and Actuators, A59, 183.
[75] Hristoforou, E. and Niarchos, D. (1992). Amorphous wires in displacement sensing techniques. Journal of Magnetism and Magnetic Materials, 116, 177.
[76] Vazquez, M., Pirota, K., Badini, G., et al. (2006a). Sensor multifuncional basado en microhilos magn´eticos multicapas con acoplamiento magnetoel´astico. Patent PCT/ES2006/070173.
[77] Vazquez, M., Castano, F., Ovari, T.A., et al. (2001). New viscosimeter based on the ac field induced rotation of magnetostrictive amorphous wires. Sensors and Actuators, A91, 112.
[78] Zhukov, A., V´azquez, M. and Beneytez, J.M. (1998). Magnetoelastic sensor for signature identification based on mechanomagnetic effect in amorphous wires. Journal de Physique IV, 8, Pr–763.
[79] Zhukov, A., Garcia Beneytez, J.M., and V´azquez, M., (1996). Dispositivo magnetoel´astico para la identificaci´on y autentificaci´on de firmas. Patent ES 9600172.
[80] M. Vazquez, H. Pfützner, K. Pirota, G. Badini, J. Torrejón, *Multifunctional sensor based on multilayer magnetic microwires with magnetoelastic coupling*, European Patent PCT/ES2005/070173(2006)
[81] L. Kraus, Z. Frait, K. Pirota, H. Chiriac, *J. Magn. Magn. Mater* **254** (2003) 399-403

[82] K. Mohri, T. Uchiyama, L. P. Shen, C. M. Cai, L. V. Panina, Y. Honkura, M. Yamamoto, *IEEE Trans. Magn.* **38** (2002) 3063-3068

Chapter 2
Experimental techniques

2.1 Introduction

In this chapter we present a brief description of the main aspects concerning the fabrication process followed by the experimental techniques used for magnetic characterization.

The first section (2.2) will focus on the fabrication process of single and biphase microwires, which is made by two steps. In the first one (2.2.1), we give a whole description about the fabrication of glass-coated microwire, and then, in the second step (2.2.2), the external phase is grown onto the glass Pyrex by using two subsequent methods: sputtering (2.2.2.a) and electroplating (2.2.2.b).

Then, in the section (2.3) we describe the characterization techniques. The sections 2.3.1 and 2.3.2 are devoted to the static magnetic characterization and high frequency, respectively.

2.2. Fabrication of single and biphase glass-coated microwires

2.2.1. Single magnetic phase glass-coated microwires production

a. Casting method

This technique is based on early works by Taylor, Ulitovsky and others [1-3], and it presents an increasing interest in recent years. Microwires are manufactured by means of modified Taylor-Ultivsky techniques [4-7] based on direct casting from the melt as schematically depicted in *Fig. 2.1*. By this method, we have been able to fabricate composite microwires consisting of a metallic nucleus with diameter ranging between 1 and 30 μm and an insulating coating 2–12 μm thick. Fig. 2.1(a) shows a picture of the whole casting units.

The first step to obtain a glass-metal as microwire shape is the preparation of master alloy, which consists of pure elements based on Fe, Co or Ni. 5g of pure elements have weighed, then mixed and compacted into a pill by using an electric Arc furnace MAM-1 Company Edmund Burde. Finally, the master alloy obtained by melting in protective atmosphere of Ar to pure elements (provided by Sigma Aldrich and Alfa Aesar and with 99.99% of purity).

The master alloy with the desired composition is put into a glass Pyrex tube and placed within a high frequency inductor heater. The master alloy is heated up to its melting points 1200–1300 ◦C, forming a droplet. While the metal melts, the portion of the glass tube adjacent to melting metal softness, enveloping the metal droplet. A glass capillary continuing the metallic core is drawn from the Pyrex tube and fixed onto a rotating coil at the bottom of the equipment. At suitable drawing conditions, the molten metal fills the glass capillary and a microwire is thus formed where the metal core is completely coated by a glass shell. The amount of glass used in the process is balanced by the continuous feeding of the glass tube through the inductor zone, whereas the formation of the metallic core is restricted by the initial quantity of the master alloy droplet. A water-cooling system injects a jet of water to the lateral surface of the capillary to allow for a quenching with the required rate of about $10^5 Ks^{-1}$. The winding system collects the solid microwire [8].

While Fig. 2.1 (b) depicts the main aspects of fabrication process:

i) Fabrication of continuous, long pieces of microwire up to around 10.000 m;

ii) Repeatability of the microwire properties in mass production;

iii) Control and adjustment of geometrical parameters (inner metallic nucleus diameter and glass thickness) during the fabrication process.

iv) Wide range of geometrical parameters and physical properties;

The geometrical parameters of microwires depend on many factors as [9]:

- Vertical drawing stress and velocity to control the core and total diameters;
- Pyrex tube thickness to determine the final insulating glass Pyrex thickness;
- Temperature of the melt to determine the amorphicity of the core;

- Vacuum under-pressure inside the Pyrex tube in order to control the diameter of the metallic core.

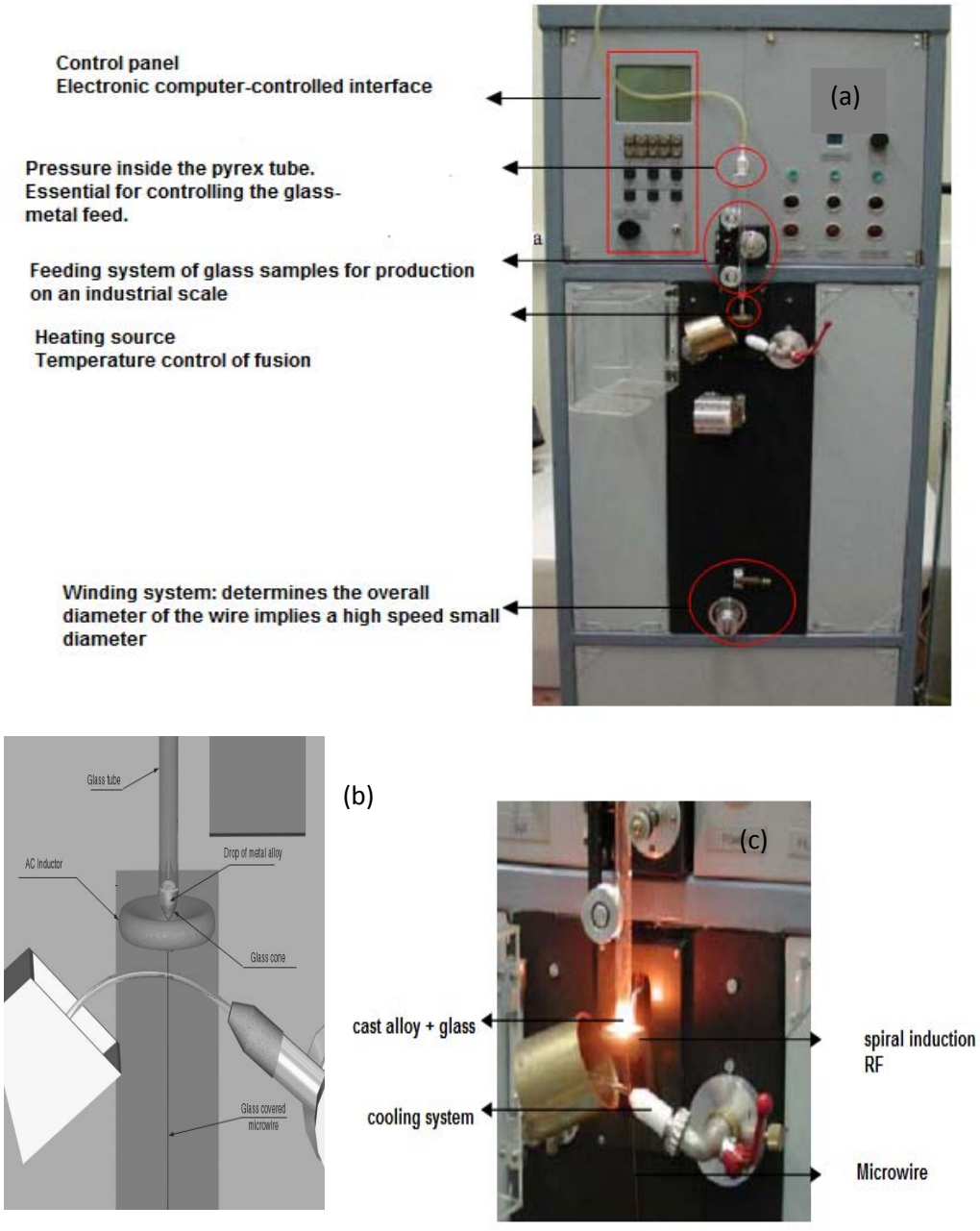

Figure 2.1fabrication of glass-coated microwires, GCM. (a) and (c) Images of quenching and drawing at the Institute of Materials Science of Madrid ,(b) Schematic drawing of microwire fabrication process by the Taylor–Ulitovsky method. [10].

Small modifications of these parameters can produce changes in the wire diameter. So, the exact diameter of the wire is checked in an optic microscope after production. The glass-coating provides electrical insulation and protects the metallic core from corrosion.

b. The composition of the metal core:

The magnetic alloys composition that can be produced with amorphous structure can be given as $TM_xM_{(1-x)}$ with x typically between 0.7 and 0.8. The main interest of magnetic microwires is their soft magnetic characteristics for which transition metals (TMs), Fe, Co, and Ni are the main elements of the alloy. In the case of amorphous microwires, the typical metalloids considered are Si and B, although elements as C, P, Al, and others, are added to enable the amorphicity of the alloys.

Many other TMs have been investigated, including rare earth metal and other metals which can react with the glass and atmosphere (Ti, V, Nb, Ta, Cr, Mo, W, Mn, Pd, or Al)[5].

The metallic alloys compositions presented in this study can be classified into three groups according to their magnetostriction, λ:

- FeSiB alloys with large and positive magnetostriction (in the order of 3×10^{-5}).
- CoFeSiB alloys with vanishing magnetostriction for the Fe/Co rate at around 5% ($\lambda\approx -1\times 10^{-7}$).
- CoFeNiSiBMo alloys with negative magnetostriction $\lambda \approx -1\times 10^{-6}$.

2.2.2. Biphase microwires production

We consider microwires with multilayer geometry and biphase ferromagnetic nature. They essentially contain a glass-coated metallic core typically with amorphous soft magnetic character, and intrinsic either axial (Fe-based) or circular (Co-based) magnetoelastic anisotropy.

The external part consists of an electroplated shell on a metallic nanolayer previously sputtered on the glass-coated microwire core. That has enabled the

fabrication of bimagnetic wires with tailored magnetic behavior namely, soft/hard, or hard/soft.

The fabrication of the external part of the biphase microwires is made in two steps. In the first one, a nanometric *Au* layer is sputtered onto the Pyrex coating by sputtering techniques. In the second step, we electroplate a magnetic softer or harder outer shell galvanostatically grown onto the *Au* layer in typical Watts type solutions.

a. Sputtering

The sputtering process is the first step to manufacture the external part of the biphase microwires. In the sputtering methods, the ionized gas is usually argon ions Ar^{+} plasma accelerated towards to a target (cathode) set at a negative voltage relative to the plasma that hits the materials to be deposited (substrate), (see *Fig. 2.2)*. The atoms are distributed throughout the enclosure, and a numbers of them are collected towards the substrate (anode), placed in front of the target, and onto which they form a thin layer.

In this work we used a commercial DC sputtering under low vacuum with a controlled gas, a ***Q150R S – metalizer*** [11]**,** which has a metal head with a deflection magnetic card easy to replace (gold / palladium as standard) as shown in the *Fig. 2.3*. The metallizer has been designed in a single module. The computer control is carried out through the color touch screen, allowing the users to enter, store and retrieve protocols. The automatic system ensures optimum vacuum conditions during evaporation / metallization. The vacuum chamber has an outer diameter of 165mm, equipped with protection against implosions. The equipment includes a vacuum locking system that keeps the vacuum in the chamber even if the system is not in operation. The metallizer is provided with a rotating sample holder platform.

In our case, we deposit Au onto the Pyrex under the following parameters: *40 mA* of current plasma, 10^{-1} *mbar* pressure in the vacuum chamber, and *3 min* time of sputtering, which according to the growth rate specified by the manufacturer, approximately correspond to a *30 nm* thick layer of Au.

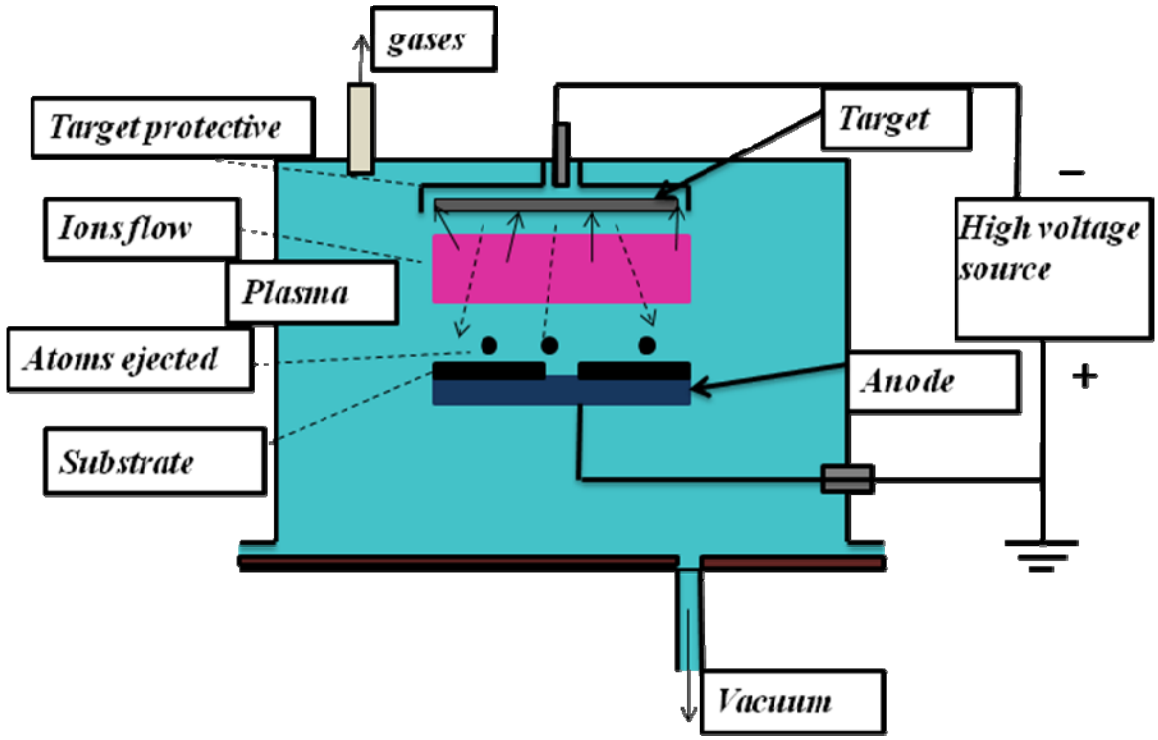

Figure 2.2 Schematic diagram of the sputtering process.

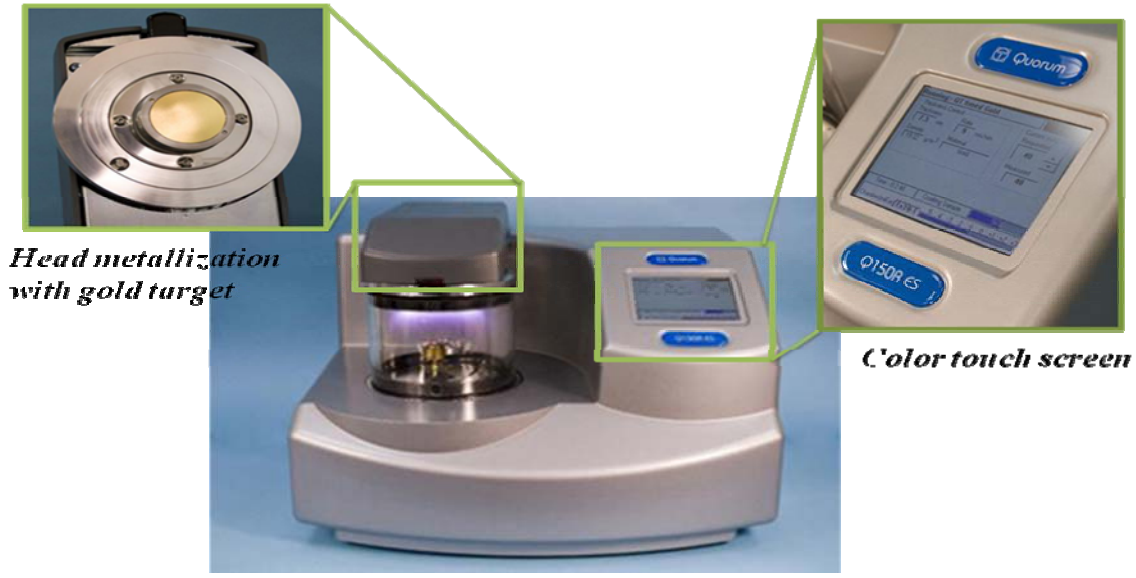

Figure 2.3 Q150R S - metalizing Images installed in the ICMM-CSIC.

In our process we used gold (Au) as noble metal to grow a film with nanometer thickness, which sputtered onto the Pyrex glass-coated microwires "GCM". This layer has a role of electrode / substrate for subsequent electroplating of the magnetic external

shell, since the electrodeposition technique requires that the substrate surface is a conductor.

b. Electrodeposition process

Electrodeposition (electroplating) refers to the deposition of a pure metal or metallic alloy from an electrolyte solution by the passing of an electric current [12]. The morphological nature of the deposit is determined by several factors including the electrolyte composition, pH, temperature, agitation, and the current density. This process holds the advantages of being a continuous process with a high rate of deposition. With these advantages identified, the electrodeposition has even been adopted by industry for preparation of magnetic materials and protective coatings [13]. Electrodeposition gives one the control over the composition and structure by pulse plating, from a single electrolyte by using a periodically varying current or potential.

Thus, electrodeposition permits the grown of a metallic coating by applying a negative charge onto a substrate in an electrochemical cell (schematically depicted in *Fig. 2.4)*. It consists of two electrodes (cathode and anode) where the electrochemical reactions occur, an electrolyte for conduction of ions, and an external conductor to provide for continuity of the circuit, through a chemical reaction type:

$$M^{n+} + ne^- \leftrightarrow M \qquad (2.1)$$

This reaction, usually reversible, is characterized by an equilibrium potential. The reduction reaction (2.1) occurs at the cathode generally accompanied by hydrogen evolution:

$$2H^+ + 2e^- \rightarrow H_2 \qquad (2.2)$$

Furthermore, different oxidation reactions occur at the anode. A possible reaction is the anodic evolution of oxygen, as in the case of an acid medium:

$$2H_2O \rightarrow 4H^+ + O_2 + 4\,e^- \qquad (2.3)$$

There are two ways to perform the electroplating process: control the current density between the anode and the cathode, or the potential difference between the substrate and a third reference electrode. The first one is the simplest, called galvanostatic electrodeposition and this is what we used in this work.

In this case, we have used a stabilized current source (or galvanostat) to control the flow of ions to the substrate. The main disadvantage of this method is the potential

between the electrodes, which varies as the deposit increases and with it the composition of the material obtained. Therefore to ensure sample homogeneity, a short plating process is required.

The elements necessary to achieve plating are shown in *Fig. 2.4*, which shows the experimental system used in this thesis, and are as follows:

Electrode: To make a galvanostatic electrodeposition two electrodes are necessary: a conductive substrate (microwires sputtered by Au) acting as a cathode and a metal anode, which in this case is a Pt mesh with cylindrical geometry sewn around a Teflon structure.

Power supply: control of the current density ($J = 12\ mA/cm^2$ in the experiments) was carried out using a potentiostat / galvanostat AMEL Instruments 2053 [14].

Electrolysis cell: The vessel containing the electrolyte is a Pyrex beaker. The cell is completed by a heating plate that controls the temperature and stirring of the electrolyte

Electrolytes: In this work, we used two baths of plating solution CoNi and FeNi:

i. In CoNi, plating has been done in an aqueous solution of $NiSO_4$-$6H_2O$ (150 g / l), $NiCl_2$-$6H_2O$ (22.5g / l), H_3BO_3 (45 g / l), $7H_2O$ $CoSO_4$ (150 g / l), $CoCl_2$ _$6H_2O$ (22.5 g / l) [15], [12]. It has been carried out in a current density regime (*12 mA /cm²*) at 40ºC. Boric acid is commonly used as an agent of amortization of these solutions to be very effective in stabilizing the pH at the cathode. CoNi solution has a pH of 4.4 and was electrodeposited under magnetic stirring for a maximum time of 90 minutes.

ii. In the FeNi, plating, the bath was composed of $FeSO_4$-$7H_2O$ (8 g/l), $NiSO_4$-$6H_2O$ (125 g/l), $NiCl_2$-$6H_2O$ (20 g/l), H_3BO_3 (40 g/l), saccharin (6 g/l) in de-mineralized water [16]. The temperature was thermostatically adjusted to 55°C. The pH of the bath was adjusted to 2 and 2.80 adding KOH to the solution. Electrodeposition was carried out under magnetic stirring at 55 ° C for a maximum of 60 minutes.

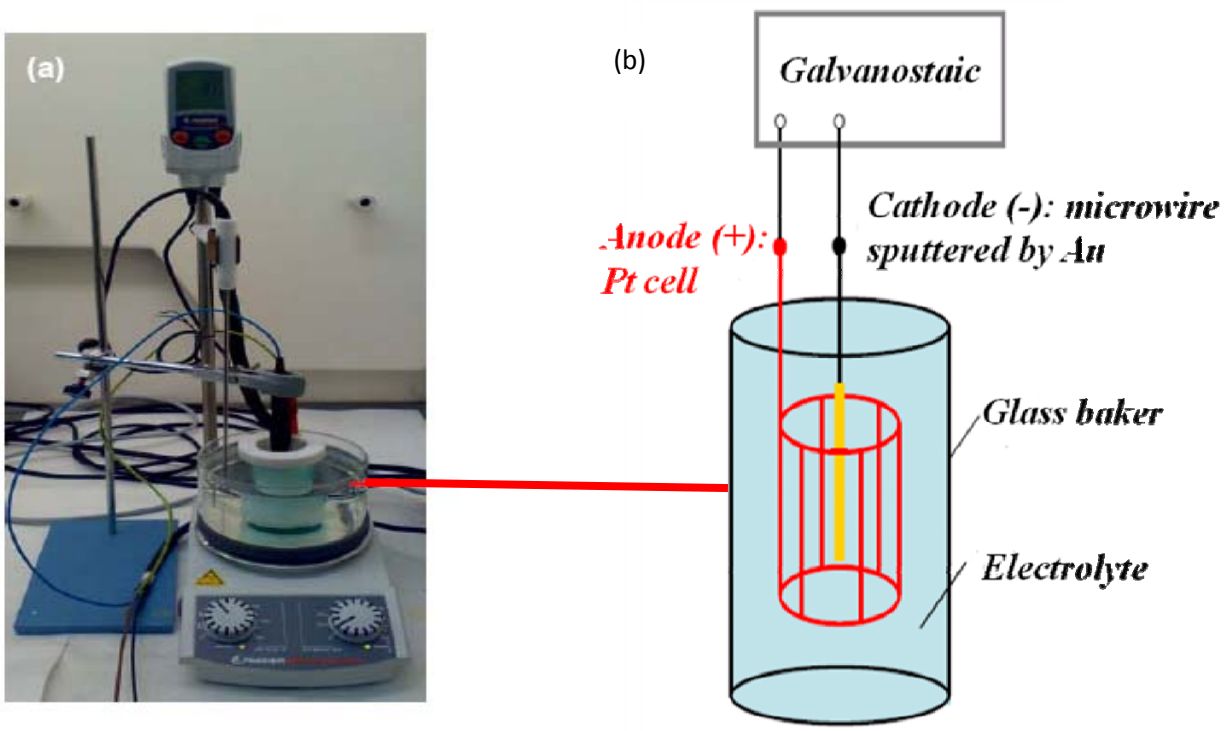

Figure 2.4 Galvanostatic electrodeposition of magnetic coating. (a) Photo of the experimental setup in the laboratories of ICMM-CSIC. (b) Schematic diagram of the electrolytic cell used.

2.3. Magnetic characterization

2.3.1. Hysteresis Loops at low frequency

This section is dedicated to the magnetic behavior measurement, where there has been a major experimental effort. The magnetization curves and hysteresis loops measurement were performed by combining two complementary equipments: i) induction magnetometer system and ii) two kinds of vibrating sample magnetometers, VSM. The first one allows one a quick and precise characterization of hysteresis loops at low field, while the second one was used for measurement of hysteresis loops in the range of high magnetic field.

a. Induction magnetometer system

The operating principle of the induction magnetometer system consists of applying an A.C. magnetic field, H, and simultaneously measuring the total change of magnetic flux induced by pick-up coil located enclosing the sample. According to Faraday's law, the voltage induced, V_{ind}, in the coil is proportional to the time derivative

of the magnetic flux. The method can have disadvantages in the case of samples with a reduced cross section. The optimization of the system was developed by our colleague Dr. ***G. Infante*** who installed an additional pick-up coil connected in series opposition to the detector coil containing the sample (see *Fig. 2.5* (down)).

This system has been employed to measure the low frequency hysteresis loops of soft magnetic materials. It has been applied successfully to characterize straight pieces of amorphous glass-coated microwires with very thin metallic nucleus.

The system is based on the electromagnetic induction law, the design is extremely simple and exploits the capabilities of commercially available data acquisition cards together with digital signal processing in order to achieve analog equipment, more details elsewhere[17].

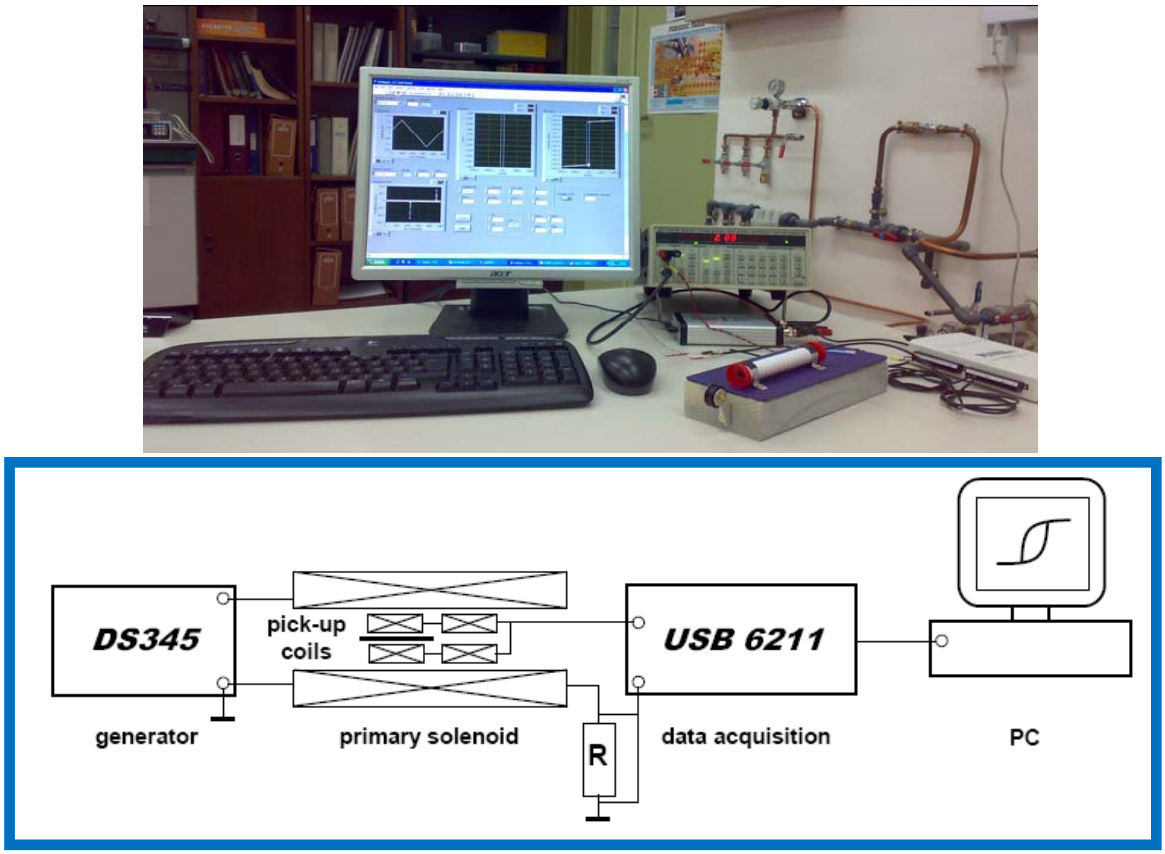

Figure 2.5 Image of the setup (upper) and schematic (down) diagram of induction magnetometer system [18].

❖ Measurement setup

Figure 2.5 is shown image (upper) and schematic diagram (down) of induction magnetometer system. The primary circuit consists of a function generator (Standford research, model DS 34S) connected to a current amplifier (UAM e- SEGAINVEX- placed under the function generator[18]) which feeds the magnetizing solenoid to provide a maximum magnetic field $H \approx \pm 8kA/m$ when fed with a 5Vpp amplitude triangular current in the frequency range between 10Hz and several 100Hz. The secondary circuit simply consists of the compensated pick-up pair.

The lab view-based software has been developed in order to acquire and process the signals and to plot the M-L loop, more details elsewhere [17].

b. Vibrating sample magnetometer

The Vibrating Sample Magnetometer is a classical instrument that was first described by Foner [19] in 1959. In the VSM, the sample vibrates in the presence of a magnetic field. The VSM is based on the Faraday's law according to which an *e.m.f.* is induced in a conductor by a time-varying magnetic flux. In VSM, a sample magnetized by a homogenous magnetic field undergoes a sinusoidal vibration at small fixed amplitude with respect to stationary pick-up coils. The motion of the sample results in an induced voltage and it can be used to determine the magnetization of the sample.

Hence the change in induction is directly proportional to the magnetization of the sample and is detected as an induced voltage. With an appropriate calibration using a sample with a known magnetization (usually Nickel), the induced voltage and magnetization relationship can be established and then employed to determine the magnetization of other samples.

The magnetization measurements of materials were performed using two vibrating sample magnetometers, VSM. The first one is the commercial KLA- Tenor EV7 VSM from LOT-Oriel Company [20], which installed in ICMM-CSIC, and the second one LakeShore VSM (7400 series) [21] installed in Immanuel Kant State University, Kaliningrad, Russia under the supervision of Dr. Valeria Rodionova .

❖ Measurement setup

i. Vibrating sample magnetometer (KLA Tandor EV7)

This equipment uses an electromagnet which, depending on the distance between its poles, applies a maximum external field of 1.8 T (for a minimum gap of ≈ 3cm). The accuracy of the system to stabilize the applied field is less than 0.1 Oe and the maximum distance between the pole pieces is 82 mm. The most important parts of the VSM are presented in the *Fig. 2.6*: the vibrator which causes the oscillatory movement of the sample; the fastening system of the rod where the sample is placed; the detection coils and the electromagnet. The sample is placed between two detector coils and begins to vibrate with simple harmonic motion.

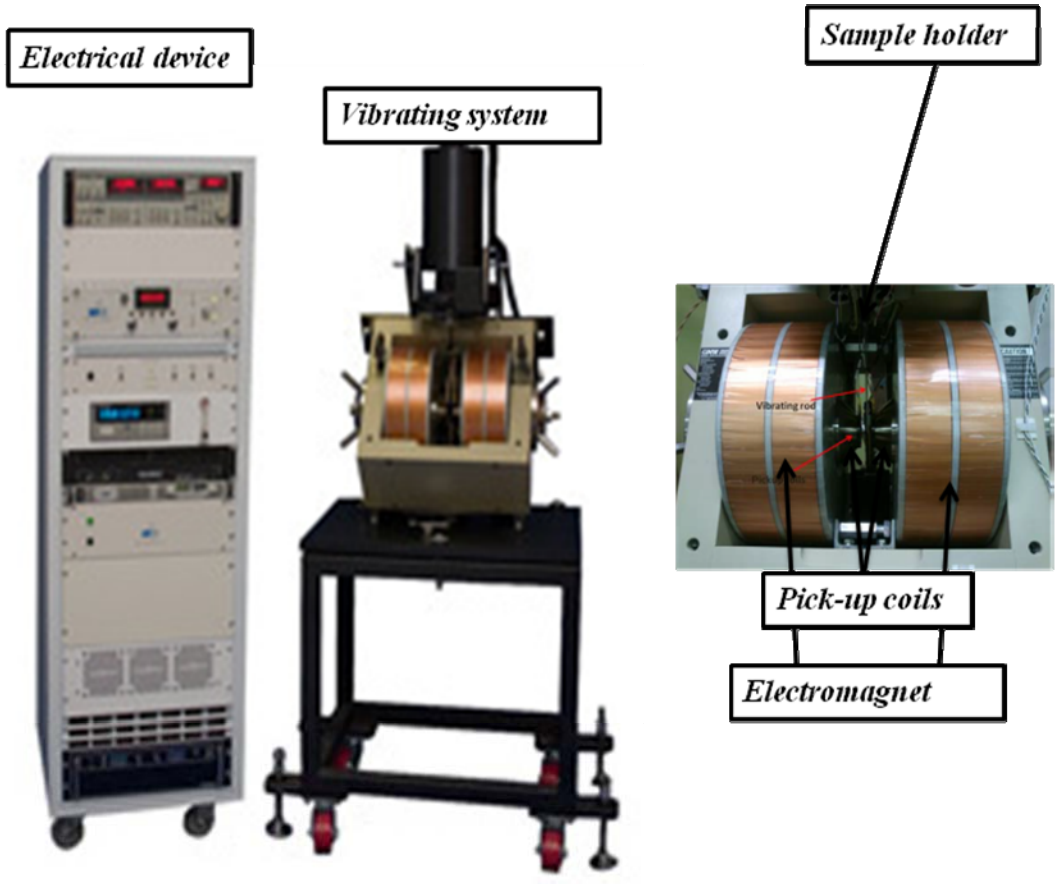

Figure 2.6 Image of the VSM installed in ICMM/CSIC, and a part where the pickup coils and the sample are located.

ii. Vibrating sample magnetometer (Lake shore 7400 Series)

The vibrating sample magnetometer [22] with high magnetic field resolution of 0.02 Oe was used to measure the magnetic behavior of materials at high temperature.

Available in three different variable gap electromagnet configurations providing fields up to 3.1 T, the Lake Shore VSM system is a sensitive electromagnet-based VSMs commercially available and feature the broadest temperature range capability from 4.2 K to 1,273 K (-269 °C to 1000 °C). The VSM measures a wide range of sample types, making them ideal tools for the most demanding materials research applications and quality control of magnetic materials.

The design of the measuring unit vibrating magnetometer is shown in *Fig.2.7 (a)*. The assortment of options including, head driver, sample holder, pick-up coils, and electromagnet. The picture of magnetometer presented in *Fig.2.7 (b),* consists of three main blocks: the electromagnet, which is powered by power supply; a vibrator unit, which is attached to the holder of the stock with the sample; and the electronics system. For high temperature measurements, it additionally uses a high temperature oven, which is placed between the electromagnet and pick-up coils (see *Fig.2.7 (c)*).

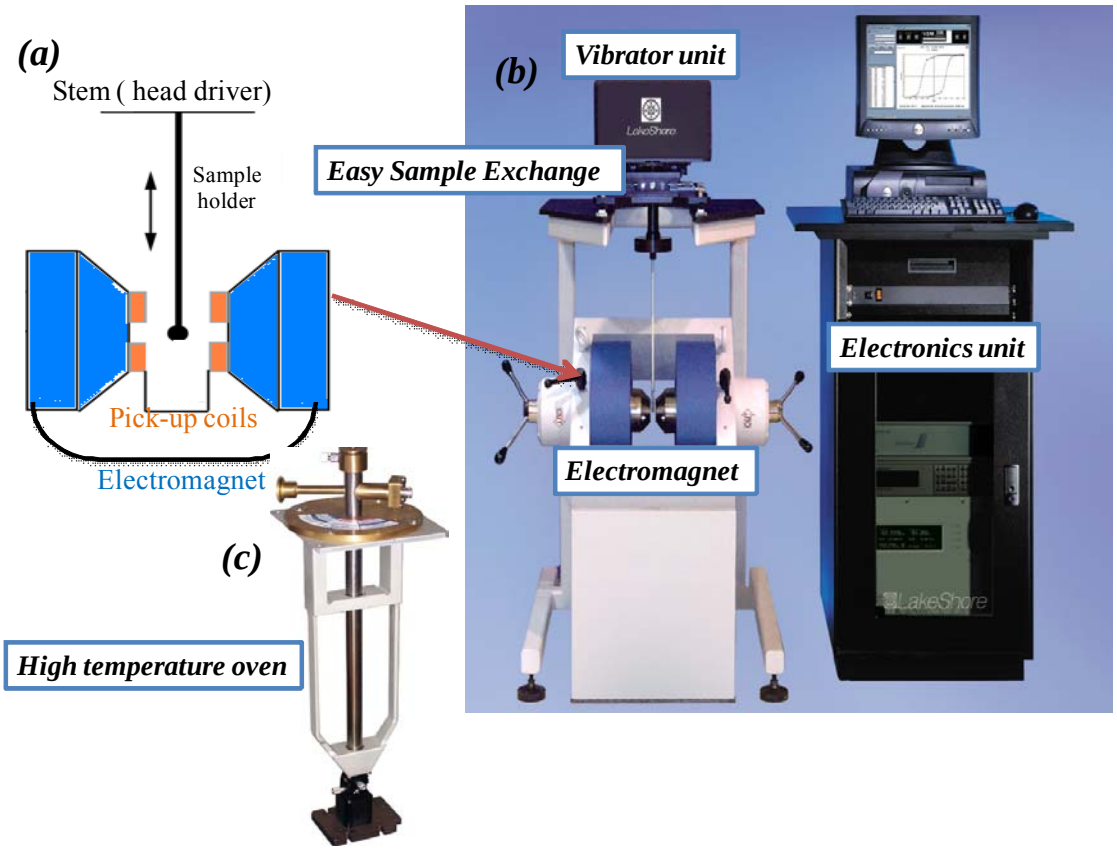

Figure 2.7 Image of the VSM installed in Immanuel Kant State University, Kaliningrad, Russia, and a part where the pickup coils and the sample are located.

2.3.2. High frequency basic: FMR Spectra

For measuring the ferromagnetic resonance, there are various techniques such as measuring in free space [23], waveguide [24] or resonant cavity [25] and measurement in transmission coaxial line, TCL, [26] or microstrip [27, 28].

In this manuscript, we focus to analyze the behavior of single and biphase magnetic microwires at high frequency by using two processes: the measurement in transmission coaxial line (which has historically been the most widely used for samples in the form of wires), and the measurement in Electron Paramagnet Resonance spectrometer (resonant cavity (X-band)).

The measurement in the transmission coaxial line requires essentially a vector network analyzer of microwave equipment. The vector network analyzer (VNA)-FMR uses a periodic RF signal emitted from the VNA as the source for exciting the magnetization. The VNA has the ability to sweep the frequency in a wide band of frequencies and at the same time the device can detect the RF signal´s phase and amplitude related to the same frequency, so that it provides a full description of the so-called scattering or S−parameters. The S-Parameters or scattering matrix, describes the way in which the traveling RF wave is affected when it passes a circuit or through the sample under test. But the design and calibration of the sample holder are the most sensitive.

In this work, we will present a new approach sample holder, which has been developed by Dr. Victor Raposo from University of Salamanca [29].

a. Measurement in Transmission Coaxial Line (TCL)

The ferromagnetic resonance, FMR, measurements up to 12 GHz at a constant static magnetic field have been achieved in the laboratory of ICMM-CSIC by a network analyzer (Agilent E8362B) [30] and a transmission coaxial line. The device is shown in *Fig. 2.8*.

The static magnetic field (0.5 T max.) is generated by an electromagnet and uses cables, SMA connectors and adapters suitable for measurements at a maximum frequency of 20 GHz. The adapted sample holder shown in *Fig. 2.8(b)* is based on a commercial SMA (SubMiniature version A) connector [31] where the inner pin has been removed in order to avoid radiation effects. The inner and outer conductors of the

holder are shorted by means of the microwire nucleus: the Au and magnetic coatings are removed from the wire ends and the amorphous nucleus (around 50Ω DC resistance) is welded using silver paint. The reflection coefficient S_{11} is analyzed, from which real R and imaginary X components of impedance are determined [32].

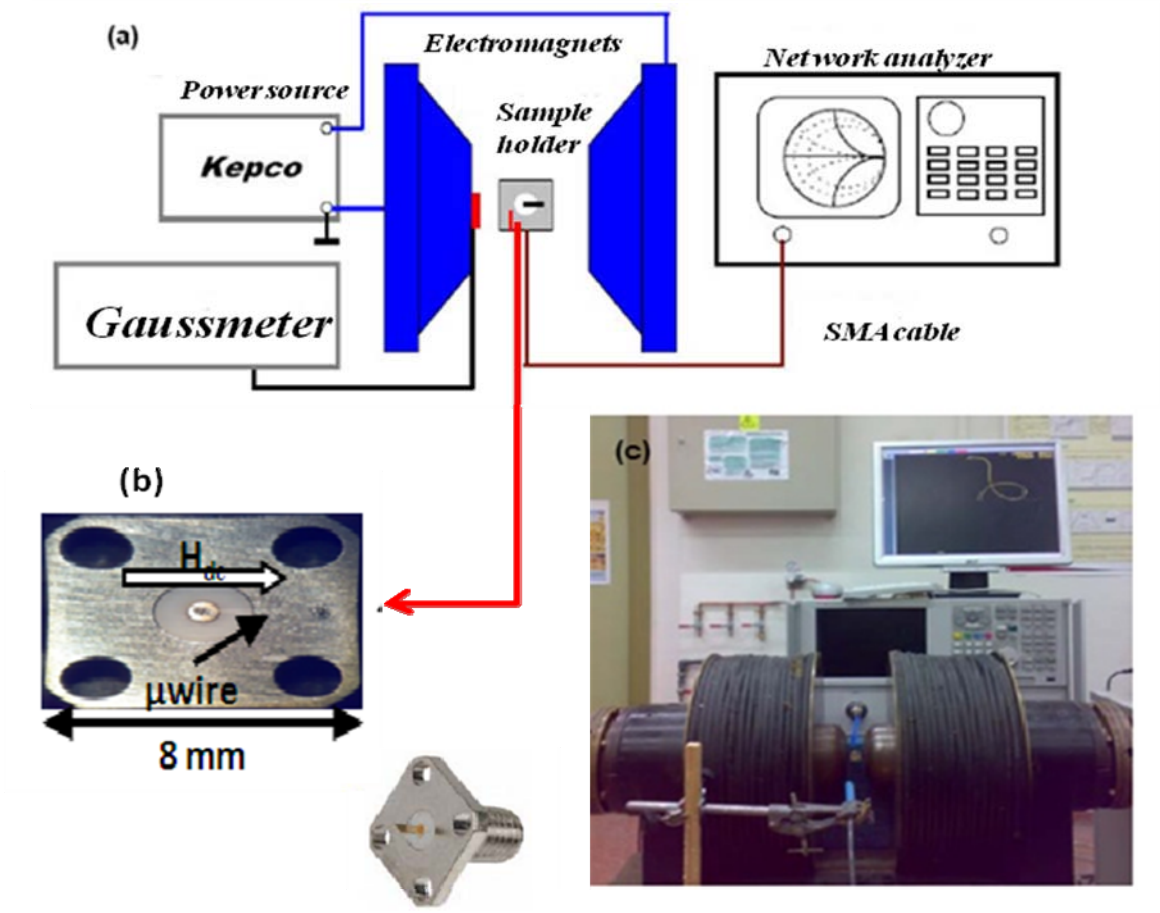

Figure 2.8 Experimental device of FMR measurement in transmission coaxial line (10 MHz-12 GHz) installed in ICMM-CSIC laboratories: (a) Schematic diagram of the measurement system (the position of the sample shown in black), (b) detail of sample holder based on a commercial SMA connector, (c) image of the system.

The impedance of the sample is calculated using the expression:

$$Z \equiv R + iX = 50\frac{1 - S_{11}}{1 + S_{11}}$$

Where S_{11} is the complex reflection coefficient measured by the network analyzer, corrected by the circuit above the sample. In resonance, the real part of the impedance is the maximum and the imaginary part crosses zero.

Real and imaginary impedance components were simultaneously measured as a function of frequency for a range of dc longitudinal applied fields (up to 80 kA/m), starting the process from the minimum field. As in common FMR experiments, the DC magnetic field is perpendicular to the *rf* magnetic field. Previous to the measurement procedure, all cables, connectors, and adapters were calibrated using a short-open-load (SOL) technique and the value of the electrical delay of the TCL terminated in the sample holder, *77 psec*, was determined by measuring the response of a 50Ω SMD resistive load using the same holder.

b. Measurement in Electron Paramagnet Resonance (EPR) spectrometer

The microwave absorption measurements were performed using a standard ER ***049X*** Electron Paramagnet Resonance (EPR) Spectrometer at 9.5 GHz at room temperature as shown in *Fig. 2.9*. The measurements of FMR were performed in the laboratory of spectroscopy and microscopy services from the University of the Basque Country Bilbao under the supervision of Dr. Galina Kurlyandskaya, and Dr. Luis Lezama.

The important parts of the EPR spectrometer are the microwave bridge and the EPR magnet as shown in *Fig. 2.9(b)*. The x-band waves at the microwave bridge are generated. These are directed through a wave guide towards the cavity where the sample under study is locked. The cavity and the sample are subjected to the magnetic field during the EPR measurements generated by EPR magnet (see *Fig. 2.7(a)*), and maximum field is 1T (with field modulation 1Oe and 100 kHz).

This technique allows one obtaining the derivatives of the absorption peaks as function of the magnetic field (dP/dH). DC magnetic field was parallel to the wire. The schematic setup is depicted in *Fig. 2.9(a)*. Samples can be measured at room temperature, with different angles, and at low temperature in the range 4-300K. For low temperature, the spectrometer can be fitted with a cryostat. Liquid and gaseous Nitrogen (Helium) comes from a large storage Dewar via a transfer line.

In our measurements, pieces of microwires 3 mm in length were taken. The samples were vertically placed into the tube between 2 small circular kapton pieces. As

the electric field at the sample position in the cavity was not exactly zero, relatively strong circumferential AC field was induced by electric polarization of the wire [33].

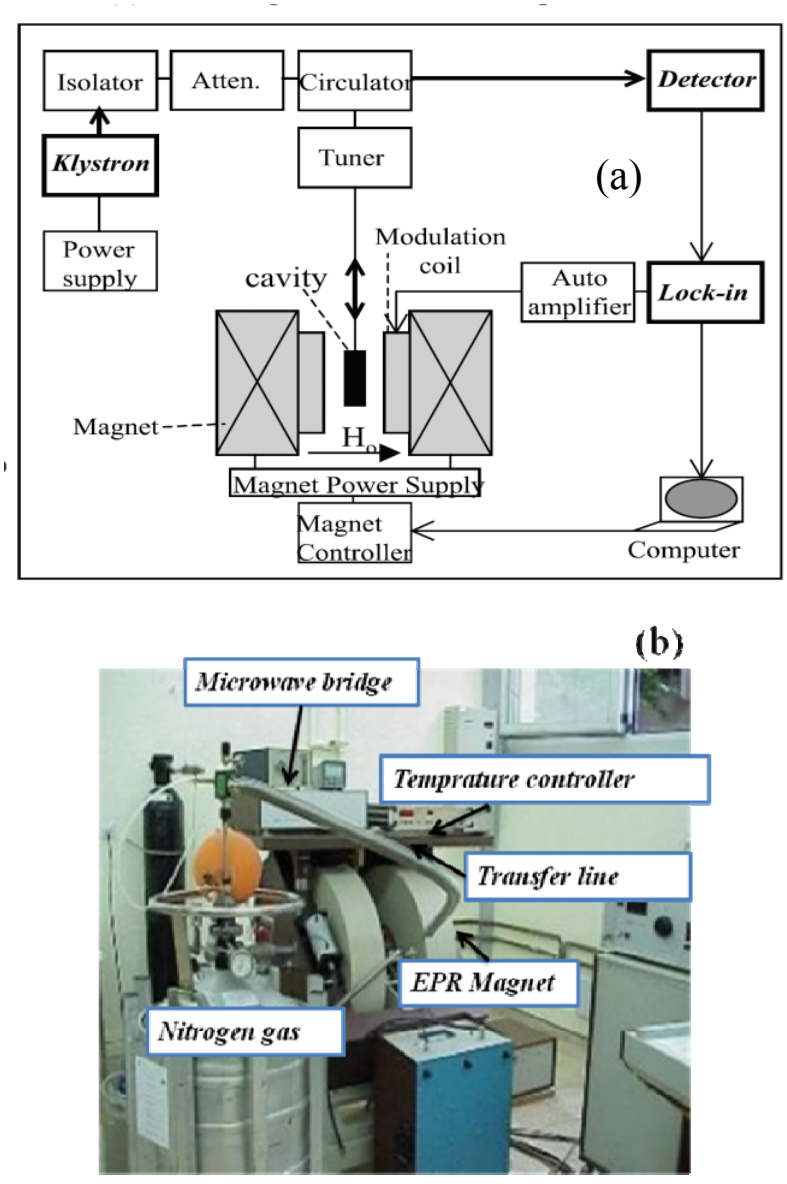

Figure 2.9 Schematic view (a) and image (b) of the cavity perturbation measurements setup, installed in the University of the Basque Country.

2.4. References:

[1] G. F. Taylor, Phys. Rev. 23, 655 (1924).

[2] G. F. Taylor, process and apparatus for making filaments, U. S. Patent 1, 793, 529, 1931.

[3] K-Y. Wang, J. Arcas, V. Lrin, J. L. Muños, A. P. Zhukov, D. X. Chen, M. Vazquez, and A. Hernando, Phys. Status, Solidi 162, R5 (1997).

[4] A. V. Ulitovsky, method of continuous fabrication of microwires coated by glass, USSR Patent, 128427, 1950.

[5] A. V. Ulitovsky in "micro-technology in desing of Electric Devices" Leningrad, 1951, Nº7, P.6.

[6] A. V. Ulitovsky and N.M. Avernin, Method of fabrication of metallic microwires, USSR Patent 161325, 1964; bulletin 7, p.14.

[7]A. V. Ulitovsky, I. M. Maianski, and A. I. Avramenco, method of continous casting of glass-coated microwires, USSR Patent 128427, 1960, bulletin 10, p. 14.

[8] V. Larin, A. Torcunov, A. Zhukov, J. Gonz_alez, M. V_azquez, and L. Panina, /Preparation and properties of glass-coated microwires," Journal of Magnetism and Magnetic Materials, vol. 24, pp. 39-45, 2002.

[9] H. Kronmuller and S. Parkin, Eds., Handbook of Magnetism and Advanced Magnetic Materials. John Wiley & Sons, Ltd., 2007, vol. 4: Novel Materials, ch. Advanced Magnetic Microwires by Manuel V_azquez, pp. 2193-2226.

[10] M. Vazquez, in: Handbook of Magnetism and Advanced Magnetic Materials, Vol. 4, edited by H. Kronmu¨ ller and S. Parkin (John Wiley and Sons, New York, 2007), p. 2193.

[11] Metalizador Quorum Technologies SC7620: http://www.quorumtech.com/products/sputter-coaterssem- carbon-coaters/sc7620-mini sputter-coater.html.

[12] J. Torrejón, "*Estudio del acoplamiento magnetoelástico y magnetoestático en microsistemas multicapas bifásicos"*, Tesis Doctoral, Universidad Autónoma de Madrid (2008).

[13] V. S. Larin, A. V. Torkunov, A. Zhukov, J. González, M. Vázquez, L. Panina, *J. Magn. Magn. Mater.* **249** (2002) 39-45.

[14] Potenciostato/galvanostato AMEL Instruments 2053: http://www.amelchem.com/product/electrochem/line2000/2053/2053.html.

[15] M. Schlesinger, M. Paunovic, *Modern Electroplating*, Wiley (2000).

[16] Li, X.P.; Seet, J.; Fan, J.: Electrodeposition and characteristics of Ni80Fe20/Cu composite wires, Journal of Magnetism and Magnetic Material, Vol. 304, Iss. 1, pp. 111-116 (2006).

[17] M. Butta, G. Infante, P. Ripka, G. A. Badini-Confalonieri, M. Vázquez, Rev. Sci. Instrum. 80 (2009) 083906.

[18] DAQ National Instruments NI USB-6211: http://sine.ni.com/nips/cds/view/p/lang/en/nid/203224
[19] S. Foner, Rev. Sci. Instrum. 30 (1959) 548-557.
[20] VSM LOT-Oriel EV7: http://www.lot-oriel.com/ib/es/home/vsm/.
[21] VSM Lakeshore Serie 7400: http://www.lakeshore.com/products/Vibrating-Sample-Magnetometer/Models/Pages/Overview.aspx
[22] N. Perov and A. A. Radkovskaya, "Vibrating sample anisometer," in *Proc. 1&2 Dimensional Magn. Meas. Testing*, 2001, pp. 104–108, -Vienna Magnetic Group Report.
[23] D. K. Ghodgaonkar, V. V. Varadan, V. K. Varadan, IEEE Trans. Instrum. Meas. 39 (1990) 387-394.
[24] S. Lefrançois, D. Pasquet, G. Mazé-Merceur, IEEE Trans. Microwave Techno. and Tech. 44 (1996)1557- 1562.
[25] A. N. Medina, M. Knobel, S. Salem-Sugui, F. G. Gandra, J. Appl. Phys. 79 (1996) 5462-5464.
[26] D. Menárd, M. Britel, P. Ciureanu, A. Yelon, V. P. Paramonov, A. S. Antonov, P. Rudkowsky, J. O. Ström-Olsen, J. Appl. Phys. 81 (1997) 4032-4034.
[27] D. de Cos, "Magnetoimpedancia en muestras planas a altas frecuencias", Tesis Doctoral, Universidad del Pais Vasco (2006).
[28] D. de Cos, A. García-Arribas, J. M. Barandiarán, Sens. Actuators A. 115 (2004) 358-375.
[29] V. Raposo, G. Infante, M. Zazo, J. Íñiguez, Measuring magnetoimpedande in multilayer amorphous microwires, Magnetic Measurements 2010, MP19.
[30] Vector Network Analyzer Agilent E8362B: http://www.home.agilent.com/agilent/product.jspx?nid=536902643.536882571.00&lc=eng&cc=US.
[31] Conector SMA Radiall R124510000: http://radiall.applixia.net/catalogue/object.do?action=datasheet&object=2660474.
[32] J. Torrejon, G. A. Badini-Confalonieri, and M. Vazquez, J. Appl. Phys. 106, 023913 (2009).
[33] D.S. Rodbell, J. Appl. Phys. 30, (1959) 1845.

3. Low frequency properties: Hysteresis Loops

3.1. Introduction and selected samples

A number of applications have been developed making use of the outstanding magnetic characteristics of amorphous alloys. Magnetic field and stress sensors profit of the giant magneto-impedance observed in non-magnetostrictive CoFe-based amorphous or Fe-based nanocrystalline alloys with extremely high initial susceptibility. Particular interest is being currently addressed to amorphous microwires prepared by rapid solidification techniques (i.e., quenching and drawing). Updated information on the achievements using amorphous wires the many applications can be found elsewhere [1].

In this study, we consider microwires with multilayer geometry and biphase ferromagnetic nature. Microwires of this family were introduced recently [5, 6]. They essentially consist of a glass-coated core typically with amorphous soft magnetic character, and intrinsic either axial (Fe-based) or circular (Co-based) magnetoelastic anisotropy. In addition, a second external concentric microlayer is grown that enhances the magnetic possibilities owing to the magnetic interactions between magnetic phases. Particularly, significant magnetostatic and magnetoelastic interactions have been systematically investigated in biphase microwires [7, 8]. For an updated review including such magnetic interactions and technological applications (i.e., multifunctional sensor, designed magnetic anisotropy) the reader is addressed to [9].

Along this chapter we will consider the following aspects:

i) Description of selected wires for the study (table with all microwires studied)

ii) Morphology, structure and compositional characteristics (SEM, XRD, composition) for both CoFe and Fe-based wires.

iii) CoFe- based single and biphase general magnetic characteristic. a) Results for single phase with different thickness of Pyrex, b) Results for biphase with different thickness of shell of CoNi and with FeNi

iv) Fe-based single and biphase general magnetic characteristics. a) Data for Fe-based single and/or biphase with different Pyrex thickness, b) Influence of annealing (with separation of data for annealing below and above 500ºC, c) Summary of influence of annealing

v) Temperature dependents magnetic behavior and its analysis: a) High temperature dependence, and b) Low temperature dependence.

vi) Summary or conclusion.

3.1.1. Morphology, compositional characteristics of studied samples

The composition and dimensions details of the studied microwires are presented in Table 3.1. And the geometry details of the microwies are given in the *Fig. 3.1*.

Composition	Dimensions	Electrodeposition Galvanostatic J=12mA/cm^2
$Co_{67.06}Fe_{3,87}Ni_{1,44}Si_{14,47}B_{11,53}Mo_{1,66}$/ $Co_{90}Ni_{10}$;$Fe_{20}Ni_{80}$	d=17µm D_{tot}=20, 34, 42µm	$t_{FeNi,\ CoNi}$= 0-7 µm
$(Co_{0.94}Fe_{0.06})_{72.5}Si_{12.5}B_{15}/Co_{90}Ni_{10}$	d=8µm D_{tot}=24µm	t_{CoNi}= 3-10µm
$Fe_{76}Si_{13}B_{11}/Co_{90}Ni_{10}$	d=18, 18, 20µm D_{tot} =24, 24, 26µm	t_{CoNi}= 0-7 µm
$Fe_{77,5}Si_{7,5}B_{15}/Co_{90}Ni_{10}$; $Fe_{20}Ni_{80}$	d=12µm D_{tot} =40-38µm	$t_{FeNi,\ CoNi}$= 0-7 µm

Table 3.1 Investigated single and biphase microwires

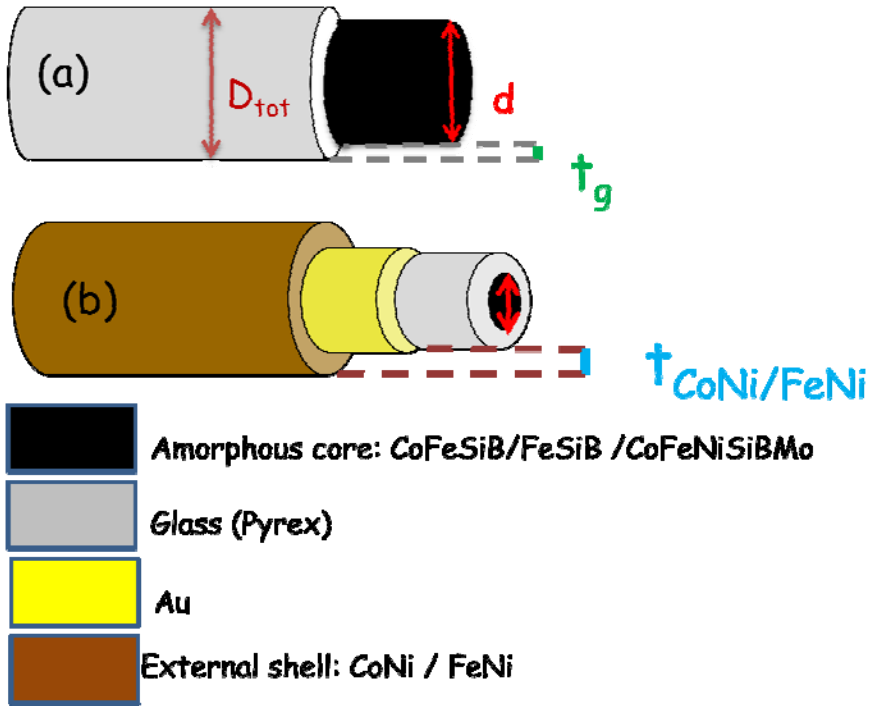

Figure 3.1 Schematic view of magnetic single (a) and biphase (b) microwires. ***d*** *is the diameter of amorphous core,* t_g *is the thickness of the intermediate insulating glass Pyrex,* D_{tot} *is the total diameter, and* $t_{FeNi/CoNi}$ *is the thickness of magnetic external shell (CoNi/FeNi).*

The composition of the different layers of each system has been determined by SEM-EDX (Scanning Electron Micrscope- Energy Dispertive Spectroscopy) technique,

which gives information and analysis on the composition corresponds only to a small region of the surface. While, the dimensions and thickness of the external shell has been checked by optical microscope techniques. Finally, the crystal structure of the magnetic layers has been analyzed by RX diffraction techniques.

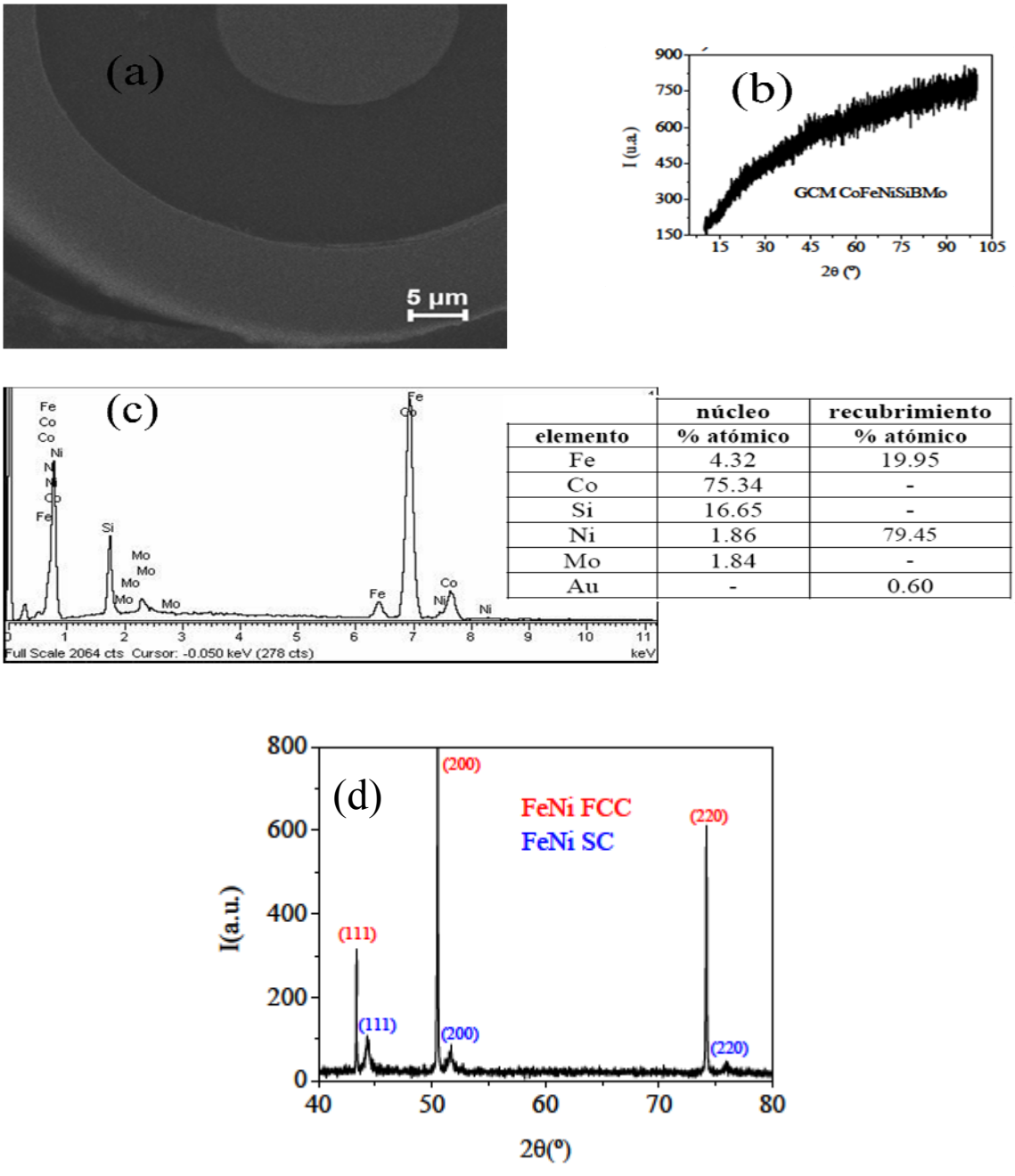

	núcleo	recubrimiento
elemento	% atómico	% atómico
Fe	4.32	19.95
Co	75.34	-
Si	16.65	-
Ni	1.86	79.45
Mo	1.84	-
Au	-	0.60

Figure 3.2 (a) SEM image of biphase microwires CoFeNiSiBMo/FeNi (a=7 µm, tg=14 µm, t=9 µm). (b) X-ray spectrum and its (c) microanalysis core composition of CoFeNiSiBMo and the external shell FeNi (source: [3]). (d) X-ray spectrum of external Shell FeNi (source [4]).

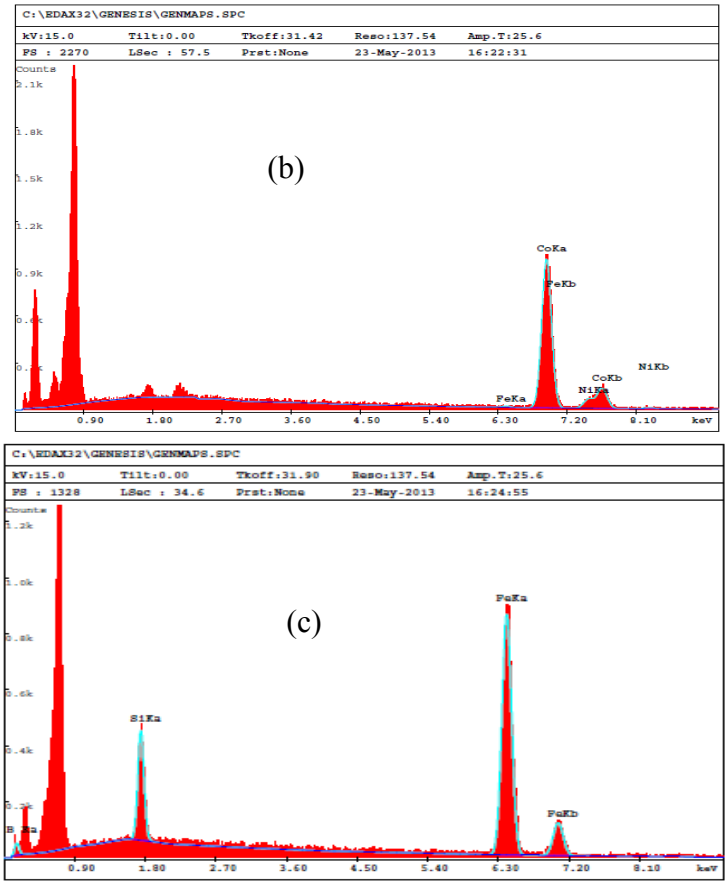

Element	Wt%	At%
FeK	74.64	40.01
SiK	6.02	6.42
BK	19.35	53.58

Element	Wt%	At%
FeK	0.70	0.74
CoK	92.15	92.09
NiK	7.15	7.17

Figure 3.3(a) SEM image of biphase microwires FeSiB/CoNi (d=18µm, D=24 µm, t_{CoNi}=3 µm). EDX microanalysis core composition of FeSiB (b) and the external shell CoNi (c).

Figures 3.2 and 3.3 present the micrographs and surface chemical analysis of CoFe/FeNi and FeSiB/CoNi biphase microwires.

Fig.3.2 (a) and Fig.3.3 (a) show a cross section SEM image. The composition, checked by SEM-EDX is found to be homogeneous, as depicted in *Fig. 3.2(c)* and *Fig. 3.3(b and c)*. X-ray spectra of CoFe and Fe core and FeNi external shell are shown in *Fig. 3.2 (b), (d)*.

3.2. Magnetic behavior of single and biphase microwires at room temperature

3.2.1. CoFe-based single and biphase: Influence of thickness of Pyrex glass-coating and of external shell

We consider first the hysteresis loop of single CoFe-based microwires. $(Co_{100-x}Fe_x)$-based amorphous microwires with composition $3<x<6$ exhibit negative but vanishing magnetostriction. Their axial hysteresis loop is nearly non-hysteretic as observed in *Fig. 3.4*, characterized by a circular anisotropy field, H_k, for a glass-coated CoFe-based microwire with a 17μm of nucleus diameter, and three different total diameters D_{tot}.

The nearly reversible magnetization process is interpreted considering a circular magnetoelastric easy axis. Under axial field, magnetization rotates towards the axis. From the reduction of the axial susceptibility with increasing Pyrex thickness, we deduce an increase of the circular anisotropy (H_k*=-6.07, -4.64, -1.60 Oe,* for D_{tot}*= 42, 34, 20μm*, respectively). This is interpreted to be a consequence of the increasing internal stresses induced by the Pyrex coupled with the negative sign of magnetostriction. It was established that the strength of such internal stress increase with increasing the glass-coating thickness.

Such large internal stresses, σ, in eq. (3.2) gives rise to a drastic change of the magnetoelastic energy, K_{me}, even for small changes of the glass-coating thickness at fixed metallic core diameter.

Additionally, such change of the geometric ratio, ρ, (where $\boldsymbol{\rho} = \mathbf{D_{tot}}$ (total diameter) /***d*** (nucleus diameter)) should be related to the change of the magnetostriction constant with applied stress [11]:

$$\lambda_s = (\mu_0 M_s/3)\,(dH_k/d\sigma) \qquad (3.1)$$

Where μ_0 is free space permeability and M_s is saturation magnetization.

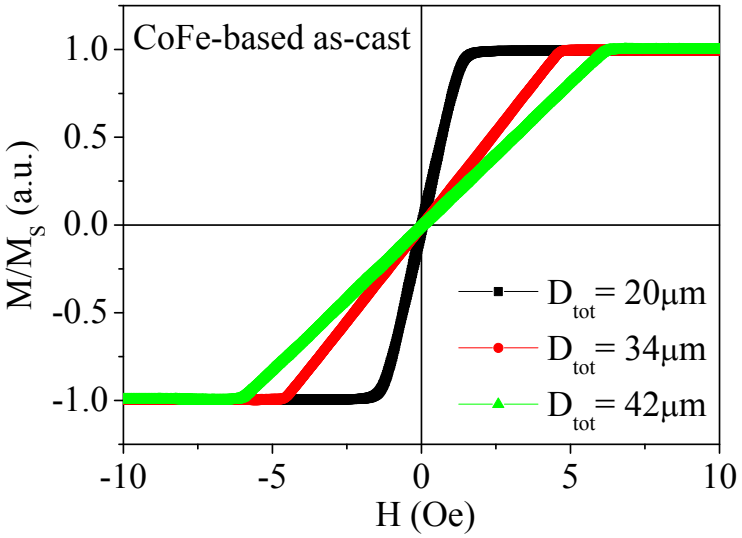

Figure 3.4 Normalized low-field hysteresis loops of CoFe-based glass-coated microwires with a 17μm nucleus diameter as a function of the total diameter D_{tot}.

As have been previously reported, outer layers, magnetic or not, induce mechanical stress onto the inner magnetic nucleus giving rise to intrinsic magnetoelastic anisotropy [12].

A strong dependence of the hysteresis loops on these parameters can be related with magnetoelastic energy.The magnetoelastic energy density is given by:

$$K_{me}=3/2\lambda_s\sigma_i \qquad (3.2)$$

Where λ_s is the magnetostriction constant and σ_i are the internal stresses originated by the different thermal expansion coefficients of metallic nucleus and glass-coating, depending strongly on the thickness of glass-coating and metallic core diameter [10]. In addition, thermal stresses are frozen during the rapid quenching fabrication as well as by the drawing process.

Fig. 3.5 shows the high-field hysteresis loop of a CoFe/ CoNi biphase microwire for a given thickness for each magnetic layer (17μm thick CoFe-based core, and a 2μm CoNi thick outer shell). *Fig.3.5 (a)* shows the hysteresis loop of single phase glass-coated microwires with a soft core is characterized by a non-hysteretic loop, with circular anisotropy field H_k = -6.07Oe, according to the vanishing magnetostriction. On the other hand, *fig.3.5 (b)* shows the hysteresis loop of hard magnetic external shell CoNi microtube with a high coercive field (the coercive field increase by increasing CoNi thicknesses). The presence of the two magnetic phases appears clearly defined by

the two large Barkhausen jumps at low (soft CoFe-based core) and high (CoNi outer shell) fields as depicted in *Fig.3.5 (c)*.

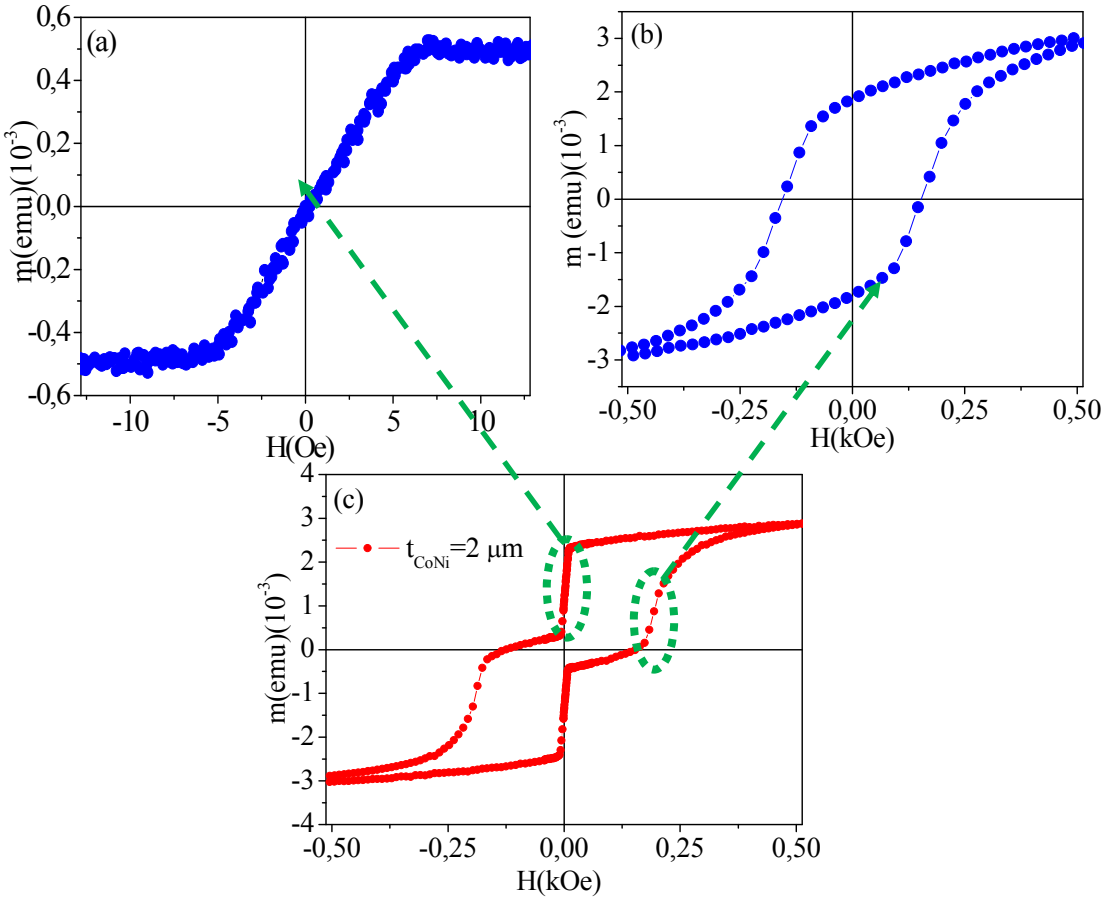

Figure 3.5 High-field hysteresis loop of a CoFe/CoNi composite microwire with a 2µm thick CoNi layer. Hysteresis loop for amorphous core (a), CoNi microtube external shell (b), and biphase microwires CoFe/CoNi (c).

Moreover, Jacob Torrejon et al., [7, 13] have investigated the magnetic behavior of biphase microwires with hard external shell. Thus, it has been observed that the hard external shell, CoNi, has an influence on the magnetic properties (i.e. coercive field, remanence, and magnetic moment) by increasing the thickness of CoNi.

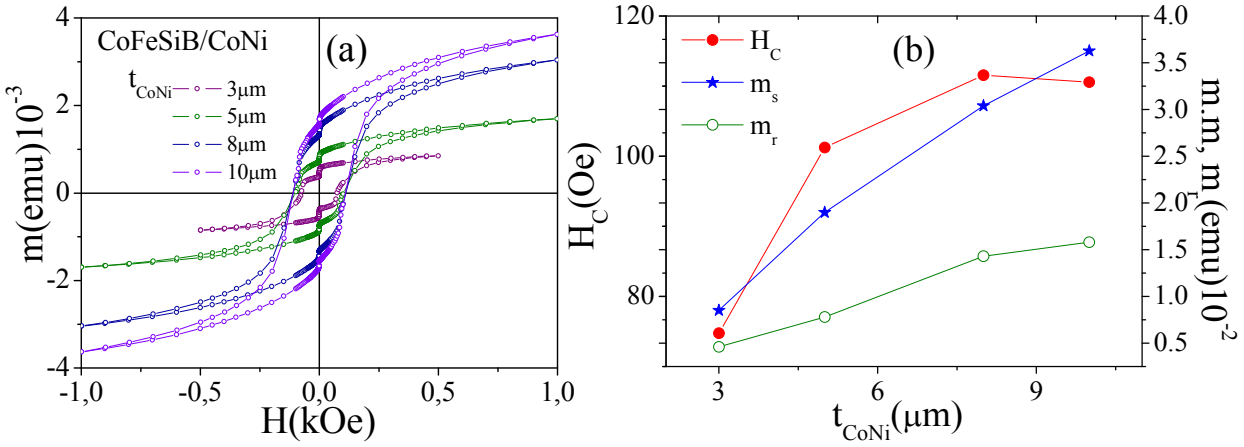

Figure 3.6 (a) Hysteresis loops of biphase CoFe/CoNi microwires measured at high field with differents CoNi thicknesses, t_{CoNi}=3, 5, 8 and 10μm. (b) The dependence of H_c, m.m, and m_r as function of CoNi thickness.

We have studied the influence of the external shell thickness on biphase wires with a nucleus of nominal composition $(Co_{0.94}Fe_{0.06})_{72.5}Si_{12.5}B_{15}$, with metallic diameter, d=8μm and total diameter, D_{tot}=24 μm. An external shell magnetic microtube was electroplated onto the Au layer with different thicknesses t_{CoNi}=3, 5, 8 and 10μm.

The hysteresis loops measured at high field for biphase microwires CoFe/CoNi with different thickness of CoNi with length *l=4 mm* are depicted in *fig. 3.6 (a)*. As can be observed, up to 5μm of CoNi thickness, two Barkhausen jumps are clearly observed corresponding to the different phases. The jump presented at low field corresponds to the amorphous core CoFe-based, the other one presented at high field is ascribed to the hard external shell, CoNi. However, for thickness higher than 5μm, the jump observed at low field becomes smaller, and almost the reversal magnetization process of the hard external shell is only observed. This is determined by the magnetoelastic coupling induced during electrodeposition process of the magnetic hard shell, CoNi, and to the reduced fractional volume of the nucleus for large thickness of the shell.

Fig. 3.6 (b) shows that H_c, m. m and m_r (the coercive field, H_c, magnetic moment, m. m, and remanence, m_r,) increase with the thickness of CoNi

The influence of the intermediate insulating glass Pyrex thicknesses, t_g on the glass-coated microwires was firstly studied by our colleague *Jacob Torrejón* in similar systems [3]. A clear dependence of the switching field was observed on the thickness of the intermediate insulating glass Pyrex.

In the case of single phase microwire without external shell, as depicted in *Fig. 3.4*, an increase in the anisotropy field was observed with increasing the thickness of glass Pyrex. This is due to the circular internal stresses induced by the Pyrex during the process of ultrafast solidification [14].

Here, we have investigated the influence of the Pyrex thickness for a biphase microwire with CoFeNiSiBMo core and FeNi external shell.

Figure 3.7 shows the hysteresis loops for CoFe/FeNi soft/soft biphase microwires with fixed thickness of core and outer magnetic phase and three particular thicknesses of the insulating Pyrex layer. The following particularities are to be noticed: (i) a large Barkausen jump is observed at similar applied fields, which should be ascribed to the soft FeNi outer layer; (ii) a second magnetization process with nearly constant magnetic susceptibility for each Pyrex coat thickness is observed that should be ascribed to the CoFe-based core as deduced from a comparison with the loops in *Fig. 3.4*.

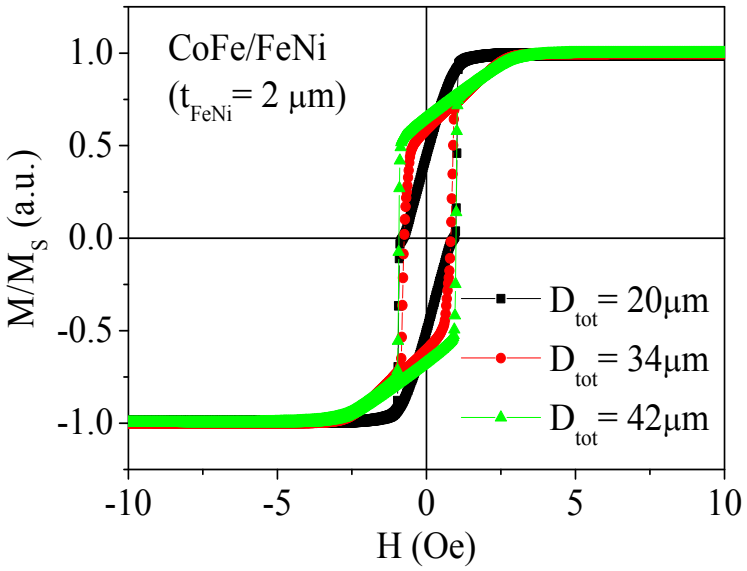

Figure 3.7 Low-field hysteresis loops of CoFe/FeNi composite microwires with a 2μm FeNi thickness, as function of different total diameter, D_{tot}. Total diameter of the glass-coated microwire precursor as a parameter.

We have also investigated the influence of the thickness of FeNi soft external shell. *Fig. 3.8* shows the hysteresis loops for CoFe/FeNi biphase microwires with different thickness of soft external shell. The following characterizations are observed:

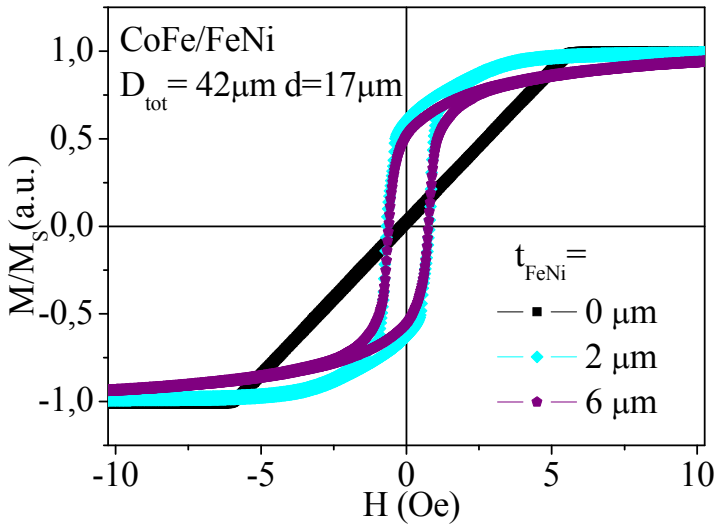

Figure 3.8 Hysteresis loops of biphase CoFe/FeNi microwire as function of thickness FeNi, t_{FeNi}. D_{tot}= 42µm, d=17µm.

i) A large Barkhausen jump which corresponds to the external shell FeNi;

ii) A second magnetization process at higher field that corresponds to the soft CoFeNiSiBMo magnetic core.

Furthermore, for large enough Py thickness between 2 and 6µm the second magnetization is reduced because of the reduced fractional volume of the nucleus. As consequence, with increasing the thickness, t_{FeNi}, the magnetic signal of FeNi gains a relative weight, whereby blurs the linear region associated to the core. Finally, for high enough thickness (for example at 6 µm and above), the behavior is practically that of the coating of Permalloy. Thus, the presence of the external shell magnetic phase modifies very significantly the magnetic behavior of the microwires.

3.2.2. Fe-based single and biphase: Influence of geometry and annealing treatment

The annealing treatment of a magnetic material can be more effective when it is performed under applied mechanical stress, magnetic field, or both [22]. The thermal treatment under applied stress induced strong magnetic anisotropy [23]. On the other hand, the thermal treatment affects the magnetoelastic anisotropy which is determined by the coupling between magnetostriction and mechanical stresses [24-26]. The magnetostriction constant of CoFe-based alloys (λ_s<0, λ_s~0) also depends on temperature and is affected by structural relaxation contribution [28, 29, 6]. As well, the

temperature dependence of switching field for magnetization reversal and coercive field of amorphous microwires with (λ_s>0) has been also taken account [5, 9]. Changes in the easy axes orientation or changes in the magnetic domain structure-are also aimed after different kinds of annealing [27]. Annealing also aims to nanaocrystalline state and very soft behavior [18].

Single and biphase wires have been exhaustively investigated from many points of view at room temperature, and only few data are available regarding the influence of the thermal annealing on the low frequency magnetic response of soft/hard biphase microwires. In this section, we consider multilayer microwires with FeSiB as nucleus, and CoNi as external shell, and we have studied the influence of such thermal treatments on samples with different thickness of Pyrex.

Bistable glass-coated amorphous microwires with nominal composition $Fe_{76}Si_{11}B_{13}$ were selected as precursor system. Series of microwires were prepared with metallic core diameter in the range of d=18, 18, and 20μm, and total diameter D_{tot}= 24, 26 and 26μm, respectively.

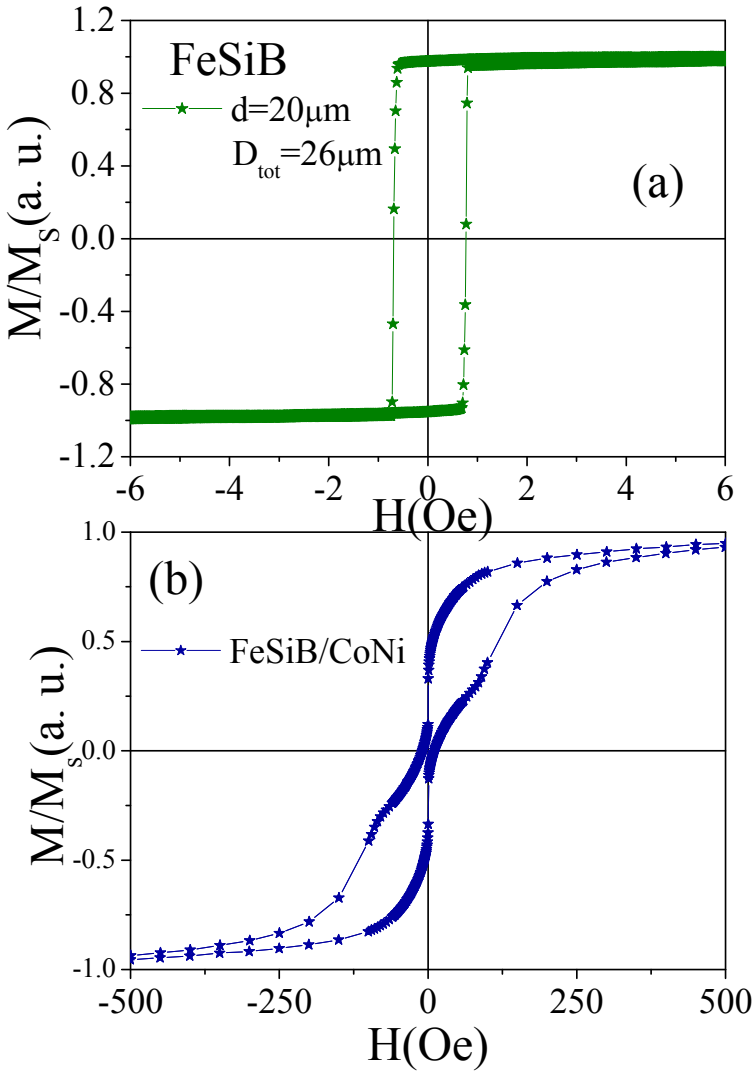

Figure 3.9 Normalized high-field hysteresis loops of as-produced single and biphase FeSiB/CoNi microwire with d=20 µm, D_{tot}=26 µm and t_{CoNi}=3µm.

Figure 3.9 shows the hysteresis loop measured at room temperature of Fe-based single phase wire (Fig.3.9 (a)) and Fe/CoNi bimagnetic microwire with 3µm of CoNi thickness (*Fig.3.9 (b)*). *Fig.3.9 (a)* shows the typical hysteresis loop of single phase FeSiB with a typical square shape, where a large Barkhausen jump is observed at low field, while at higher field the magnetization rotates until it reaches the saturation. *Fig.3.9 (b)* shows the loop for a biphase wire where we observe the large Barkhausen jump at low field from the FeSiB core and the second jump at higher field from the harder CoNi shell.

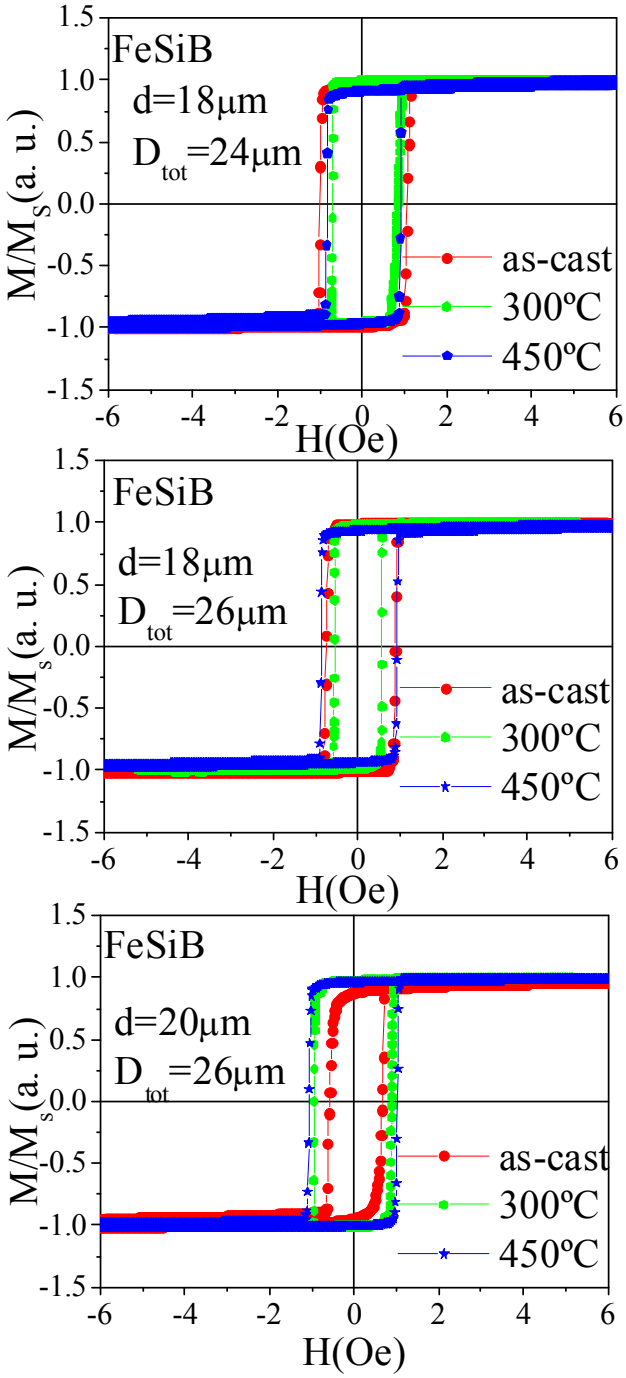

Figure 3.10 Normalized low-field hysteresis loops for single phase FeSiB microwires with different diameter and total diameter, measured before and after annealing treatment at moderate temperature.

It is well known that the Fe-based microwires with high magnetostriction constant show the magnetic bistability in the as-cast state due to the stress induced during the fabrication. On the other hand, annealing treatments at temperature lower

than the crystallization temperature gives arise the structural relaxation of the amorphous materials that results in the loss of magnetic bistability [16].

The objective of this section has been to study the effects of annealing treatments on the magnetic behavior of the single and biphase microwires Fe/CoNi before and after annealing treatments below and above the crystallization temperature. Pieces of 3cm in length were annealed in argon atmosphere for 1h at various temperatures from 100ºC up to 700ºC.

Thermal treatment results in drastic changes of the hysteresis loops. We can define two ranges of annealing temperature, below and above the crystallization temperature, around T_{cry}=500ºC, for the amorphous FeSiB core.

Fig. 3.10 shows low field hysteresis loops measured at room temperature by means of fluxmetric induction technique for single-phase microwires with different diameter (d=18, 18, 20 μm) and total diameter (D_{tot}=24, 24, 26μm), respectively, and after annealing treatments (below crystallization temperature) up to 450ºC . As observed, the hysteresis loops retain the magnetic bistability over the whole range of annealing treatments and only relatively small variations in the coercivity are observed. At moderate annealing temperature the amorphous structure is kept and the mechanical stresses are expected to relax, giving rise to a slight reduction of coercivity that keeps a value of the order of 1Oe.

Annealing at above crystallization temperature, the loops show different behavior with much increased coercivity not suitable for measurements using fluxmetric induction technique. In this regard, all the samples annealed at above crystallization temperature were measured using VSM magnetometer.

Fig. 3.11 displays the hysteresis loops measured at room T of single and biphase microwires as a function of annealing temperature, in the range from 500ºC to 700ºC for different diameter (d=18, 18, 20 μm) and total diameter (D_{tot}=24, 24, 26μm). We observed a drastic increase of coercivity of two orders of magnitude up to reach around 100Oe. That increase of magnetic hardness is typically observed in amorphous samples after crystallization.

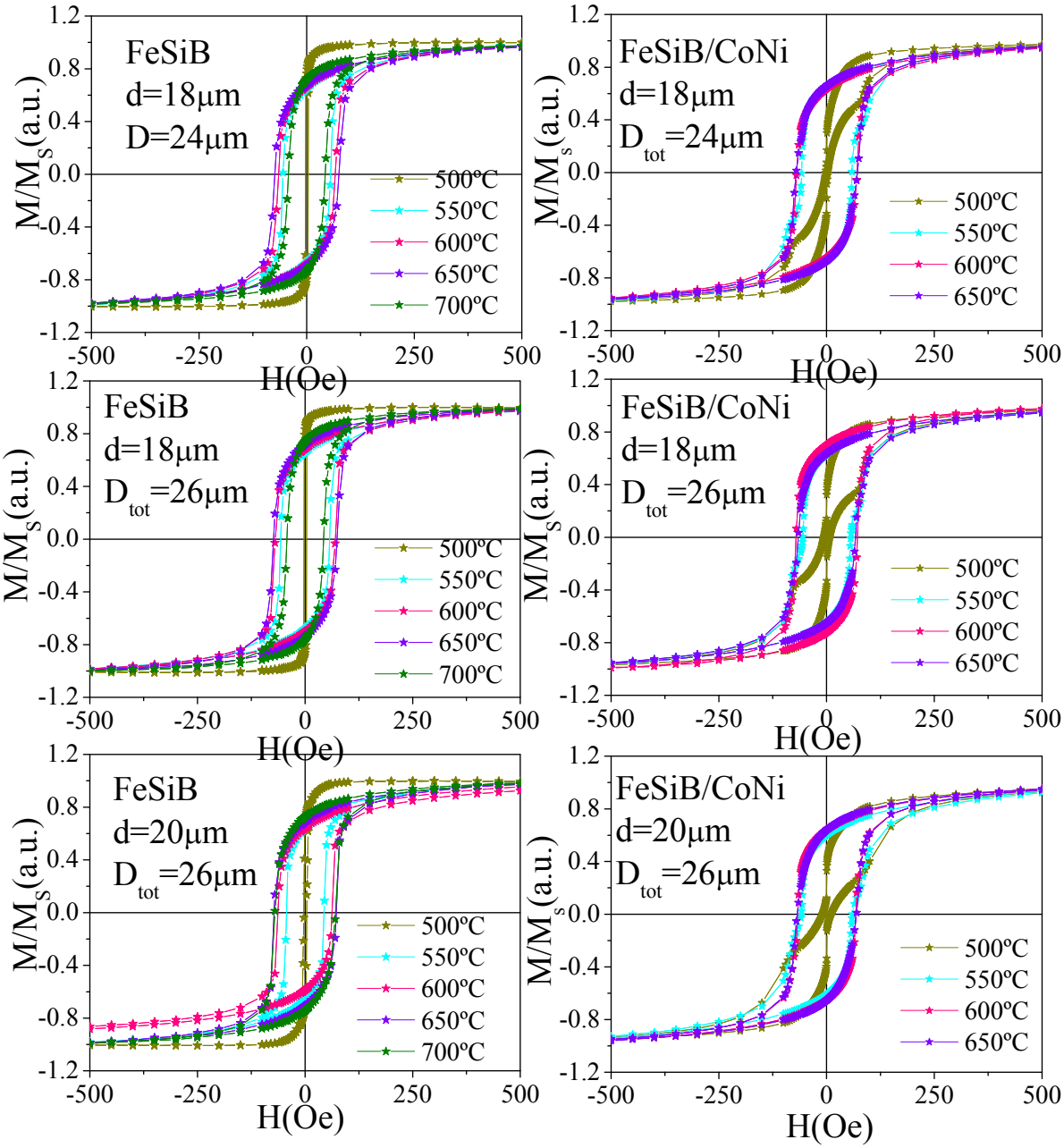

Figure 3.11 Normalized high-field hysteresis loops for FeSiB glass-coated and FeSiB/CoNi amorphous microwires with different diameter and total diameter D_{tot}, and above the crystallization temperature.

In addition, after annealing above 500ºC the magnetic bistability is lost. In both, single and biphase wires the hardening of the core is a consequence of the crystallization process by which new magnetic phases grow (particularly Fe_2B) [17].

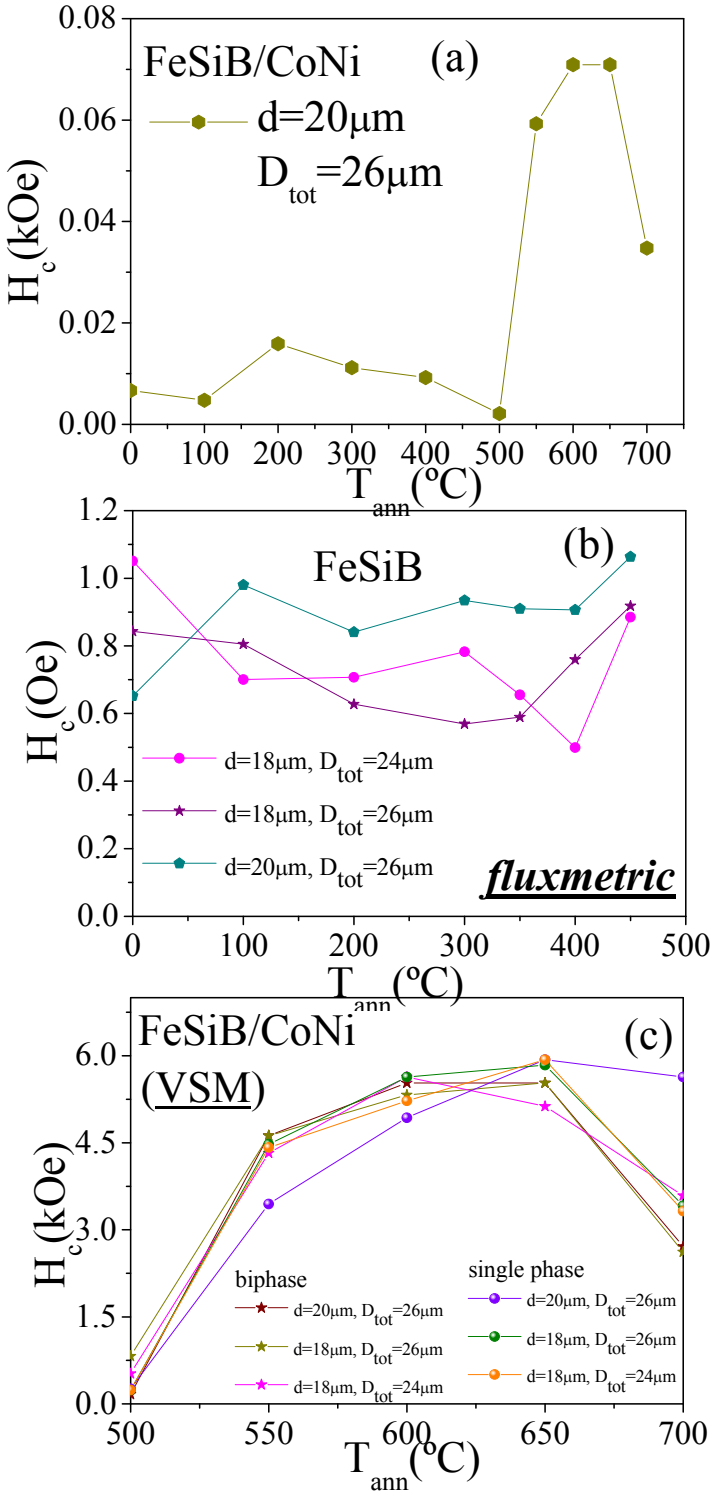

Figure 3.12 Evolution of coercive field, H_c, with annealing temperature for below and above crystallization temperature for biphase microwires with d=20μm and D_{tot}=26μm (a), below crystallization temperature for single phase (b), and (c) above crystallization temperature for biphase microwires with different diameter and total diameter.

A similar behavior has been observed in the case of FeSiB/CoNi biphase microwires. The two Barkhausen jumps are still observed at the T=500ºC. After

annealing above 500ºC, a quite noticeable magnetic hardening is also observed, and magnetization reversal takes place.

Fig. 3.12 summarizes the evolution of the coercivity as a function of annealing temperature measured at room temperature for single and biphase microwires with different diameter and total diameter.

Fig. 3.12(a) shows a magnetic softening slightly reduced coercivity in biphasse wires with $d=20\mu m$ *and* $D_{tot}=26\mu m$ treated in the range 400ºC-500ºC, which can be related to a first crystallization process has been developed, leading to fine nanocrysatlline α-Fe(Si), such as it has been widely reported in Finement ribbons [21]. A sudden increase of the coercivity is then shown at temperature above 600ºC indicating the precipitation of ion Borides.

Fig. 3.12(b) summarizes the effect of annealing temperature (below crystallization temperature) for FeSiB wire, where only a small annealing effect is presented for the three samples.

Fig. 3.12(c) summarizes the quantitative effect of annealing temperature (above crystallization temperature) for single and biphase microwires showing in both cases the large increase coercivity. We should underline that the coercivity takes similar values for both single and biphase microwires denoting that it is the crystallized core which determines the macroscopic coercivity.

We can summarized the effect of thermal treatment confirming that the annealing treatments below crystallization T induce very modest influence on the low frequency properties of both single and biphase microwires. This is ascribed to the relaxation of the amorphous structure of the core which nevertheless undergoes the action of Pyrex coating and external shell. In addition, the square shape of hysteresis loops between 100ºC 450ºC denoting the existence of single domain structure and the magnetization reversal by a single Barkhausen jump. In turn, when annealing at temperature above crystallization temperature at around 500ºC the effect of annealing treatment is to deteriorate the magnetization process giving a rise to the disappearance of bistability of the core and its significant magnetic hardening.

3.3. Temperature dependent magnetic behavior and its analysis

The influence of thermal treatments as a function of annealing is investigated in the previous section. Regarding the measuring the temperature measurements, there are only few works devoted to the thermal effects in the microwires properties [19-21], whereas this information is important to understand the mechanisms of the magnetization properties, their evolution and the interaction between biphase components.

Single and biphase microwires have been exhaustively investigated from many points of view at room T. Particularly; significant magnetostatic and magnetoelastic interactions have been systematically investigated in biphase microwires, only few data are available regarding their temperature behavior. Reported high temperature studies were mainly focused towards thermal treatments to achieve specific field induced magnetic softness [30, 31] and more recently to Hopkinson effect just below Curie temperature [32].

3.3.1. High temperature dependence

In this section, we study the high temperature (i.e., up to 925ºC) behavior of single and biphase microwires. In a previous report [33], the temperature behavior of a specific soft/hard biphase microwire was considered. Here we consider the cases where the internal core is a soft amorphous phase (i.e., Fe-based and Co-based microwires with respectively different anisotropies) and the external shell is a polycrystalline alloy with very soft (i.e., Permalloy) or relatively hard (i.e., CoNi alloy) behavior. That is, we consider the cases of soft/hard as well as soft/soft biphase wires. However, we are not addressing an exhaustive study to properly determine the high temperature behavior but to establishing some of the main magnetic features where contributions from each phase change with temperature. The effects of increasing temperature are considered as magnetic phase transitions and structural changes resulting in modified magnetic moment and magnetization mechanism.

For these experiments, two precursor glass-coated microwires with nominal compositions were selected namely, $Co_{68.15}Fe_{4.35}Si_{12.5}B_{15}$ with small negative magnetostriction ($\lambda s \approx -1x10^{-6}$) and $Fe_{77.5}Si_{7.5}B_{15}$ with positive high magnetostriction ($\lambda s \approx +3x10^{-5}$). The metallic diameter of these microwires were d = 8μm and d = 12μm, and the total diameter D_{tot} = 24μm and D_{tot} = 40-38μm, for Co and Fe-based wires,

respectively. Then, an external magnetic microtube was electroplated onto the Au layer. Two alloy compositions were considered for the external shell: i) $Co_{90}Ni_{10}$ with relatively hard magnetic character, and ii) Permalloy, $Fe_{20}Ni_{80}$, with well known soft magnetic character.

a. Room temperature behaviour

The magnetic behavior was firstly determined at room temperature for single and biphase systems. Figure 3.13 (left) collects the loops for CoFe single phase (in green), CoFe/FeNi soft/soft biphase (in blue) and CoFe/CoNi soft/hard biphase (in red) systems. Insets (a) and (b) show the low-field loops for CoFe and CoFe/FeNi microwires, respectively. Note that for the CoFe microwire, a nearly non-hysteretic behavior with well defined circular anisotropy field of around 6 Oe is observed, typical of negative-magnetostriction microwires. In the case of CoFe/FeNi the loop shows an irreversible low-field region with coercivity of 1.42Oe corresponding to the FeNi shell superposed to the reversible region at slightly higher field which is ascribed to the CoFe core. In the high-field loop of CoFe/CoNi microwire, we can observe a low-field high susceptibility corresponding to the CoFe core. At higher field, an irreversible loop is observed with maximum differential susceptibility at around 52Oe, which is correlates to the value of the coercivity of the hard CoNi shell. Note that irreversible region of the biphase loop closes at around 500 Oe applied field (not shown in the figure).

Note finally that for the CoFe/CoNi biphase system, the coercivity of the biphase loop corresponds roughly to that of the individual CoNi external shell. In turn, for the Fe/CoNi biphase system, the coercivity of the biphase loop is determined by that of the individual Fe core. In fact, that is purely a consequence of the relative values of the fractional volume and magnetization of each phase.

Figure 3.13 (right) depicts the hysteresis loops for Fe single phase (in green), Fe/FeNi soft/soft biphase (in blue) and Fe/CoNi soft/hard biphase (in red) systems. Insets (a) and (b) show the low field loops for Fe and Fe/FeNi microwires, respectively. Inset (a) for the Fe microwire shows a bistable magnetic behavior typical of positive magnetostrictive microwire, with a switching field of 0.72Oe. Inset (b) for the Fe/FeNi soft/soft biphase wire shows the contributions of the two soft phases. The first large Barkausen jump at 0.73 Oe ascribed to the FeNi shell, the switching field of the

amorphous core is now 4.7 Oe. Note that the presence of the FeNi external phase introduces significant magnetoelastic anisotropy which modifies the magnetic response of the Fe soft core [14]. The high-field loop of the Fe/CoNi microwire shows the low-field high susceptibility, corresponding to the Fe core, and the higher field maximum differential susceptibility, at around 77Oe, ascribed to the coercivity of the hard CoNi shell.

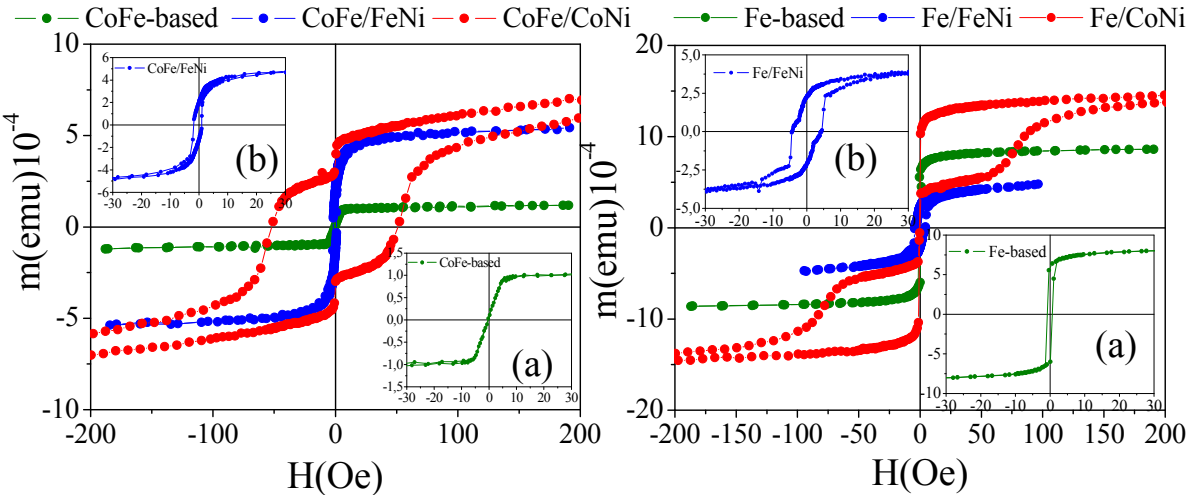

Figure 3.13 (Left)-Room-temperature hysteresis loops of CoFeSiB (green) single and biphase microwires with different external shell (CoFeSiB/FeNi, blue, and CoFeSiB/FeNi, red). Insets show the low-field loops ofCoFeSiB(a) and CoFeSiB/FeNi (b) microwires. (Right)-Room-temperature hysteresis loops of Fe (green) single and biphase microwires with different external shell (CoFeSiB/FeNi, blue, and CoFeSiB/FeNi, red). Insets show the low-field loops ofFeSiB(a) and FeSiB/FeNi (b) microwires.

b. Temperature dependence of hysteresis loops

Figure 3.14 presents dependence of hysteresis loops on the measuring temperature for selected biphase microwires (Fe/CoNi-FeNi and CoFe/CoNi-FeNi) with a fixed outer shell thickness of $t_{CoNi/FeNi}$ =1μm.

Fig. 3.14 (a, and c) shows the hysteresis loops for CoFe-Fe/CoNi. From 25 to 325ºC the loops show two Barkhausen jumps, BJ, corresponding to the magnetization process of both phases. The first jump, observed at very low field is ascribed to the magnetization reversal of the soft core, while the second one presented at high fields, between 50 and 200Oe, and denotes the reversal of magnetization of the CoNi shell. In addition, the amplitude of the first BJ of the loop decrease and the coercive field decreases by increasing the measuring temperature, T (see also Fig. 3.15(a)).

Above 325ºC the loops lose the bistability and the two Barkhausen jumps disappear, which is in principle ascribed to crystallization and re-crystallization of the amorphous and polycrystalline phases, respectively, as will be later discussed. In the range of measuring T from 625ºC up to 925ºC the loops show irreversible changes of magnetic properties due to additional structure transformations.

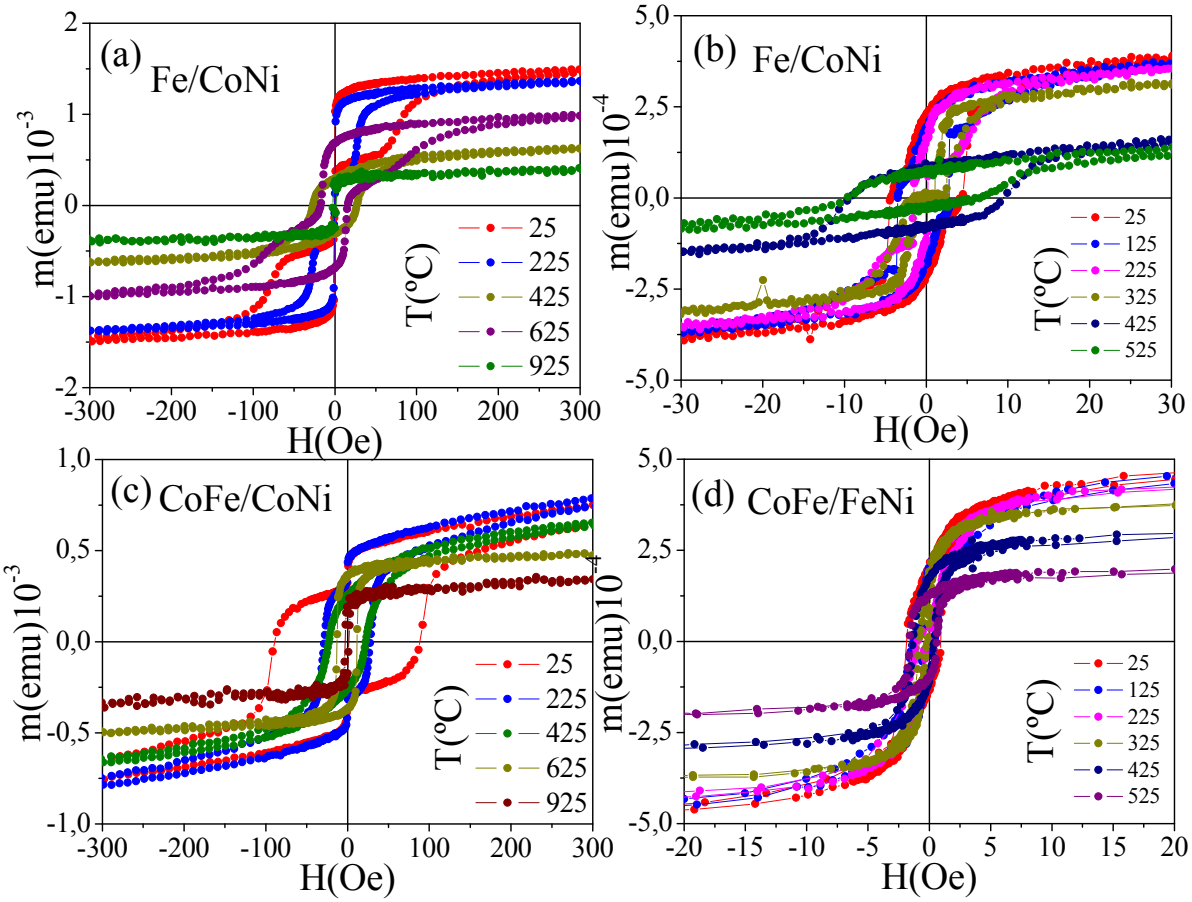

Figure 3.14 Hysteresis loops of biphase microwire CoFe/CoNi (1µm) measured in the range (25-925ºC).

A similar study has been performed in CoFe-Fe/FeNi with soft external shell. In the case of CoFe/FeNi (fig.3.14(d)) the loop shows an irreversible low field region with coercivity of 1.42Oe corresponding to the FeNi shell superposed to the reversible region at slightly higher field which is ascribed to the CoFe core as discussed above at room T (see fig. 3.13 (left inset(a)). As can be observed (Fig. 3.14 (d), the amplitude of the B.J. decreases by increasing the temperature in the range from 25 to 325ºC. Between 325ºC and 525ºC, the biphase microwires lose the bistabilty when reaching the Curie temperature of the CoFe core. Above 525ºC, only noises signal is recorded.

For the Fe/FeNi soft/soft biphase wire, the contributions of the two soft phases are depicted in Fig. 3.14(b). The first jump at very low field is ascribed to the FeNi shell, and the second large jump corresponds to Fe-based core as shown in Fig.3.13 (right (inset (b)). In the range from 25 to 375-425ºC, only small variations in each magnetic phase are detected. Indeed, the large jump, which corresponds to Fe-based core, decrease by increasing the temperature in this range.

Note that, as expected, in that temperature range coercivity is larger for the magnetostrictive Fe-rich amorphous core than for the less-magnetostrictive CoFe-rich one as clearly shown in figure 3.15 (b).

c. Temperature dependence of the magnetic moment

The temperature measurements of the magnetic moment of the samples were first performed. That will allow us to follow the structural and magnetic phase transformations which can be sensitively detected by the thermomagnetic analysis. These data are needed for the subsequent interpretation of the evolution of coercivity with temperature. Also, Curie, T_C, and crystallization temperature, T_X, are compared with previously reported data for amorphous ribbons.

The temperature dependence of magnetic moment is shown in Figures 3.15(a) and 3.15(b) for the different CoFe-based and Fe-based single and biphase systems, respectively. Figure 3.15(a) depicts the results for CoFeSiB single phase microwire for which the curie temperature takes the value of $T_{c,CoFe} \approx 377$ºC. In the literature, for CoFeSiB amorphous alloy ribbons of similar compositions, we find $T_{c,CoFe} \approx 388$ºC [34], ≈ 413ºC [35], ≈ 418ºC [36], ≈ 308ºC [37]. As the measuring temperature further increases, the magnetic moment remains with a very small value (about 0.1×10^{-4}emu). Although we expect the crystallization into Co-rich phases at crystallization temperature of $T_{x,CoFe} \approx 567$ºC [37], the applied field is likely not large enough to receive a significant magnetic response. In the case of CoFe/FeNi biphase wire, apart from T_c of the CoFe amorphous phase, we can identify the magnetic phase transition of the FeNi shell, at $T_{c,FeNi} \approx 601$ºC that agrees well with data reported in the literature [38]. Finally, for the CoFe/CoNi biphase system, the reduction of the magnetic signal at the Curie point of the CoFe amorphous phase is now less pronounced owing to its small fractional magnetic weight. The Curie point, 1075ºC [39], of the crystalline CoNi external shell is not reached at the highest measuring temperature.

From the results in Figure 3.15(b) for Fe microwire, we estimate $T_{c,Fe} \approx 425$ºC in agreement with the literature $T_{c,Fe} \approx 433$ºC [40, 35].

The increase of the measured magnetic moment at and above $T_{x,Fe} \approx 525$ºC is ascribed to the first crystallization to a relatively soft α-Fe(Si) phase at $T_{x,Fe} \approx 533$ºC [35]. That crystalline phase reaches the Curie point at $T_{c,Fe\text{-}crys} \approx 701$ºC, in agreement with the literature[41]. In the case of Fe/FeNi biphase microwire, we detect the magnetic phase transitions at $T_{c,Fe} \approx 427$ºC, and $T_{c,FeNi} \approx 601$ºC of the amorphous core and the crystalline FeNi shell, respectively. Also, we estimate the crystallization temperature of the amorphous core at around $T_{x,Fe} \approx 525$ºC, as well as its Curie point at around $T_{c,Fe\text{-}crys} \approx 645$ºC. Finally, for the Fe/CoNi biphase microwire we identify $T_{c,Fe} \approx 427$ºC, and $T_{c,Fe\text{-}cryst} \approx 675$ºC.

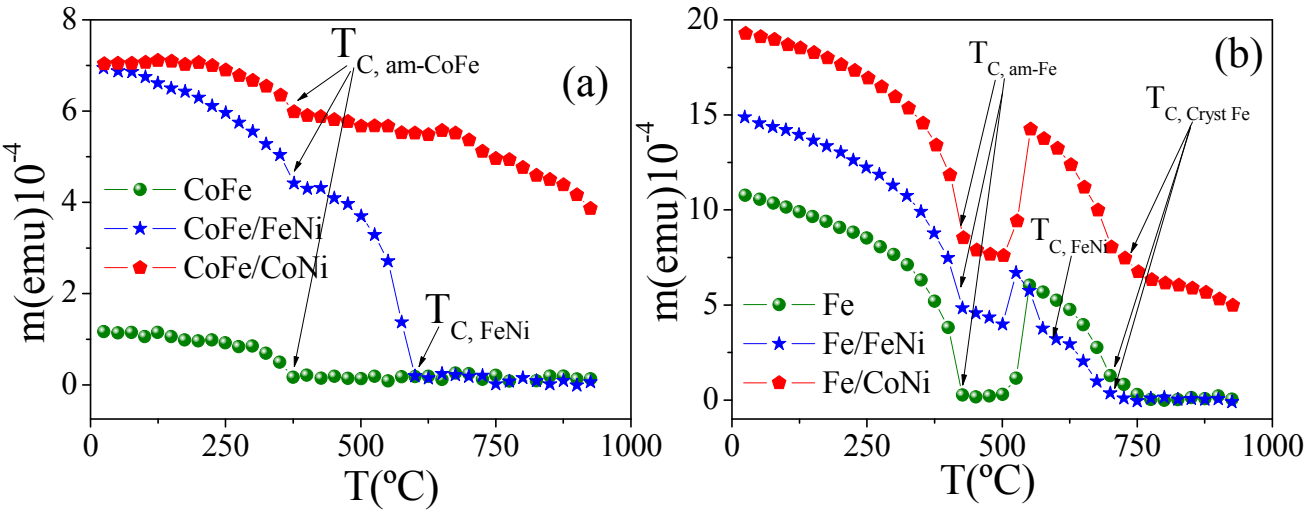

Figure 3.15 Temperature dependence of magnetic moment for single, CoFeSiB, and biphase,CoFeSiB/FeNi-CoNi (a) microwires, as well as for single, Fe, and biphase FeSiB/FeNi-CoNimicrowires (b). Arrows indicate the Curie temperature, T_c, of the different phases.

Note that very similar values of Curie and crystallization temperatures are experimentally measured for individual magnetic phases in the different single and biphase microwires. Only a small difference is found in the case of crystallized Fe core. That difference, as well as the differences obtained in comparison with data in the literature for amorphous alloy ribbons, should be ascribed to small differences in the heating rate when measuring. The apparent anomalous small increase of magnetic moment with temperature found for CoFe/CoNi up to 175ºC should be a consequence

of the magnetic softening consequence of relaxation of mechanical stresses during the heating.

d. Temperature dependence of Coercivity

The coercivity of individual magnetic phases of biphase systems has been analyzed as a function of the temperature. It has been evaluated from the corresponding hysteresis loops. In principle, the hysteresis loop of biphase system presents two steps reversal process typical of two phase magnetic materials composed a soft phase (inner core) with coercivity, H_{C1}, and hard/soft phase (outer shell) with coercivity, H_{C2}.

Fig.3. 16 (a, and b) present the temperature dependence of coercivity of soft/hard and soft/soft biphase microwires, respectively. As can observed both figures characterized by three values of coercivity as a function of temperature labeled (H_{C1}, H_{C2} and H_{C3} (the coercive field value when the loop lose the two B. J. at a specific temperature)). For H_{C1} and H_{C2}, are observed in the temperature range of 25- 325ºC, while, H_{C3} is observed in the temperature range 350-950ºC.

In the soft/hard biphase systems (i.e., containing CoNi external shell), we can identify the evolution of the coercive field for the soft (CoFe and Fe) amorphous core and the harder shell phases in the temperature range from 25ºC up to around 325ºC. In that temperature range, similarly to those observed in Fig. 3.13 at room temperature two large Barkhausen jumps can be identified for each biphase system, although becoming smaller in amplitude as temperature increases as shown in Fig.3.14(a and c). Coercivity of the CoNi shell decreases significantly in both cases from around 80-90 Oe at room temperature down to around 12 Oe. Note their ultrasoft magnetic character with coercivities in the range 0.05 to 0.5 Oe. Changes observed with temperature should be connected with the structural modifications.

At more elevated temperatures, at and above 425ºC, only a single broad Barkhausen jump can be identified, and the corresponding coercivity, H_{C3}, increases up to maximum values of 30-40 Oe at around 525ºC followed by a continuous decrease until the maximum measuring temperature. The interpretation of this behavior is not straightforward. We have to consider that within the range 375 to 425ºC, the Curie temperature of both amorphous cores is reached so that, above that temperature only crystallized phases contribute to hysteretic irreversibilities. We could assume that the evolution of coercivity for the CoNi shell should continue the trend observed at low temperatures. In that case, we could ascribe the observed maxima at 525ºC to the

coercivity of crystallized cores of amorphous precursors. That is reasonable in the case of the Fe/CoNi biphase system where coercivity is ascribed to that of α-Fe (Si) crystallites. In the case of the CoFe/CoNi biphase system, the interpretation is difficult since any expected crystallized Co-rich phase core was not magnetically detected in the first experiment in Fig. 3.13(a).The final decrease at temperatures above 725ºC should be ascribed to the CoNi shell.

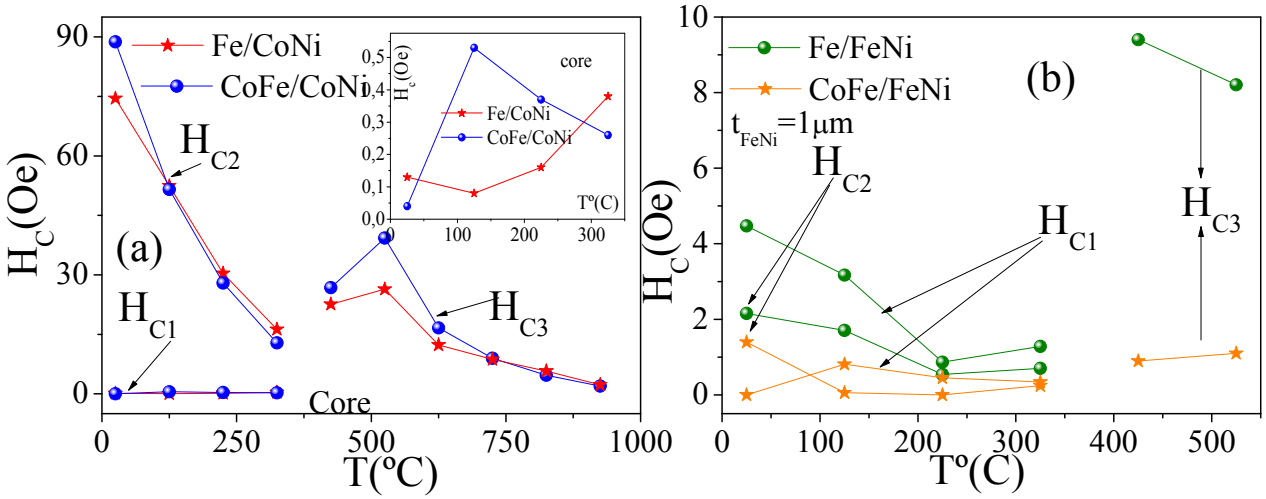

Figure 3.16 Temperature dependence of coercivity of individual phases of soft/hard (a), and soft/soft (b) biphase microwires.

The results for the coercive field of soft/soft biphase microwires are collected in Fig.3.16 (b) where arrows indicate the coercivity for the corresponding core/shell phases. Only small variations are observed in each magnetic phase in the temperature range up to 375-425ºC. Note that, as expected in that temperature range coercivity is larger for the magnetostrictive Fe-rich amorphous core than for the less-magnetostrictive CoFe-rich one. In the case of the FeNi shell, coercivity decreases with increasing temperature in both samples. In addition, it takes larger value in the Fe/NiFe than in CoFe/NiFe biphase wire. That can arise from differences in the magnetic interactions core/shell, from the different radius of the NiFe shell, or even from small differences in magnetostriction in the NiFe shell [42].

At 525ºC and above, few experimental data are obtained where only a single irreversible process with coercivity H_{C3} can be identified. The interpretation of coercivity becomes nevertheless a bit doubtful. Based on the evolution of the hysteresis loops with temperature (see Fig. 3.14), we ascribe H_{C3} of the Fe/NiFe wire to the

crystallized Fe core. The NiFe shell is in this temperature range close to approach its Curie point. In the case of CoFe/NiFe wire, small values of H_{C3} should be likely come to crystallites from CoFe core. Finally, above 575ºC, no apparent irreversibility is detected in the small received signal.

A similar temperature dependence of magnetic behavior has been investigated at low temperature in the range from -175 to 25ºC. In the next section, we present the low temperature magnetic behavior of same selected single microwires Fe and CoFe as presented in section 3.3.1, and biphase microwires with soft/soft system (CoFe/FeNi).

3.3.2. Low temperature dependence

Most of the high temperature studies reported until now are actually focused towards the influence of thermal treatments to achieve nanocrystalline structure with optimal magnetic softness [43, 44] or to field-induced specific magnetic anisotropies. Only few reports have been published about the low-temperature studies some time ago of view [45, 46]. Particularly, there is no previous report on the low-temperature behavior of biphase microwires.

In this section we introduce a phenomenological study on the temperature dependence of magnetic characteristics of single and biphase microwires and a comparative analysis of the magnetization reversal.

The low frequency magnetic characterization under applied field (up to ± 10 kOe) parallel to the axis of microwires was performed in a Vibrating Sample Magnetometer, Tandore E7, VSM, in the temperature range from -173 to 27ºC. In this case, 3 mm long pieces of microwires were taken for measurements.

a. Room temperature behavior

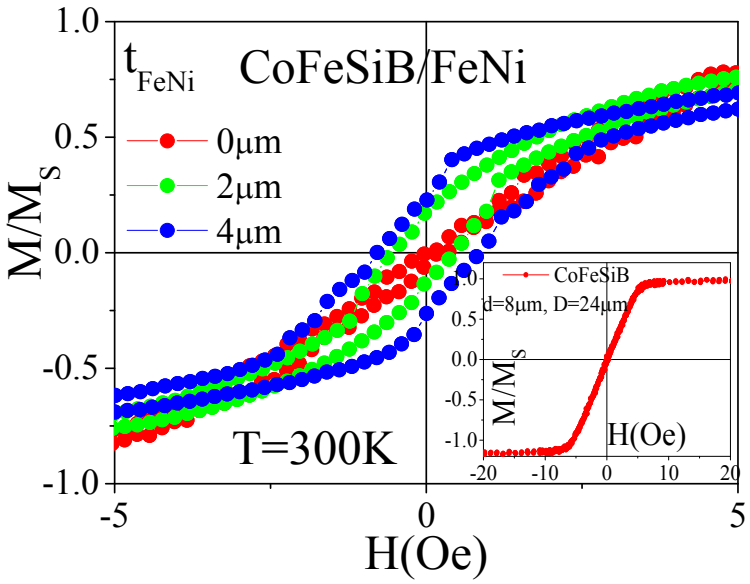

Figure 3.17 Low frequency hysteresis loops of single and biphase (2 and 4 μm FeNi thickness) taken at room T. Inset shows the enlarged loop for the single phase wire.

Figure 3.17 shows the longitudinal hysteresis loops of single and biphase microwires measured at room temperature. The hysteresis loop for the single phase CoFeSiB microwire (inset in Fig.3.17) is typical of glass-coated amorphous microwires with circular magnetic anisotropy characterized by an almost constant susceptibility up to nearly reaching the transverse (circular) anisotropy field at (H_K = 6.2 Oe in this case) , and very reduced hysteresis (0.2 Oe coercivity). The origin for this circular anisotropy has been assumed to be magnetoelastic so that, its anisotropy field can be expressed as:

$$H_K = \frac{3\sigma\lambda_s}{4\pi M_S} \tag{3.4}$$

Here, since H_K takes a negative (circular) value, the net stress, σ, induced during fabrication is derived to be positive (tensile) owing to the negative character of magnetostriction, (λs of about – $3x10^{-7}$).

For biphase microwires, the hysteresis loops show the contribution of each phase. Now, we observe a non-constant susceptibility, and the Barkhausen jumps, ascribed to the FeNi external microtube, superposed to the continuous magnetization increase coming from the amorphous core. Note, that the biphase microwires saturate magnetically under magnetic field of few kOe (not shown here).

b. Low temperature behavior of CoFe-based and CoFe/FeNi microwires

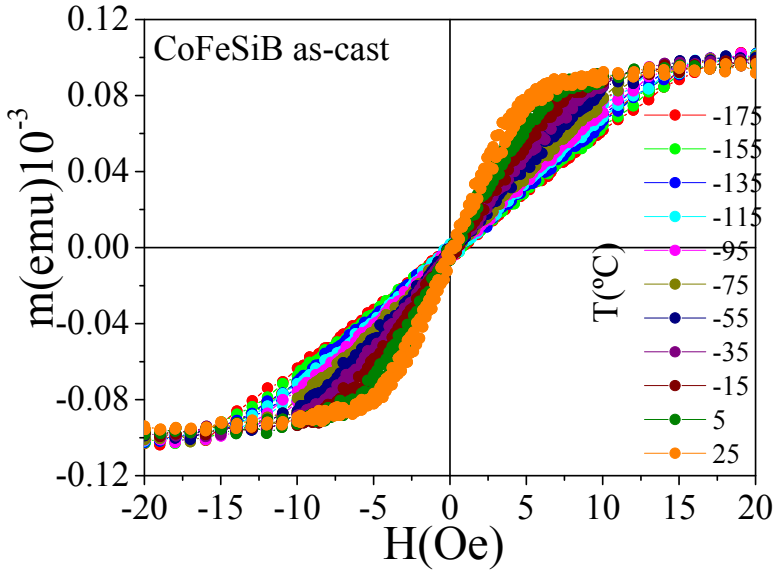

Figure 3.18 Hysteresis loops of microwires at indicated selected measuring temperatures for single phase of CoFeSiB microwires

Fig.3.18 displays the temperature dependence of the hysteresis loops for selected single phase microwires of CoFe-based. As in the case of data at room temperature, the precursor glass-coated microwires shows typical nearly non-hysteretic loops with an effective transverse anisotropy field, considered as the applied field required to reach the near saturation state extrapolated from initial susceptibility [47]. The magnetization process under longitudinal applied field taken place mainly by rotation of the magnetic moments from the easy circumferential direction towards the longitudinal directions.

Figure 3.19 shows the dependence of the circular anisotropy field, H_K, field and saturation magnetization, $4\pi M_s$, (taken as the magnetization value under 2 kOe applied field) for the single phase CoFeSiB microwire.

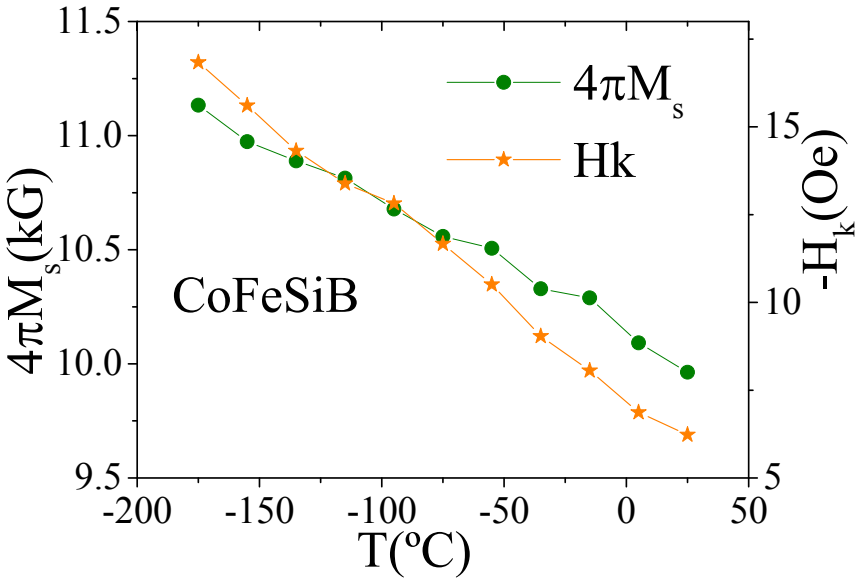

Figure 3.19 Dependence of saturation magnetization, 4πMs, and circular anisotropy field, H_K as function of temperature for single phase CoFe-based mirowires.

As observed, the circular anisotropy (i.e., anisotropy field, H_K) increases notably as measuring temperature decreases, while its remanence nearly vanishes in the whole temperature range (not shown here).

A quantitative analysis of the temperature dependence of H_k is complex since $\boldsymbol{\lambda}_s$ and M_s depend on temperature as well as σ due to the different thermal expansion coefficients of the metal core and Pyrex cover.

A similar study has been performed for biphase microwires CoFe/FeNi with two different thicknesses of FeNi (2 and 4μm). The temperature dependence of hysteresis loops at selected temperatures is presented in *Fig.3 20 (a)* and *3.20 (b)*.

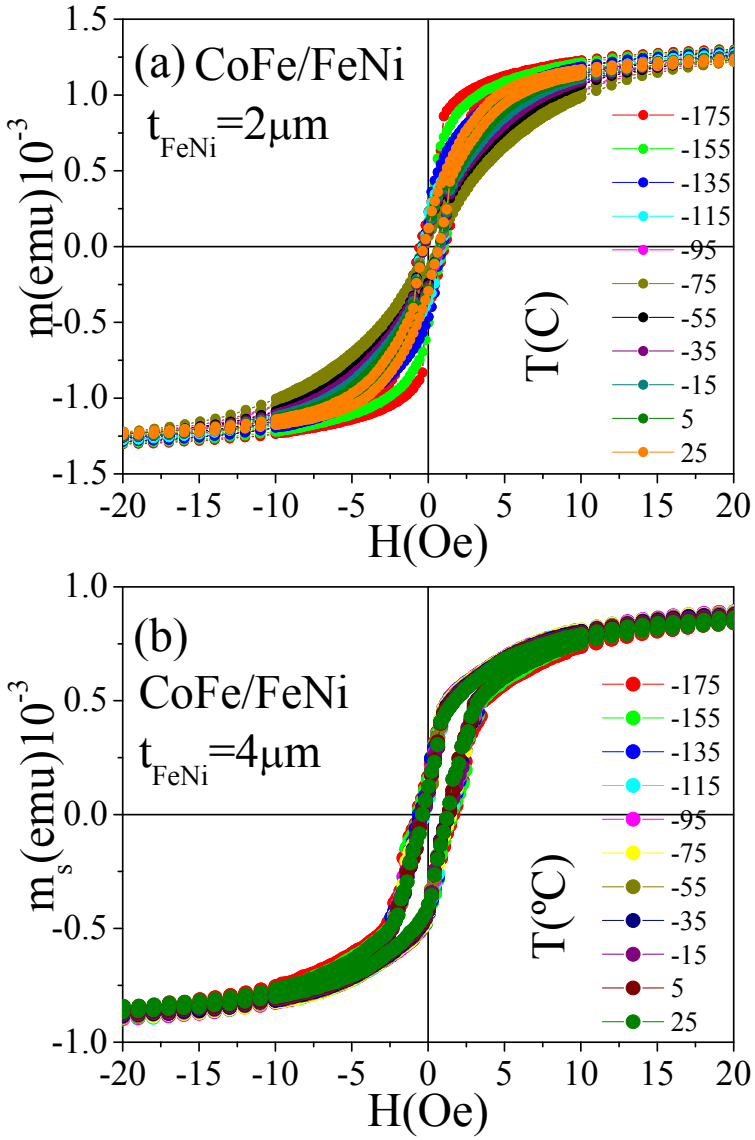

Figure 3.20 Hysteresis loops of microwires at selected measuring temperatures for biphase, microwires with two different thicknesses (a) 2μm and (b) 4μm of FeNi thick.

As mentioned in previous section (3.2.1) the soft external shell FeNi has an influence on the inner core by increasing the thickness of FeNi (Permalloy). Furthermore, for the larger Py thickness, the fractional magnetization of the core becomes smaller, while the magnetic signal of FeNi gains a relative weight. As a consequence, the behavior is practically that of the coating Permalloy.The hysteresis of the loops of biphase wires should be ascribed to that of Permalloy shell.

Nevertheless, at low temperature the loops exhibit a significant Barkhausen Jump in the whole temperature range. Due to the negative value of magnetostrictive, induced longitudinal anisotropies by the electroplated FeNi layer arise from the equivalent compressive stresses [49]. After electroplating, the reduction of temperature

also induces an additional axial anisotropy, but the switching field in this case shows relatively similar values as depicted in *Fig.3.20*. Therefore, the temperature behavior after electroplating process (biphase microwires) seems to be lower than insulating coating (single phase microwires).

From these loops, *Fig. 3.21* collects the temperature dependence of coercivity for biphase microwires with different thickness of FeNi (0, 2, and 4μm). As can be observed, the coercive field increases by increasing the thickness of FeNi. Additionally, it increases moderately by reducing the temperature for all samples single and biphase microwires. It seems reasonable to assume that the increase of the coercivity can be ascribed to magnetic softness of FeNi Permalloy.

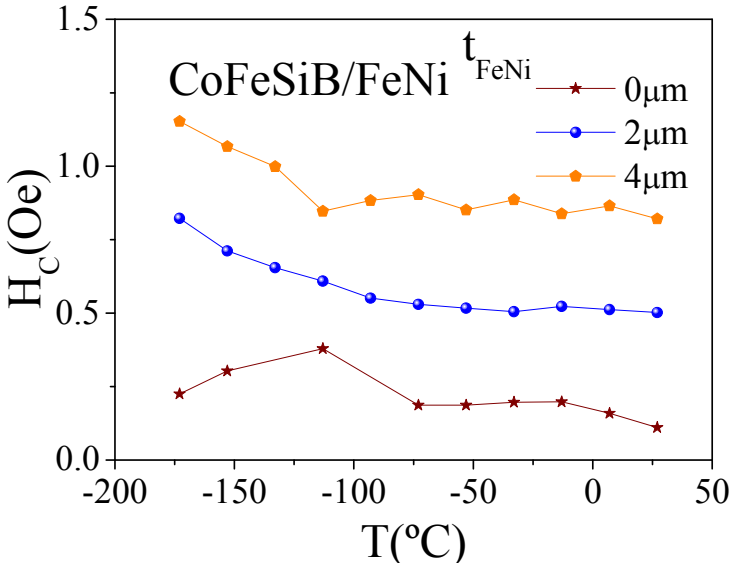

Figure 3.21 Temperature dependence of coercivity for single and biphase mirowires CoFe/FeNi for different thickness, 0, 2, and 4μm.

c. Low temperature dependence of Fe-based and Fe/CoNi

Fig. 3.22 shows a hysteresis loops measured in the temperature range from -175ºC to 25ºC for FeSiB glass coated microwire with positive magnetostriction. As observed, the magnetization process takes place by a single quite large Barkhausen jump in the whole range of temperatures. This is expected due to its high magnetostriction and strong stresses of fabrication.

On the other hand, an additional influence of induced mechanical stresses when decreasing the temperature should be expected due to the different thermal expansion coefficients of metallic nucleus and insulating coating. A general expression for the stresses arising from the coating and induced by a temperature change, ΔT, is:

$$\sigma(T) = E(\alpha_g - \alpha_m)\Delta T + \sigma_r \quad (3.5)$$

Where σ_r denotes the internal stresses induced during fabrication. An estimation of the effective thermally induced tensile stresses when decreasing temperature down to around 10K is of the order of 200–300 MPa [50, 51].

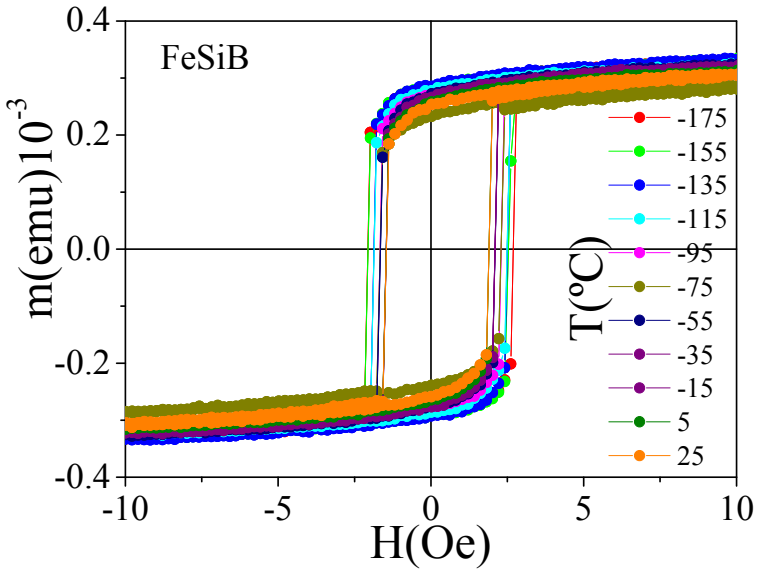

Figure 3.22 Hysteresis loops of microwires at selected measuring temperatures for single phase of FeSiB microwires

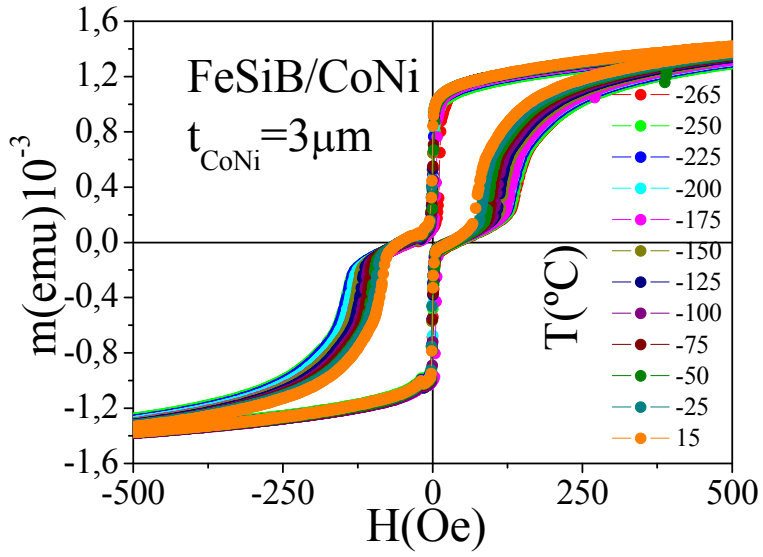

Figure 3.23 Hysteresis loops of microwires at selected measuring temperatures for biphase Fe/CoNi microwires

Such additional internal stresses should induce changes in the hysteresis loops at low temperature. Particularly, the increase of the coercivity with decreasing the temperature as observed inset *Fig.3.24* can be attributed to this contribution.

In the case of biphase microwires Fe/CoNi two Barkhausen jump are observed. *Fig. 2.23* shows the hysteresis loop for FeSiB/CoNi biphase microwires (with t_{CoNi} =3μm). The low field Barkhausen Jump is observed at around *0.017Oe* at room T and it is ascribed to the soft core. The high field Barkhausen Jump corresponds to the harder CoNi shell.

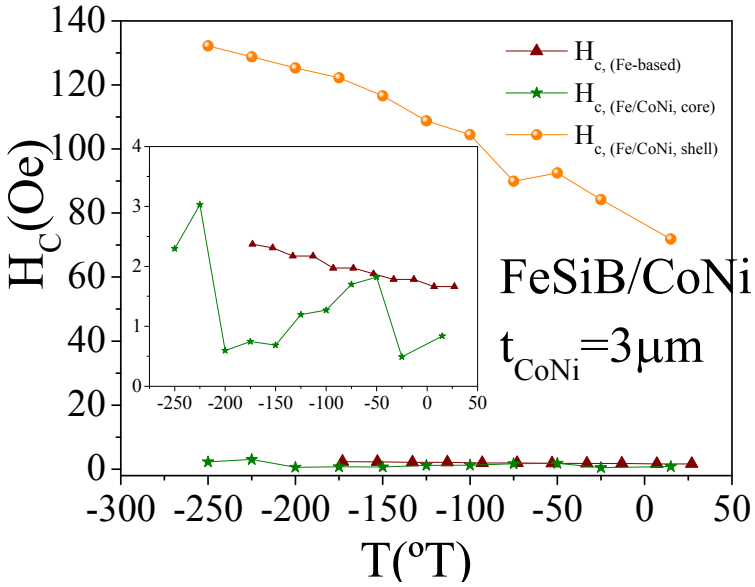

Figure 3.24 Temperature dependence of coercivity for single and biphase Fe/CoNi microwires.

Fig.3.24 shows the evolution of coercivity with temperature for FeSiB single phase microwire as well as the field of two Barkhausen jumps of the FeSiB/CoNi biphase microwire.

3.4. Influence of electroplated FeNi on magnetic behavior of glass-coated microwires

As discussed in the chapter 4, relatively small variations in the composition of FeNi alloy gives rise to significant variation of the magnetic properties. To investigate the influence of electroplated FeNi on magnetic properties for glass-coated microwires, we prepared a several samples with a nominal composition CoFeSiB with 8μm of metallic diameter and 24μm of total diameter. Then, we electroplated FeNi (Permalloy) over glass-coated microwires with a constant thickness (t_{FeNi}=1μm of thick) using different current density. The aim was to intentionally modify the FeNi alloy composition. In this regards, we characterized the composition of the electroplated FeNi

alloy by using of Energy Dispersive X-ray spectroscopy (EDX), to obtain for each sample the percentage of Fe and Ni.

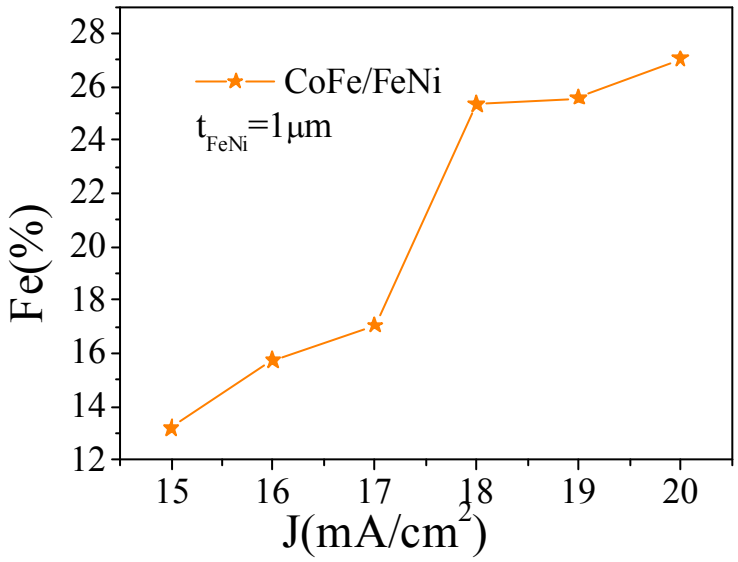

Figure 3.25 Dependence of the percentage of iron in the FeNi layer on the current density used during electroplating of the magnetic microwires.

Figure 3.25 depicts the dependence of the percentage of Fe in the FeNi external layer as function of the current density. As can be observed, different current density modifies the composition and consequently its magnetostriction constant. We should emphasize that percentage of Fe can be controlled with the current density.

Fe content is confirmed to increase with the current density. However, its precise value is very hard to maintain. One of the possible variables which might affect the composition is the speed of stirring, and additionally, the order of the sample electroplated: as we electroplate one sample after another the composition of the bath can change, and Fe or Ni might result higher than the nominal composition of the bath.

Very recently, a similar study have been reported by M. Butta et al. [52], in FeNi thin film electroplated over a cupper core ring with different current density. It has been found that the magnetostriction is shifts from negative to positive values as the % Fe increased (see Fig. 3.26).

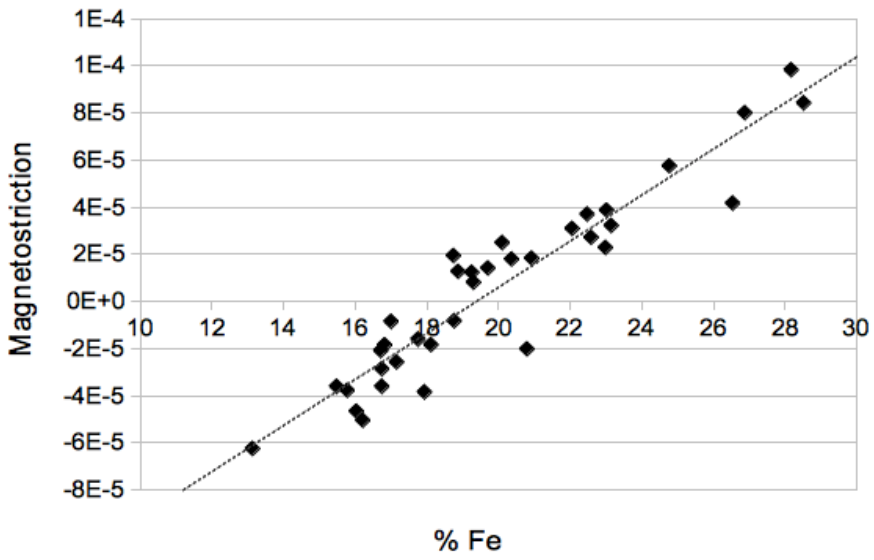

Figure 3.26 Dependence of magnetostriction of the percentage of iron in the magnetic film (nickel is complimentary to 100%). The ideal zero-magnetostrictionis achieved for $Fe_{19}Ni_{81}$ composition [50].

Its known that the ideal zero magnetostriction corresponds to $Fe_{19}Ni_{81}$ obtained for current density values (17.5 and 20 mA/cm^2) in the case of ring core with FeNi electroplated film as shown in *Fig. 3.26*, while in the case of microwires the same mutual composition of FeNi should be found approximately between 17 and 17.5 mA/cm^2 of current density as presented in *Fig. 3.25*.

We should also note that the change in composition, and accordingly in magnetostriction affects the magnetic behavior. Fig. 3.27 shows the hysteresis loops as function of different current density for biphase microwires CoFe/FeNi.

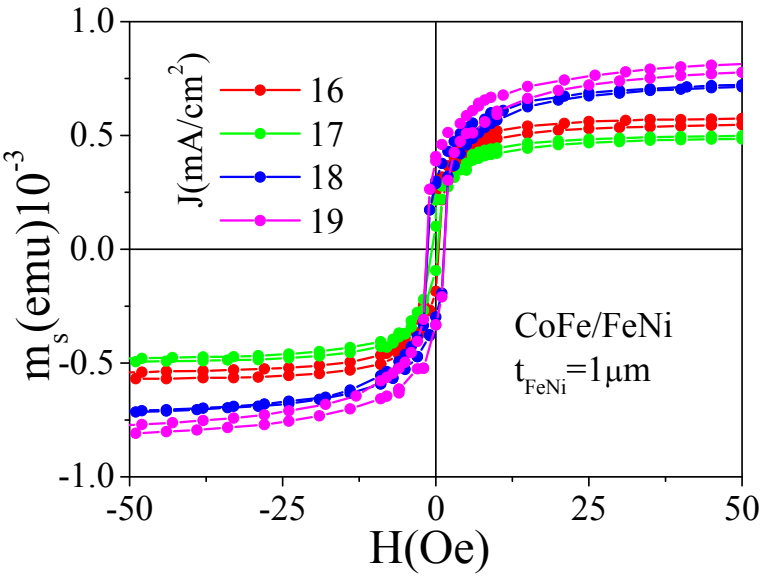

Figure .3.27 High field hysteresis loops as function of different current density for biphase microwires CoFe/FeNi.

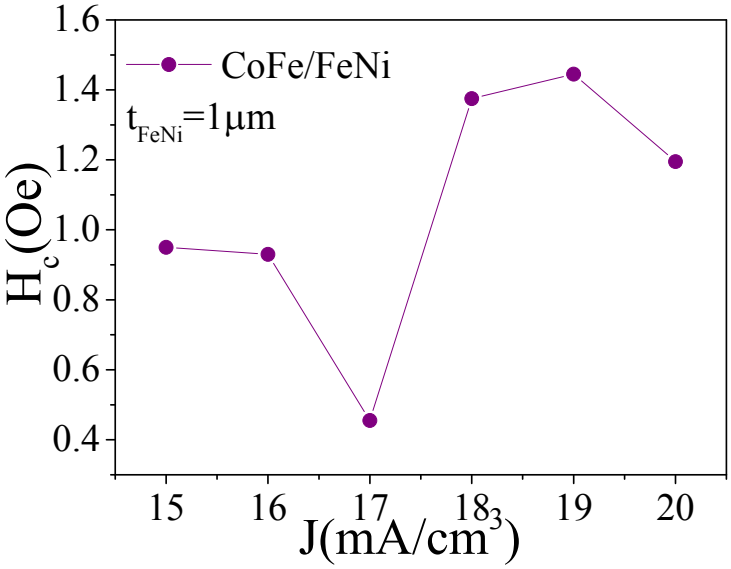

Figure 3.28 dependence of coercive field on the current density for biphase microwires CoFe/FeNi.

As can be concluded, the current density is responsible for the composition of the electroplated FeNi alloy and therefore of the magnetostriction and the magnetic properties. The standard deviation of the composition indeed sometime differs of few units of percent when we consider the amount of Fe and Ni. In order to obtain an ideal $Fe_{19}Ni_{81}$ we should electroplate several samples and select the best one. Finally, the electroplating process should be further improved in order to fully control the

composition of the FeNi alloy (Permalloy).

3.5. Conclusion

The conclusion of this chapter, the magnetic behavior of different families of microwires we can summarize the following:

- In the first section we found that, the role of increasing the Pyrex thickness is reflected in the modification of the circular magnetoelastic anisotropy of the soft core for single phase microwires. In this regard the anisotropy field increases by increasing the Pyrex thickness. For both biphase investigated systems (CoFe/CoNi and CoFe/FeNi); a similar effect of the Pyrex thickness is observed.
- In the second section, the annealing effect on single and biphase microwires has been studied. Thermal treatment below the crystallization temperature (from 100ºC up to 500ºC) induces modest magnetic softening on the low frequency properties of both families of microwires. This is ascribed to the relaxation of the amorphous structure of the core which nevertheless undergoes the action of Pyrex coating and external shell. Annealing at higher temperatures (above crystallization temperature, from 500ºC up to 700ºC) deteriorates the magnetization process in two magnetic stages, and we observe a general hardening of the microwires.
- In the third section, the high measuring temperature dependence of the magnetic properties of selected ferromagnetic biphase microwires has been presented in the temperature range from 300 to 1200K. Analysis of temperature dependence of the coercive field of each phase has been performed. The identification of Curie temperature of different phases has been performed. On the other hand, the evolution of the coercive field of individual phases, obtained from an analysis of the whole hysteresis loops is discussed in view of the magnetic and structural phase transitions.

3.6. References

[1] M.Vazquez, M.Knobel, M.L.Sanchez, R.Valenzuela and A.Zhukov. Sensors and Actuators A 59, (1997) 20.

[2] K. Pirota, M. Hernandez-Velez, D. Navas, A. Zhukov and M. Vazquez, Adv. Funct.Mater.14 (2004) 266.

[3] J. Torrejón, "Estudio del acoplamiento magnetoelástico y magnetoestático en microsistemas multicapas bifásicos". Tesis Doctoral, Universidad Autónoma de Madrid (2008).

[4] G. Infante, "Propiedades magnéticas y de transporte de nuevos microhilos mono y bifásicos". Tesis Doctoral, Universidad Autónoma de Madrid (2010)

[5] R.A.Alben, J.I.Budnick and G.B.Cargill (III). In: J.J.Gilman and H.J.Leamyeds. Metallic glasses. American Society of Metals, Metals Park, Ohio, (1978), 394.

[6] J. Olivera, R. Varga, P. Vojtanik, V. M. Prida, M. L. Sanchez, B. Hernando, A. Zhukov. J. Magn. Magn. Mater 320 (2008) 2534.

[7] J Torrejon, G. Badini, K. Pirota, and M. Vazquez. Acta materials 55 (2007) 4271.

[8] J. Escrig, S. Allende, D. Altbir, M. Bahiana, J Torrejon, G. Badini, and M. Vazquez. J. ppl. Phys. 105 (2009) 023907.

[9] J. Olivera, R. Varga, V. M. Prida, M. L. Sanchez, B. Hernando, A. Zhukov. Phys. Rev. B 82 (2010) 094414.

[10] J. Velazquez, M. Vazquez, A. Zhukov, J. Mater, Rev. 11 (1996) 2499.

[11] J. Gonzalez, K. Kulakowski, P. Aragoneses, J. M. Blanco, E. Irurieta, J. Mater. Sci. 30 (1995) 5173.

[12] G. A. Badini-Confalonieria, G. Infantea, J. Torrejo´na, and M. Vazquez, J. Magn. Magn. Mater. 320, 2443 (2008).

[13] J. Torrejón, L. Kraus, K. Pirota, G. Badini and M. Vázquez; J. Appl. Phys. 101 (2007) 09N105.

[14] G. Infante, G. A. Badini- Confalonieri, R. P. del Real, M. Vázquez, J. Phys D: Appl. Phys. 43 (2010) 345002.

[15] F. E. Atalay, and S. Atalay, J. Alloys Compd. 392 (2005) 322-328

[16]P. Marin, J. Arcas, A. Zhukov, M. Vazquez, and A. Hernando, in: G.C. Hadjipanayis _Ed.., Magnetic Hysteresis in Novel Magnetic Materials, Kluwer Academic Publishers, Netherlands, (1997) 743.

[17] M. Vazquez, "Magnetism and Advenced Magnetic Materials," in Handbook of Magnetism and Advenced Magnetic Materials, H. Kronmuller and S. Parkin, Eds. Hoboken, NJ: Wiley, 2007, vol. 4, ch. XX, p. 2193.

[18] J. Arcas, C. Gomez-Polo, A. Zhukov, M. Vazquez, V. Larin, and A. Hernando, nanostruct. Mater. 7 (1996) 823.

[19] A. A. Rakhmanov, N. Perov, P. Sheverdyaeva, A. Granovsky, and A. S. Antonov, *Sens. Actuators A*, vol. 106, pp. 240–242, 2003.

[20] M. Vázquez, A. P. Zhukov, K. L. Garcia, and K. R. Pirota, *Mater. Sci. Eng. A*, vol. 375–377, pp. 1145–1148, 2004.

[21] J. Torrejon, G. Badini-Confalonieri, and M. Vazquez, *J. Appl. Phys.*, vol. 103, p. 07E712, 2008.

[22] J. Torrejo, G. Badini, K. Pirota, and M. Vazquez, J. Magn. Magn. Mater., vol. 316, pp. E 575–e 578, 2007.

[23] Kikuchi, M., H Fujimori, Y. Obi and T. Masumoto. Jap. J. Appl. Phys. **14**: 1077 (1975).

[24] Luborsky, F.E. and H.H. Liebermann. Mater. Sci. Eng. 49: 257 (1981)

[25] Luborsky, F.E., S.C. Huang and H.C. Fiedler. IEEE Trans. Magn. Mag-17: 3463 (1981).

[26] González, J. J. Appl. Phys. **79**: 376 (1996).

[27] J. Gonzalez, E. Iruriea, P. Aragineses, J. M. Blanco, I. Ibarrondo, M. Vazquez, J.

M. Gonzalez, and F. Cebollada, IEEE Trans. Magn. 30, 1015 (1994).

[28] Hernando, A., M. Vázquez, V. Madurga and H Kronmüller. J. Magn. Magn. Mat. 37 (1983)

[29] Barandiarán, J.M., A. Hernando, V. Madurga, O.V. Nielsen, M. Vázquez and M. Vázquez-López. Phys. Rev. B 35: 5066 (1987).

[30] H. Chiriac, T.A. Ovari, Gh. Pop and F. Barariu, J. Appl. Phys. 81 (1997) 1.

[31] A. Talaat, M. Ipatov, V. Zhukova, J.M. Blanco, M. Churyukanova, S. Kaloshkin and A. Zhukov, Phys. Status Solidi C 11 (2014) 1120.

[32] V. Zhukova, M. Ipatov, A. Talaat, and A. Zhukov, Phys. Status Solidi C, 11, 1130 (2014).

[33] V. Rodionova, A. Nikoshin, J. Torrejon, G.A. Badini-Conflanieri, N.Perov and M. Vazquez. IEEE Trans. Magn. 47 (2011) 3787.

[34] V. Madurga, M. Vazquez, A. Hernando and O. Nielsen, Sol. Stat. Commun. 52 (1984) 701.

[35] E. Michel, Mc Henry, M. A. Willard and D. E. Laughlin. Progr. Mater. Science 44 (1999) 291.

[36] C. Nuñez de Villavicencio, M. Vazquez, V. Madurga and A. Hernando. J. Magn. Magn. Mater 59 (1986) 333.

[37] F. Celegato, M. Coisson, E. Olivetti, P. Tiberto and F. Vinai. Phys. Stat. Sol. (a), 205 (2008) 1745.

[38] R. M. Bozorth, in "Ferromagnetism" (Van Nostrand, London, 1968).pp. 276.

[39] P. Yu, X. F. Jin, J. Kudrnovský, D. S. Wang and P. Bruno. Phy.Rev.B 77 (2008) 4431.

[40] G. Herzer, IEEE Trans. Magn. Mag. 26 (1990) 1397.

[41] M. Vazquez and A.P. Zhukov, J. Magn. Magn. Mater. 160 (1996) 223.

[42] R. El Kammouni, M. Vázquez, L. Lezama, G. Kurlyandskaya and L. Kraus, J. Magn. Magn. Mater. 368 (2014) 126.

[43] K. Pirota,M.Hernandez-Velez,D.Navas,A.Zhukov,M.Vazquez,Adv.Funct. Mater.14 (2004)266.

[44] K. Pirota, M.Provencio, K.Garcıa, P.Mendoza, M.Hernandez-Velez, M. Vazquez, J.Magn.Magn.Mater.290 (2005)68.

[45] M. Vazquez, L.Kraus, K.Pirota, G.Badini, J.Torrejon, J.Non-Cryst.Solids353 (2007)763.

[46] M.H. Phan, H. X. Peng, M. T. Tung, N. V. Dung, N. H. Nghi, J. Magn. Magn. Mater. 316 (2007) 244.

[47] M. Vazquez, K. Pirota, J. Torrejon, G. Badini, and A. Torcunov, J. Magn. Magn., Mater. 304 (2006) 197-202.

[48] M. Vazquez, and D. X. Chen, IEEE Trans. Magn. 31 (1994) 1229.

[49] J. Lluma, M. Vazquez, J. M. Hernandez, J. M. Ruiz, J. M. Garcia- Beneytez, A. Zhukov, F. J. Castaño, X. X. Zhang, J. Tejada, J. Magn., Magn., Mater. 196-197 (1999) 821-823.
[50]
[51]
[52] M. Butta, M. Janosek, P. Ripka, L. Kraus, and R. El Kammouni, IEEE Trans., on Magn. Vol 50 Nº 11 (Nov 2014) 4006504.

Chapter 4 High frequency basic: FMR Spectra

4.1. Introduction

Ferromagnetic resonance, FMR, or, to be more precise, resonant absorption of external electromagnetic radiation in ferromagnetic substances is a phenomenon of microwave spectroscopy, which is a relatively young branch of physics. The FMR is a technique used today by various groups for the investigation of the magnetic microwires [1, 2]. From a technological point of view, the knowledge of microwave behavior of single and biphase magnetic microwires is very promising.

The study of ferromagnetic resonance, FMR, is often used for the investigation of the structural changes in amorphous alloys. The main features of FMR in amorphous microwires have been analyzed in several reports [3, 4], where it is accepted that the FMR frequency follows the Kittel equation by which it increases linearly with the square root of the effective total magnetic field. Multipeak absorption has been observed as a consequence of the presence of the external shell [5]; but the origin of the FMR spectra is in some cases not fully interpreted since the experiments were done in nonfully saturated samples.

FMR experiments in wires can be basically divided into two categories. They are either measurement under a fixed dc magnetic field varying the microwave frequency or measurements at constant frequency varying the dc magnetic field. The former are done by means of network analyzer and coaxial or microstrip microwave circuits. The latter make use of classical FMR spectrometers and waveguide microwave techniques.

For Network Analyzer (Agilent, model E8362B) measurements, the microwave characterization in this manuscript was carried out at room temperature and performed in the frequency range between 10 MHz and 20 GHz. DC magnetic field (up to 5 kOe) was applied parallel to wire axis. Pieces of microwires 5 mm in length were taken for these measurements. The electric contacts between the inner metallic core and the measuring circuit were done by a silver paint. The microwave current passing through the wire induced a circumferential AC field in the core and the surrounding external shell (FeNi or CoNi) microtube. Additional experimental details can be found elsewhere [6, 7].

Parallel measurements were performed by using cavity-perturbation technique (DC magnetic field dependence of microwave-absorption) at microwave X-band frequency of 9.5 GHz and carried out at room temperature and at low temperature range from 4 to 300 K. DC magnetic field (up to 30kOe) was parallel to the wire (with field

modulation 1Oe and 100 kHz). For these measurements, pieces of microwires 3 mm in length were taken. The samples were vertically placed into the tube between 2 small circular kapton pieces. As the electric field at the sample position in the cavity was not exactly zero, relatively strong circumferential AC field was induced by electric polarization of the wire [8].

The ferromagnetic resonance, FMR, has been investigated in the two families of multilayer microwires with soft core and two different outer layers (hard and soft): CoFe/CoNi, CoFe/FeNi, and Fe/CoNi. Under the maximum applied field, the soft phases CoFe, FeNi and Fe can be assumed to reach magnetic saturation, while the semi-hard CoNi phase is still relatively far from saturation. For each family of microwires, we first present the study of the FMR for single phase microwires without external magnetic layer (*GCM*) to be later compared with the FMR data of biphase multilayer microwires so that, we can observe the influence of the presence of hard or soft external shell.

The first issue to be addressed in this chapter has been the influence of the thickness of the insulting Pyrex layer and magnetic character of outer magnetic shell. FMR experimental results will be presented in single microwires CoFe-based with metallic radius of 17μm and three different glass insulting thicknesses (D_{tot}=20, 34, 42 μm). Then, it is followed by analyzing in detail the FMR spectrum of CoFe/CoNi (hard external shell) biphasic microwires [9]. The measurement of microwires CoFe/FeNi (two very soft and weakly coupled magnetic phases) we observed three resonant absorptions, two of them due to the FMR magnetic phases and a third one at low frequency ascribed to a capacitance effect caused by the geometrical nature of these multilayer structures.

The second issue corresponds to the effects of annealing treatment on ferromagnetic resonance of single amorphous microwires FeSiB with diameter of metallic cores of 18, 18, 20μm and total diameter of 24, 26, and 26 μm. Afterwards, we analyze the FMR spectrum of 3μm thick CoFe/CoNi (hard external shell) biphase microwires. After annealing, the observed different absorption peaks, which FMR frequency was analyzed through the Kittel equation, are correlated with the presence of the soft core and hard external shell.

The last issue has been to obtain a deeper knowledge on the microwave phenomena in single and biphase microwires through the temperature dependence of

their FMR absorptions peaks. To reach this goal, we have selected a soft/soft biphase microwire. It consists of a 8 μm diameter small magnetostriction amorphous CoFeSiB single-phase microwire, coated by micrometric Pyrex layer, and after electroplating an external shell, 2 μm or 4 μm thick, of FeNi alloys. An additional study was performed on the angular dependence, which carried out at room temperature for two different glass-coated amorphous microwires: CoFe-based and Fe-based.

The measurements of FMR at room T and temperature dependence of FMR were performed in the laboratory of spectroscopy and microscopy services from the University of the Basque Country Bilbao under the supervision of Dr. Galina Kurlyandskaya, and Dr. Luis Lezama by using a standard ER ***049X*** Electron Paramagnet Resonance (EPR) Spectrometer at 9.5 GHz at room temperature as shown in *Fig. 2.9 (chapter 2 Section 2.3.2.b)*, and the measurement of FMR in biphase microwire; electroplated by hard external shell; were carried out under the supervision of *Prof. Ludek Kraus* from Institute of Physics, Academy of Sciences of the Czech Republic in Prague by using cavity- perturbation technique with two different microwave frequencies of 9.5GHz (X-band) and 69GHz (K-band).

4.2. Ferromagnetic resonance in single and biphase microwires

4.2.1. Influence of the thickness of Pyrex in CoFe-based single and biphase microwires

Magnetic amorphous glass-coated microwires with vanishing magnetostriction ($\lambda_s \sim -10^{-7}$) of a nominal composition $Co_{67.06}Fe_{3.84}Ni_{1.44}B_{11.53}Si_{14.53}Mo_{1.66}$ have been first considered. Three samples are taken with the same metallic diameter (17 μm), but different Pyrex thickness so that the total diameter is D_{tot}=20, 34, and 42 μm. The magnetic core is subjected to strong stresses induced during the fabrication process that depend on the thickness of the Pyrex, thus influencing the resulting magnetoelastic anisotropy. The corresponding anisotropy field, H_k, can be evaluated directly from its dependence on applied stress [10]. In fact, the easy axis of that magnetoelastic anisotropy is determined by the sign of the alloy magnetostriction. Consequently, either an axial or a circular magnetic domain configuration will result for positive and negative magnetostriction, respectively. Therefore, the sign and magnitude of the magnetostriction constant together with the strength of the internal stresses are the key parameters that allow one to understand the magnetic phenomena in these materials [11]. For example, as has been shown in previous studies, the magnetoimpedance, MI,

effect in CoFe glass-coated amorphous microwires is strongly dependent on the glass thickness. A first aim of this study has been thus to confirm the role played by the increasing thickness of the insulting glass Pyrex on that magnetic anisotropy.

a. Single phase magnetic microwires

The main features of FMR in single phase amorphous microwires have been analyzed in several reports [3, 4]. The evolution of the impedance spectra (real R component of impedance) with dc magnetic field for CoFe glass-coated microwires as a function of its total diameter presented in F*ig. 4.1*. The spectra are smooth and show the typical behavior for FMR, i.e., the maximum of R is observed at the resonance frequency.

As shown in *Fig. 4.1 (d)*, the resonance frequency satisfies the Kittel resonance condition for a uniaxial thin film magnetized along the in-plane easy axis [12]:

$$\frac{\omega}{\gamma} = \sqrt{(H + H_k)(H + H_k + 4\pi M_s)} \approx \sqrt{(H + H_k)4\pi M_s} \qquad (4.1)$$

We assumed that $4\pi M_s >> H+H_k$

$$f_r^2 = \frac{\gamma^2 \mu_0^2 M_s}{4\pi^2}(H \mp H_K) \qquad (4.2)$$

where $\omega=2\pi f$ is the angular frequency of the microwave field, γ is the gyromagnetic ratio, $4\pi M_S$ is the saturation magnetization and H_k is the anisotropy field. The field, H, is the effective field, which includes the applied field, H_{app}, plus the anisotropy field, H_k of the wire, H_k, $H=H_{app}+H_k$. the sign of H_k in eq. (4.2) indicates the parallel or perpendicular anisotropy field, H_k.

From the fitting to experimental results to Eq. (4.2) (*see Fig. 4.1 (d)*) it is possible to obtain the saturation magnetization $4\pi M_S$=7.1 kG for all samples, in good agreement with previous results on the same kind of wires [9]. The anisotropy field values are deduced from extrapolation of the linear behavior, and the obtained negative values, $H_k<0$, denote weak circular magnetoelastic anisotropy the values of Hk are very small and negative. Only small variation is obtained as a consequence of the small value of the magnetostriction constant. H_k becomes less negative as the thickness of the glass coating is increased; reflecting the stress effect induced by the insulating layer, in agreement with the hysteresis loops behavior depicted in Fig. 3.4 in chapter3.

In the case of biphase microwires, the appearance of multipeak absorption spectra has been recently reported [5, 9]; but the origin of the FMR spectra is not clear since the experiments involving the CoNi external shell were done for nonfully

saturated samples. In the present work, we want to deepen into the knowledge of the microwave behavior. Therefore, we have compared the response of non saturated CoFe/CoNi microwires to that of fully saturated CoFe/FeNi ones. The influence of the thickness of the Pyrex layer is also presented in those layered systems.

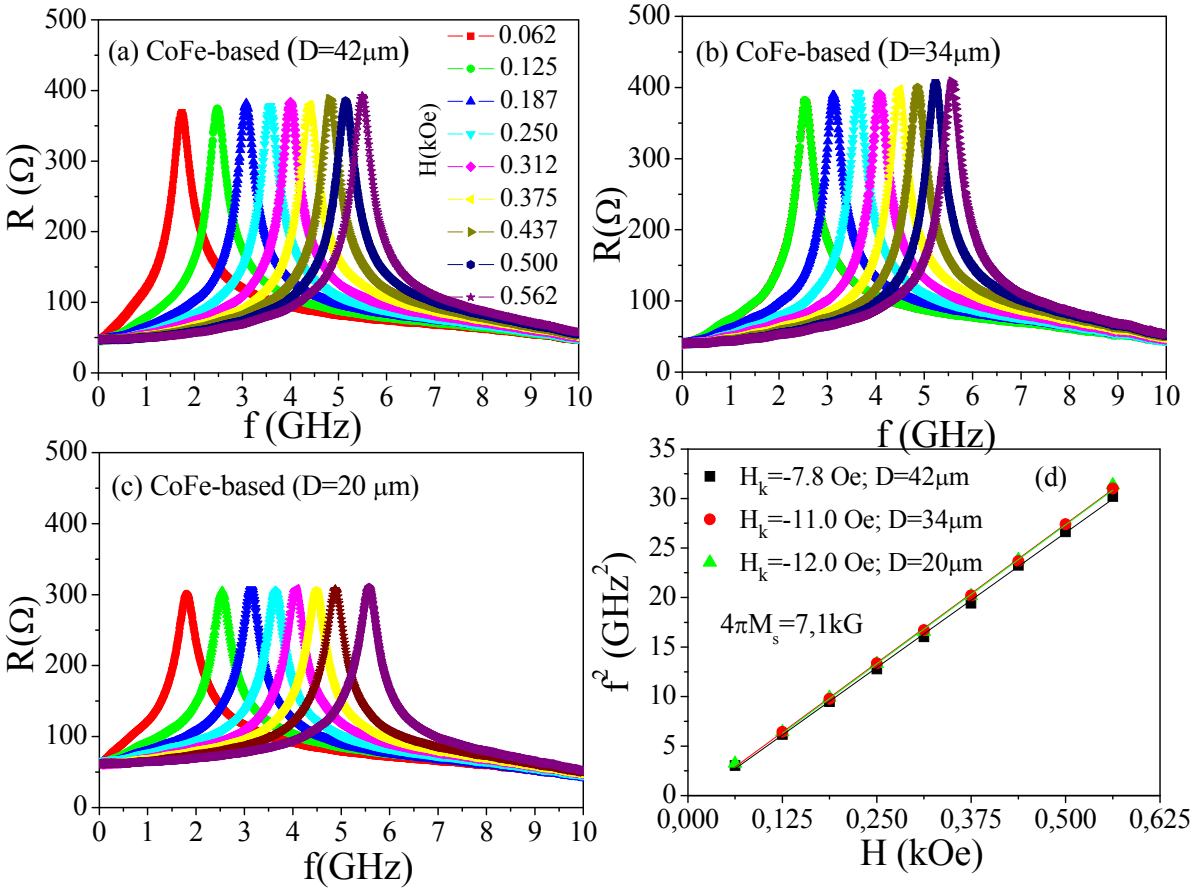

Figure 4.1 *Evolution of the FMR spectra (real part of impedance) with indicated static magnetic field for CoFe glass-coated microwires with a 17 μm thick amorphous nucleus. Total diameter as a parameter: (a) D= 42 μm, (b) D= 34 μm, (c) D= 20 μm. (d) FMR condition for the data shown (a), (b), and (c). Lines represent a linear fit according to Eq. (4.2).*

Let us turn to analyzing the FMR spectra of the biphase wires. *Fig.4.2* a to c shows the evolution of the impedance spectra (real part of impedance) with dc magnetic field for CoFe/CoNi microwires with a 2μm thick CoNi outer shell as a function of the thickness of the insulating Pyrex layer. The applied dc magnetic field is not high enough to saturate the hard external shell (see the M–H loop of Fig.3.5) and 2 absorption peaks appear for all cases (FMR1 and FMR2, respectively at high and low frequencies). In order to obtain the intrinsic impedance of the sample, correction procedures such as the one mentioned in Ref. [9] should be applied. However, the scope

of this contribution is the study of the resonance condition; which can be precisely determined from the real part of the resonance spectra.

Fig.4.2 (d) shows the fitting of the different absorption peaks to *Eq. (4.2)*. Again, a modest influence of Pyrex thickness is observed, and the anisotropy field reflects the small increases induced by the stresses of the glass Pyrex. The most interesting results concern the FMR condition: FMR1 follows the resonance condition given by *Eq. (4.2)*, with a fitted value $4\pi M_S$=7.1 kG, which allows one to ascribe it to the inner CoFe core.

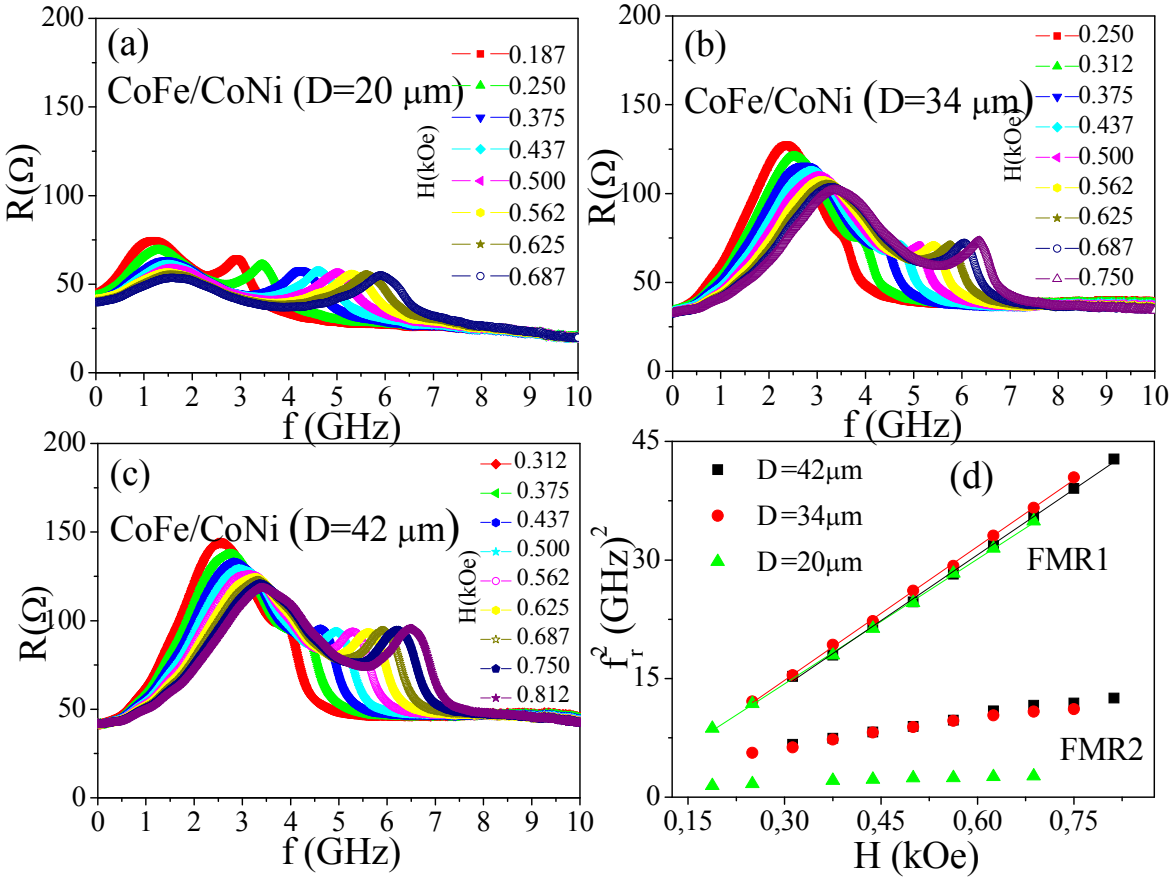

Figure 4.2 *Evolution of FMR spectra (real and imaginary part of impedance) with static magnetic applied field for CoFe/CoNi microwires with a 2 μm thick CoNi layer. Total diameter D of the glass-coated microwire precursor as a parameter: (a) D= 20 μm, (b) D= 34 μm, (c) D= 42 μm. (d) FMR condition for the data shown in (a), (b), and(c) lines represent a linear fit according to Eq. (4.2).*

On the other hand, FMR2 does not follow a linear relation f^2 versus H and, moreover, its resonance condition is clearly dependent on the dimension of the dielectric (Pyrex) layer: it increases with D for a given H. This latter trend suggests that FMR2 is not of magnetic origin.

In order to further clarify the origin of the low-frequency magnetoabsorption FMR2, the same kind of measurements have been done in CoFe/FeNi composite wires

of the same dimensions as those in *Fig. 4.2*. These soft/soft wires can be taken as magnetically saturated under the maximumdc field applied during the microwae measurements (*see the M– H loops of Fig.3.7*) and, according to previous comments, more useful information concerning FMR can be expected.

The results, presented in *Fig. 4.3*, clearly show not 2 but 3 absorption peaks of soft/soft biphase wires that shift with the applied field: the two already found in CoFe/CoNi wires (FMR1 and FMR2) and a new one appearing at higher frequencies (labeled as FMR3 in *Fig. 4.3(a, b, and c*).

Again, the resonance condition provides useful information about their physical origin. The results are plotted in *Fig. 4.3(d)*. Linear fittings provide $4\pi M_S$ values of 7.0 kG for FMR1 (i.e., it corresponds to the CoFe nucleus) and 11.5 kG for FMR3, which is a reasonable value for electroplated Permalloy [14]. Therefore, FMR1 and FMR3 correspond to the two magnetic phases (CoFe nucleus and FeNi shell); and FMR2, the one at lower frequency is not of magnetic origin as was presumed in References [5, 9]. Therefore, as discussed in [5, 9] that FMR2 were associated to the hard shell, but what actually happens in these experiments is that neither frequency nor applied field is high enough to observe and saturate the hard external shell CoNi. That is why, we appreciate only 2 not 3 resonant absorption characteristics of these two phase wires CoFe/CoNi.

It can be also observed in *Fig. 4.3(d)* that this low-frequency resonance depends again on the thickness of the Pyrex layer in such a way that it seems reasonable to ascribe it to a geometrical feature; probably the capacitance formed between the two magnetic conductors and the insulating Pyrex layer.

The capacitive character of these layered structures [15, 16] has to be taken into account when explaining the multipeak FMR spectra; the wire is a cylindrical capacitor (see figure 4.4 (a)) with a given capacity:

$$C = \frac{2\pi\varepsilon_0\varepsilon_r l}{\ln(b|a)} \tag{4.3}$$

Therefore, together the wire and measurement system formed the LRC resonant circuit, which is schematically depicted in Figure 4.4 (b), and the resonance frequency is given by:

$$f_r = \frac{1}{2\pi\sqrt{L(H)C}} \tag{4.4}$$

where, L (H) is the inductance of the two magnetic phase structure.

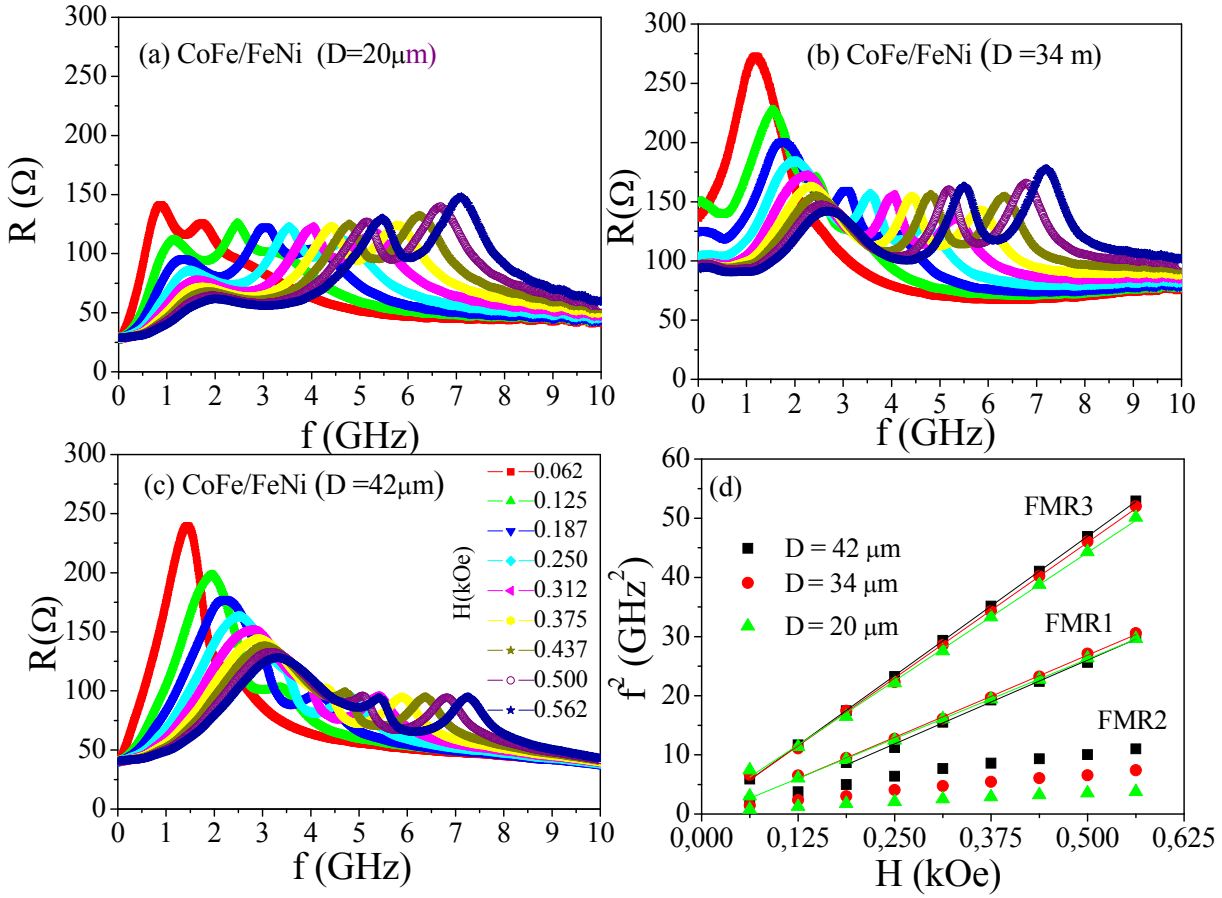

Figure 4.3 *Evolution of the FMR spectra (real part of impedance) with static magnetic field for CoFe/FeNi microwires with a 2 μm thick FeNi layer. Total diameter D of the glass-coated microwire precursor as a parameter: (a) D= 20 μm, (b) D= 34 μm, (c) D= 42 μm. (d) FMR condition for the data shown in (a, b, and c). Lines represent a linear fit according to Eq. (4.2).*

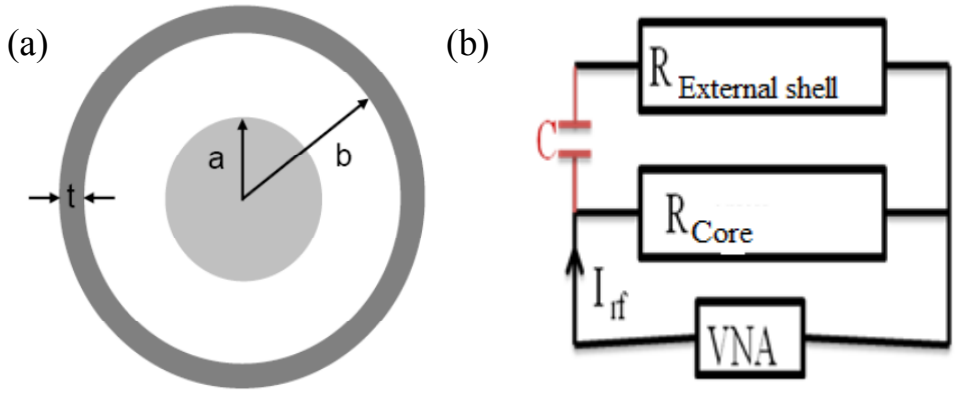

Figure 4.4 *Resonant circuits LRC diagram formed by the two-phase microwires and microwave network analyzer (VNA). Rcore presents the electrical resistance of the core, External shell presents the electrical resistance of the external shell FeNi, and C is the capacitance of the biphase wire.*

This circuit reproduces qualitatively the FMR behavior observed for the biphase microwires CoFe/FeNi. First, we will explain why it is possible to observe the magnetic resonance of the FeNi outer layer (FMR3).

Therefore, in *Fig. 4.4(b)* the capacitance C (red) is formed between the inner core and external shell, where the insulting Pyrex layer is taken as a dielectric layer. As a result, the alternating current passes through not only the inner ferromagnetic core but also the outer shell of the microwire CoFe/FeNi (FMR1 and FMR3 in *Fig. 4.3*). Thus, the biphase microwire consists of two impedances in parallel (one much larger than the other since l=5mm, R_{core}≈50Ω, $R_{External\ shell}$=1-5 Ω), which would involve that the values of theirspectrum of resistance should be modified with respect to the single phase CoFe microwire as we observe in *Fig. 4.5(a)*. Thus, the resonance shifted to the applied field due to the resonance frequency.

Fig. 4.5(a) presents the absorption spectra at a constant applied field (H_{app}=0.375 kOe) of single phase microwires CoFe (black), of the same microwire sputtered with a thin Au nanolayer (orange), and of the wire after electroplated by FeNi soft external shell (green). Indeed, the resistance of biphase microwires (electroplated by magnetic or not magnetic metal layer) is much smaller than the single phase microwires. On the other hand, in the *Fig. 4.5(a)* we observed that the FMR2 appears in the case of a non-magnetic coating of Au, which confirms the capacitance origin of its absorption peak.

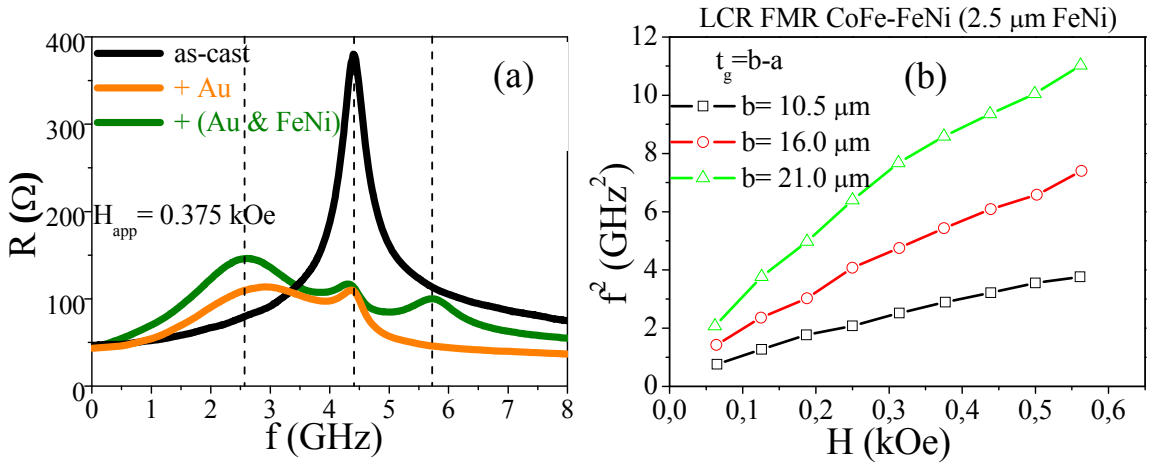

Figure 4.5 (a) Comparisons of absorption spectra of CoFe-based, CoFe/Au, and CoFe/FeNi with 2.5μm of FeNi thick measured at a constant applied field, l=5mm and other dimensions are the same as in Fig.4.3. The vertical lines indicate the position of FMR1, FMR2, and FMR3. (b) Dependence of the resonance condition for FMR2 with dielectric thickness t_g = b-a in biphase microwires CoFe / FeNi with l = 5 mm, t_{FeNi} = 2.5 μm, d = 17 μm. The microwave output is -10 dBm.

This phenomenon illustrates that the composite wire constructs an LRC circuit by itself. The LRC- FMR should depend on the geometry of the associated capacitor as shown in *Fig.4.4 (b)*.

In addition, the dependence of FMR2 with the dimensions of the microwire is the definitive point confirming its capacitive origin. In the *Fig.4.5 (b)* presents the low frequency absorption, FMR2, in CoFe/FeNi composite microwires as a function of the thickness of the dielectric layer (Pyrex) :(l= 5mm, d=17 μm, b= 10.5, 16, 21 μm, t=2.5 μm). It's observed that, for a given, H_{app}, the resonance frequency increases as the thickness of dielectric increase. Thus, the capacitance C of the structure decreases as b is increased. Therefore, for a given value of H_{app}, the associated resonance frequency f_r increases (see eq. 4.3 and eq. 4.4).

It can be concluded that: (i) for single-phase microwires the role of increasing the Pyrex thickness is reflected in a moderate increase of the circular magnetoelastic anisotropy of the soft core. (ii) For both biphase investigated systems (CoFe/CoNi and CoFe/FeNi), a similar effect of the Pyrex thickness is observed, and (iii) biphase microwires show in addition the presence of an unexpected third absorption peak that is clearly of nonmagnetic origin. These multilayer microwires actually represent a new family of magnetic materials with potential applications in microwave circuits.

The study of ferromagnetic resonance, FMR, is often used for the investigation of the structural changes in amorphous alloys as CoFe-based. Similar high frequency studies have been done on other composition as FeSiB microwires with a positive magnetostriction, $\lambda_0>0$. Previously, FeSiB glass-coated microwires have been considered less interesting for giant magnetoimpedance, GMI, because of their positive and high magnetostriction, which promotes longitudinal domains and reduces the circular permeability. In the next section, we will present a FMR behavior of single and biphase FeSiB/CoNi microwires, and a particular emphasis have been investigated on the effect of annealing treatment in single and biphase FeSiB/CoNi microwires.

4.2.2. Effect of annealing treatment in FeSiB single and biphase microwires

The influence of thermal treatments on the magnetic behavior of amorphous alloys was systematically performed years ago. While treatments at moderate

temperature result in relaxation of the amorphous structure, annealing at higher temperatures leads to crystallization of amorphous microstructure and to the growing of new crystal phases with size in the nano and microscale that deteriorates the magnetic behavior and the soft magnetic response itself [17-19].

The objective of this section is to investigate the influence of the annealing treatment on the ferromagnetic resonance behavior of soft/hard bimagnetic microwires with different thicknesses of the insulating intermediate microlayer. The study is performed on magnetic microwires whose core is $Fe_{76}Si_{13}B_{11}$ amorphous alloy with high and positive magnetostriction, (λ_s=3x10^{-5}), which ensures their soft and bistable magnetic behavior. Series of microwires have been selected with metallic core diameter, *d*, in the range of 18 to 20 μm, and total diameter *D* = 24 to 26 μm. Three particular microwires with different geometric ratio ($\rho=d/D$), ρ=0.69, 0.75 and 0.77 were selected for measurements. The external shell is a polycrystalline $Co_{90}Ni_{10}$ alloy with magnetically harder character and 3μm thickness.

The annealing treatment before full crystallization is achieved. Single and biphase microwires were annealed at various annealing temperatures, T_{ann}, ranging from 100ºC to 700ºC in Argon atmosphere for 1h. The cooling to room temperature took between 1 and 2h, depending on the annealing temperature. Thermal treatments performed at such temperature range results in structural transformations, including amorphous relaxation and crystallization. The evolution of the high frequency behavior is studied with annealing temperature and in comparison with the parallel evolution for single phase precursor glass-coated microwire.

a. Single phase microwires FeSiB: before and after annealing treatment

For single phase FeSiB microwires, FMR is observed typically in the frequency range between 7 and 12 GHz as analyzed and ascribed in [5, 9]. Here, we have measured the absorption characteristics for the as-prepared microwires before and after thermal annealing treatments.

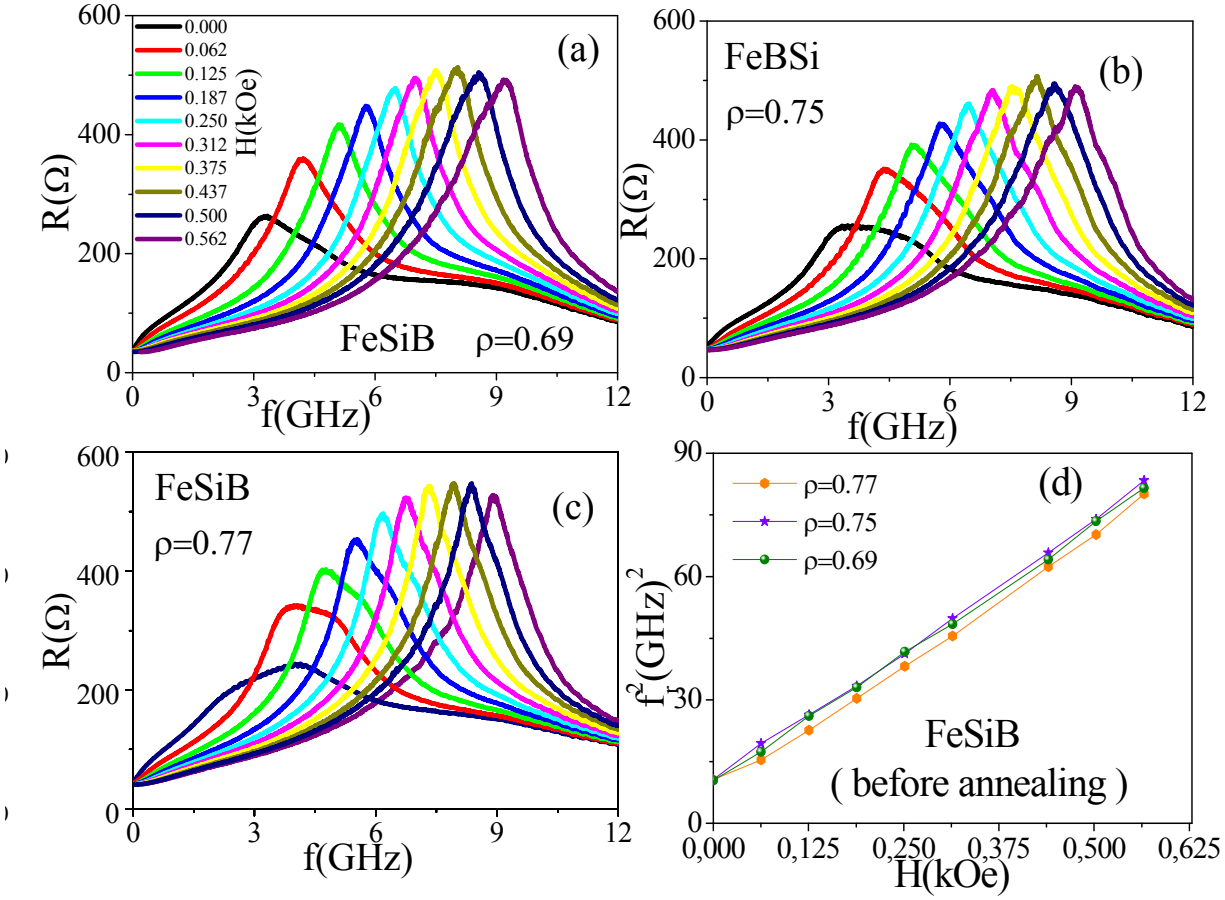

Figure 4.6 Evolution of resonance spectra (real part of impedance) with static magnetic applied field for FeSiB glass-coated microwires with different geometrical ratios (a), (b), and (c). (d) Square of the resonance frequency as a function of applied static magnetic field for single phase FeSiB microwires before annealing treatment.

The absorption spectra (real component of impedance) for single phase as-prepared amorphous FeSiB glass-coated microwires before annealing treatment as shown in *Fig. 4.6* are sharp and show a typical single absorption peak at the FMR frequency which increases from around 4 to 10 GHz as the applied field increases up to 0.562kOe. In addition, the absorption peak amplitude slightly increases with increasing the geometric ratio, ρ.

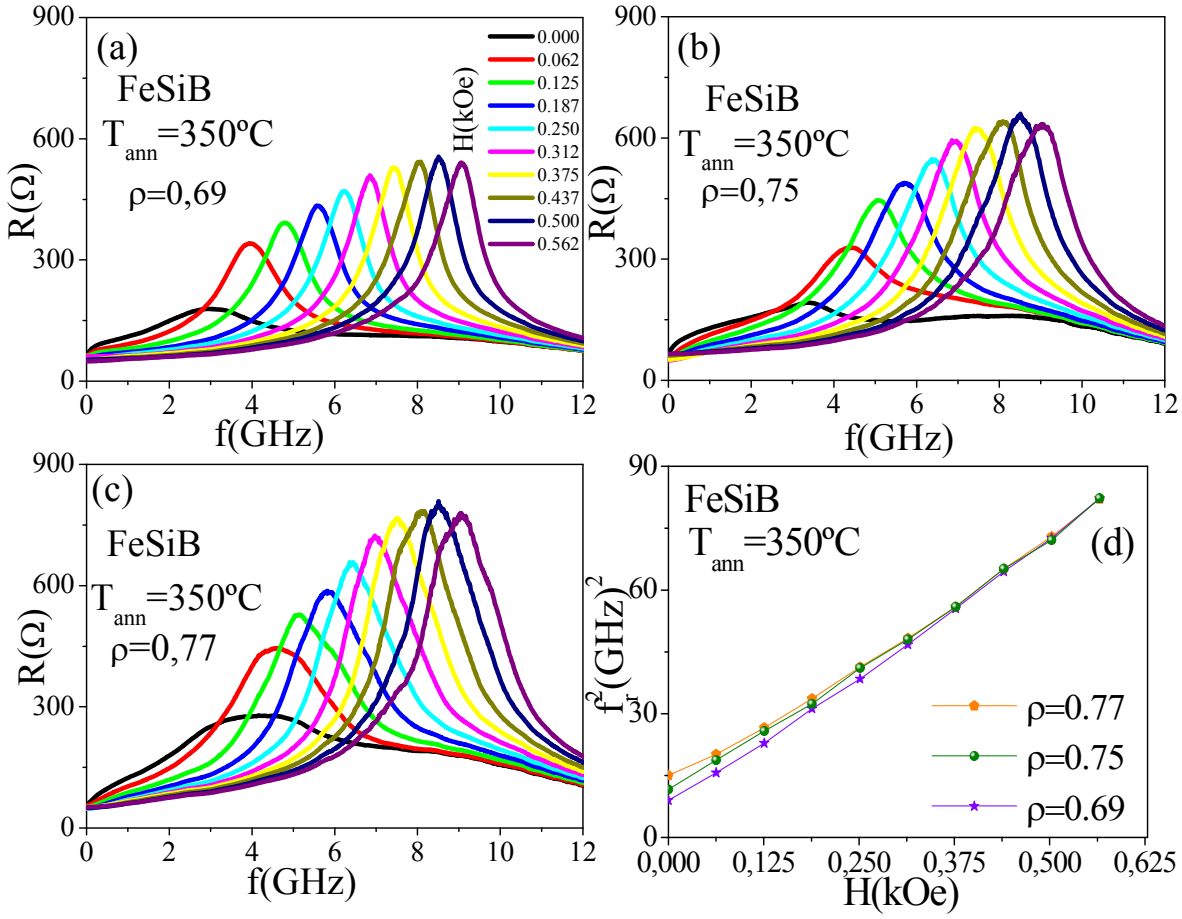

Figure 4.7 *Evolution of resonance spectra (real part of impedance) with static magnetic applied field for annealed FeSiB glass-coated microwires at 350ºC, with different geometrical ratios (a), (b), and (c). (d) Square of the resonance frequency as a function of applied static magnetic field for single phase FeSiB microwires before and after annealing at 350ºC.*

After annealing up to around 500ºC (below crystallization temperature) only small changes are observed in the FMR absorption characteristics. However, after annealing above 500ºC (above crystallization temperature) , the absorption peaks show much less amplitude and their FMR frequency changes only slightly with the applied field. *Fig. 4.7* shows the data for annealing temperatures below crystallization temperature, i.e., 350ºC, while in *Fig. 4.8* present the data for annealing temperature above crystallization, i.e., 650ºC.

Thus, for samples treated at a temperature up to 350ºC we still observed sharp absorption peaks. However, above the crystallization temperature, for example T_{ann}=650ºC, as shown in *Fig. 4.8*, the absorption peaks show much less amplitude and are not so well defined. These facts are interpreted as a consequence of the crystallization of the sample.

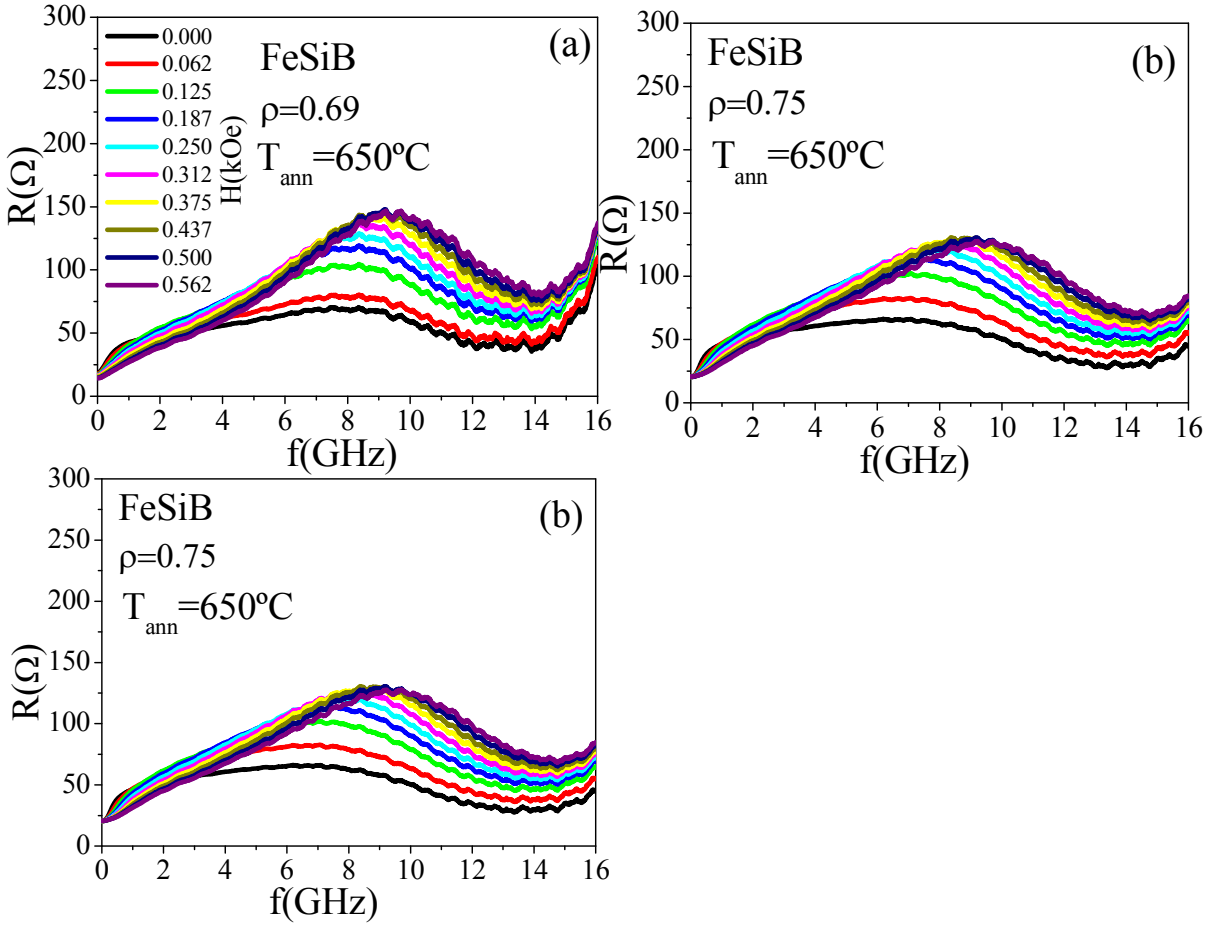

Figure 4.8 *Evolution of resonance spectra (real part of impedance) with static magnetic applied field for annealed FeSiB glass-coated microwires at 650ºC, with different geometrical ratios (a), (b), and (c).*

Experimental evolution of the FMR frequency with applied static field, H, has been well fitted to Eq. 4.2 for single phase FeSiB microwires in as-cast state and after annealed at 350ºC as shown in *Fig. 4.6(d)*, and *Fig. 4.7(d)* respectively, from which a saturation magnetization value of $4\pi M_S \approx 16$kG has been obtained. This agrees reasonably with values in the literature.

After 500ºC exactly at 650ºC, it is not possible to obtain the value of saturation magnetization because of non linear fitting.

b. Biphase microwires soft/hard FeSiB/CoNi: before and after annealing treatment

Thermal treatments have been done for biphase microwires. *Fig. 4.9* and *Fig. 4.10* show the data for biphase microwires measured before and after annealing treatment (below 500ºC). Two absorption peaks are observed, the one at high frequency

(FMR1) is ascribed to the FMR of the FeSiB core, since it is observed at similar frequencies as for the single phase FeSiB microwire. The peak at lower frequency (FMR2) does not evolve significantly with the applied field, and it has been ascribed to the capacitance effect due to the presence of the external shell (the two coaxial magnetic conductors and the intermediate insulting Pyrex layer) [6] as interpreted in the previous section.

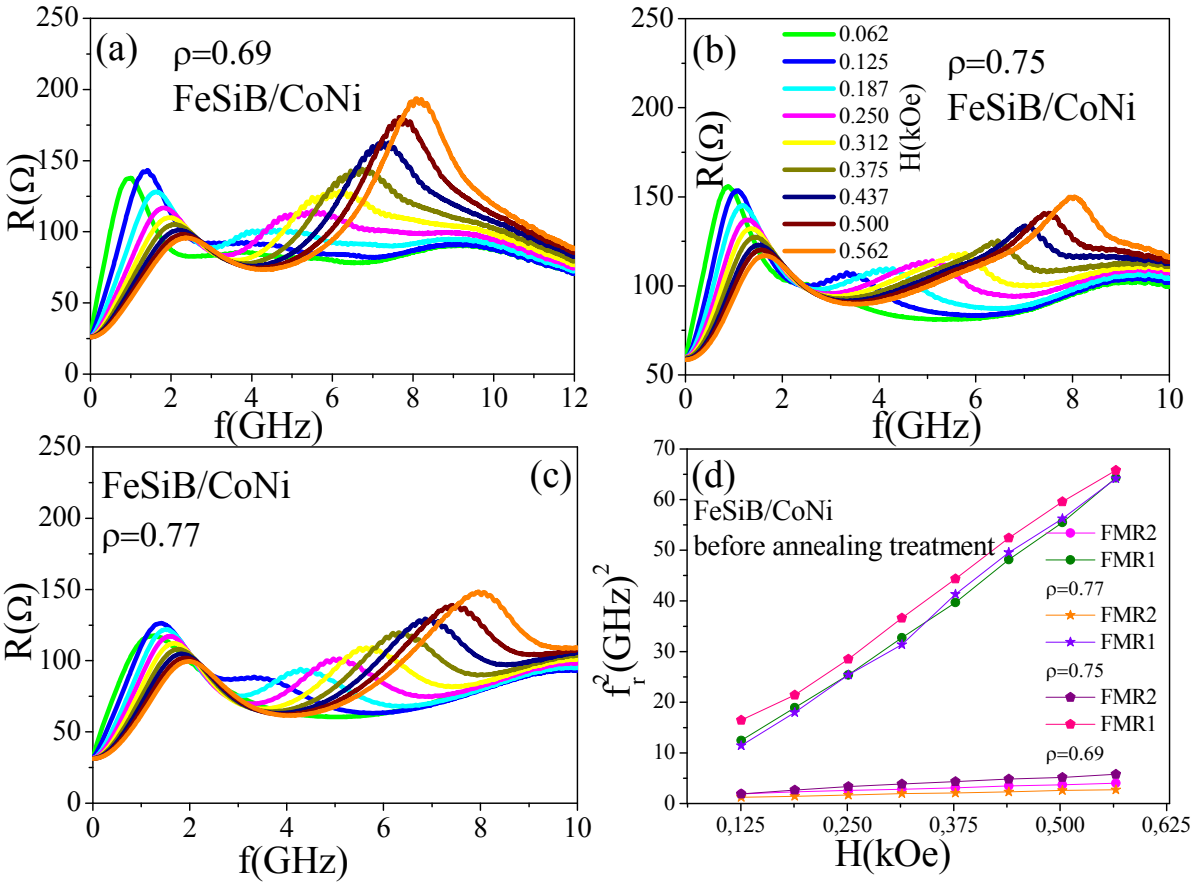

Figure 4.9 *Evolution of resonance spectra (real part of impedance) with static magnetic applied field for biphase FeSiB/CoNi glass-coated microwires, t_{CoNi}=3μm, with different geometrical ratio before annealing temperature. (d) Square of the resonance frequency as a function of applied static magnetic field for biphase FeSiB/CoNi microwires before annealing treatment.*

After annealing treatment at 500ºC, we still observe two absorption peaks, although the peak (FMR1) corresponds to the soft core shows much less amplitude, and eventually it should be ascribed to the partially crystallized FeSiB core, while the first absorption peak (FMR2) does not change so significantly as can be observed in *Fig. 4.11* for the sample annealed at 650ºC.

Indeed, the first absorption peak (FMR2), which presented at low frequency is not magnetic and this is confirmed that it depends on the thickness of insulting glass Pyrex. As we mentioned above (4.2.1.a) it can be the capacitance, as well as, there is no effect on this peak during annealing treatment.

Fig. 4.9(d) and *Fig. 4.10(d)* show the fitting to the Eq. (4.2) corresponding to biphase FeSiB/CoNi microwires before and after annealing at 500ºC just before crystallization of the amorphous core. The peak FMR1 ascribed to the soft core follows the resonance condition given by Eq. (4.2), with fitted value $4\pi M_s \approx 15$kGand $4\pi M_S \approx 17$kG before and after annealing, respectively. Data for FMR2 does not follow the resonance condition and is ascribed to the mentioned capacitive effect. In addition, CoNi shell is not sufficiently saturated magnetically so that it does not show properly ferromagnetic absorption effect.

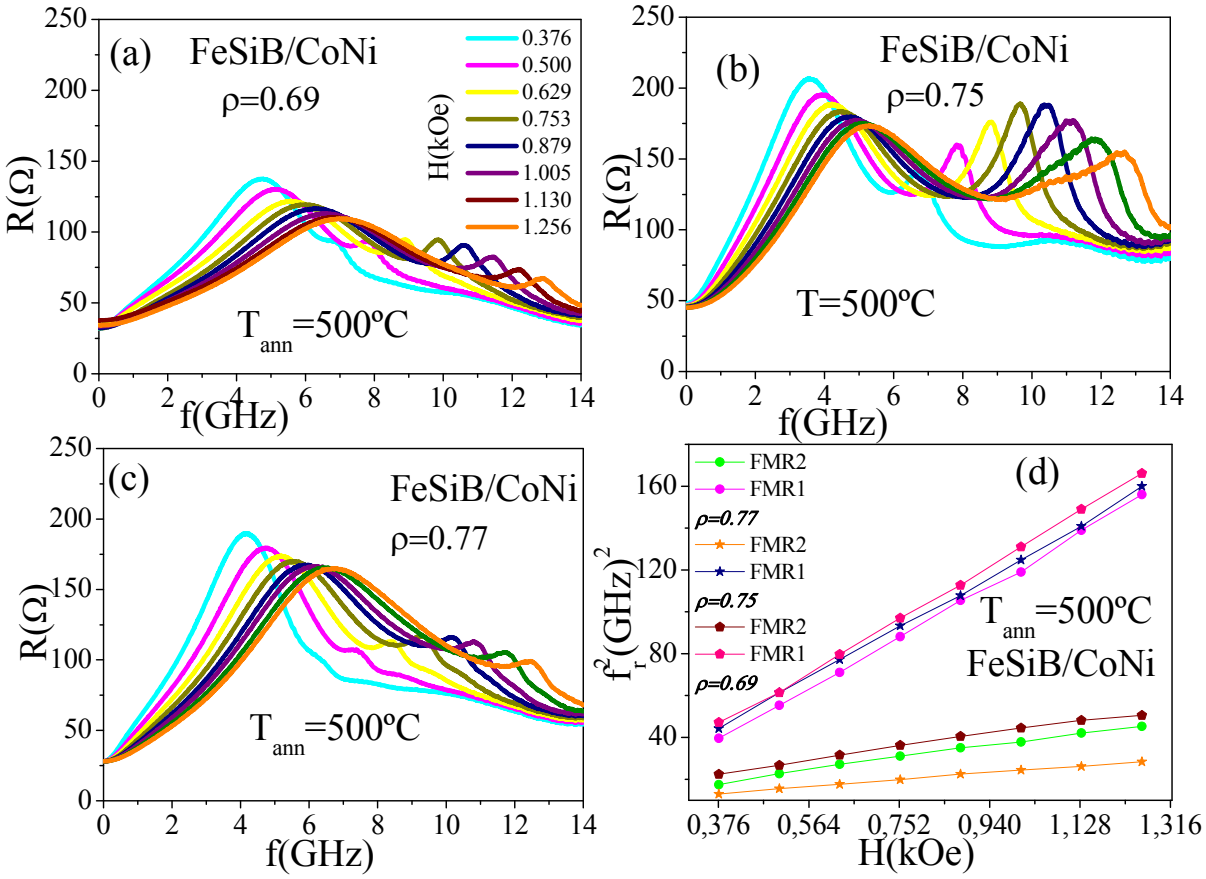

Figure 4.10 *Evolution of resonance spectra (real part of impedance) with static magnetic applied field for biphase FeSiB-CoNi glass-coated microwires, t_{CoNi}=3μm, with different geometrical ratio annealed at 500ºC. (d) Square of the resonance frequency as a function of applied static magnetic field for biphase FeSiB/CoNi microwires before and after annealing at 500ºC.*

In summary, the annealing effect on single and biphase microwires has been investigated. Annealing treatments (up to 500ºC) induce very modest influence on high-frequency properties of both families of microwires.

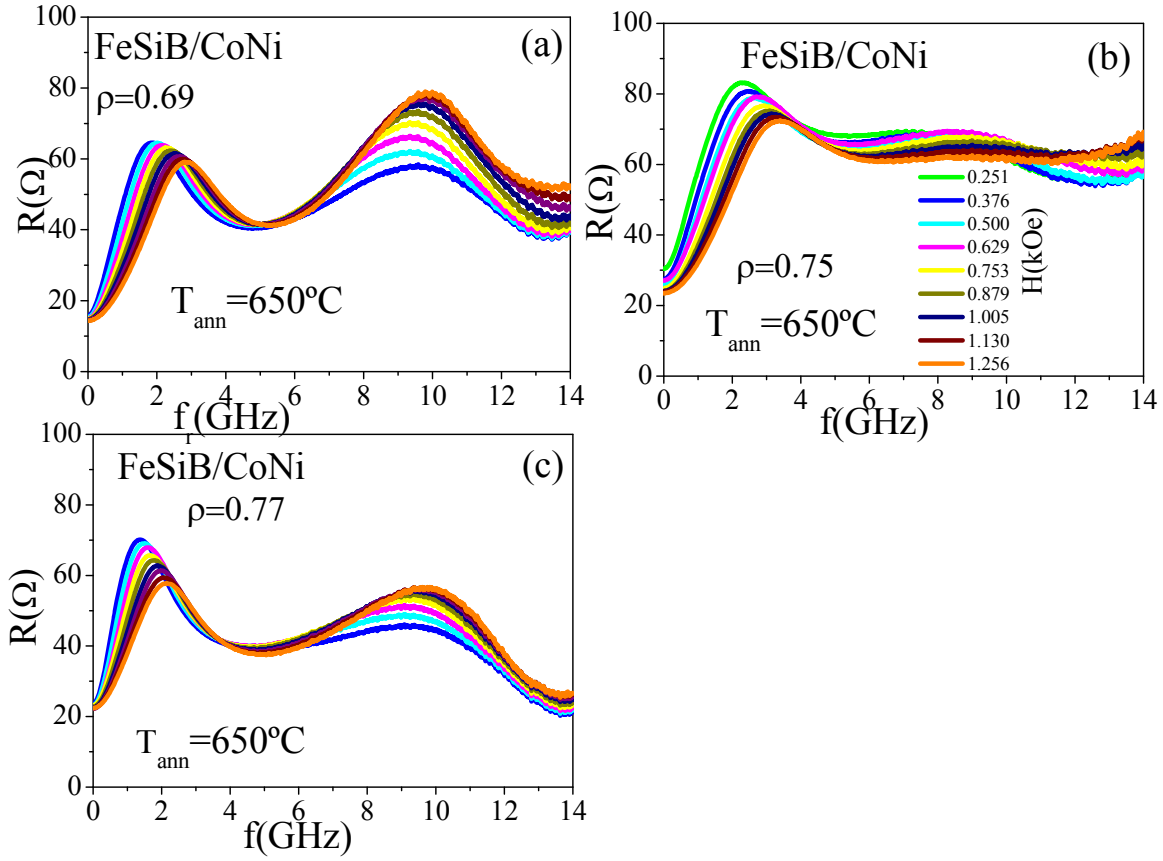

Figure 4.11 *Evolution of resonance spectra (real part of impedance) with static magnetic applied field for biphase FeSiB-CoNi glass-coated microwires, t_{CoNi}=3μm, with ρ=0.69, 0.75, and 0.77 respectively, annealed at 650ºC.*

FMR data indicate that for single phase microwires annealed up to 500ºC (below crystallization temperature), the absorption peaks are found in the range from 3 to 9 GHz for increasing applied fields from which we derive saturation magnetization value. In biphase microwires, the presence of the external shell gives rise to a second absorption peak ascribed to a capacitive effect. It is understood that CoNi shell is not sufficiently saturated magnetically so that it does not show properly ferromagnetic absorption. After crystallization, the absorption peaks show much reduced dependence on applied field, and the FMR behavior cannot be fitted properly to the characteristics of the biphase material. That crystallization gives rise to new crystal phases with magnetically hard character so that, no absorption peak is observed at the range of applied fields.

In short, we can conclude that biphase microwires maintain their magnetic properties after annealing treatments below crystallization temperature of the soft amorphous core so that, they are good candidates as sensing elements to be employed at moderate temperature.

4.2.3 Microwave behavior at high frequency for biphase wires with hard shell

From early works [20], the high-frequency, at the microwave range, behavior of microwires has been also reported by several groups [21-29]. The interpretation of rather complex experimental data for multilayer wires with and without intermediate glassy layer has been, however, sometimes contradictory.

In the case of biphase wires with glassy interlayer, several difficulties have been pointed out to interpret their multiabsorption spectra [5, 6, 7, and 9]. While single phase microwires are characterized by single ferromagnetic resonance absorption ascribed to the only phase, in the case of biphase microwires two or even three different absorption peaks are observed depending on the soft/hard nature of the two phases. The evolution of the resonance frequency with DC applied field has been fitted to Kittel's equation for thin films which is applicable also to metallic wires if the skin depth is small compared to the wire diameter [30]. Thus, the diversity of interpretation specifically occurs if the skin effect in ferromagnetic metal is not properly taken into account. This fact justifies the present updating of recent progress in understanding FMR aspects of ferromagnetic metallic wires.

As deduced from (section 4.2.1 and 4.2.2) measurements using Network Analyzer, the biphase microwires with hard external shell, CoNi, do not saturate magnetically in the range up to 20GHz under the maximum applied field, at room temperature, neither in as-cast nor after annealing.

Here, we report on FMR in biphase microwire; electroplated by hard external shell; obtained by means of cavity- perturbation technique with two different microwave frequencies of 9.5GHz (X-band) and 69GHz (K-band), were compared.

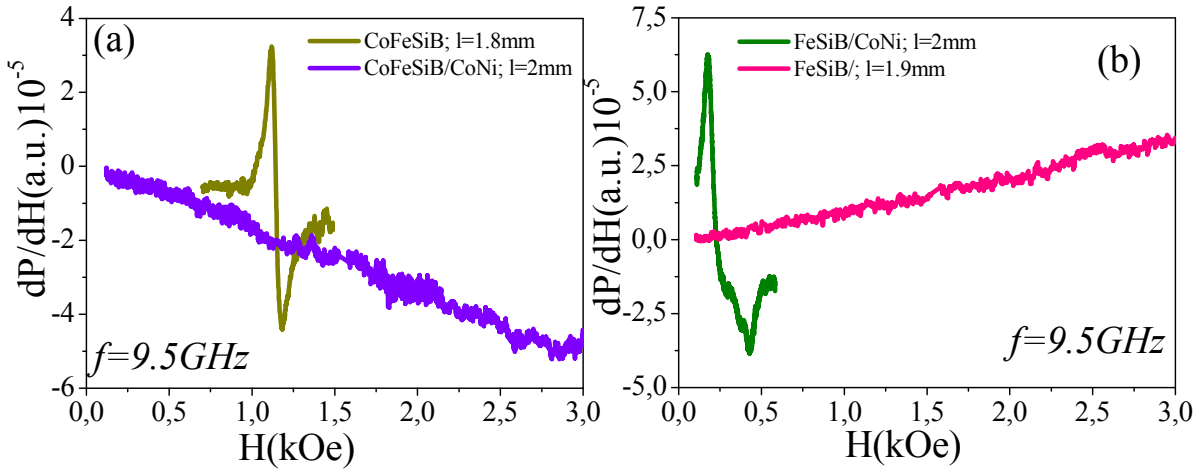

Figure 4.12 *Resonance spectra for single and biphase microwires measured in microwave frequency of 9.5GHz. (a) CoFeSiB and CoFe/CoNi; (b) FeSiB and Fe/CoNi.*

The classical FMR experiments were done on two different amorphous glass-coated microwires with nominal composition FeSiB and CoFeSiB, with metallic core diameters 12.5 and 8μm, and total diameters 40 and 24μm, respectively. These two samples were selected and electroplated by a hard external shell, CoNi, with 3μm of thickness.

Pieces with different length (see *Fig.4.12* and *Fig.4.13*) were cut from the selected wires inserted into quartz capillarity and placed into the middle of circular waveguide with sample axis along the electric field vector.

The FMR spectra measured at frequency 9.5GHz for selected single and biphase microwires are shown in *Fig.4.12*. Low absorption is observed in single phase wires. In this case, the CoNi layer completely screens the internal core, and the resonance of CoNi shell is not observed since it is not magnetically saturated.

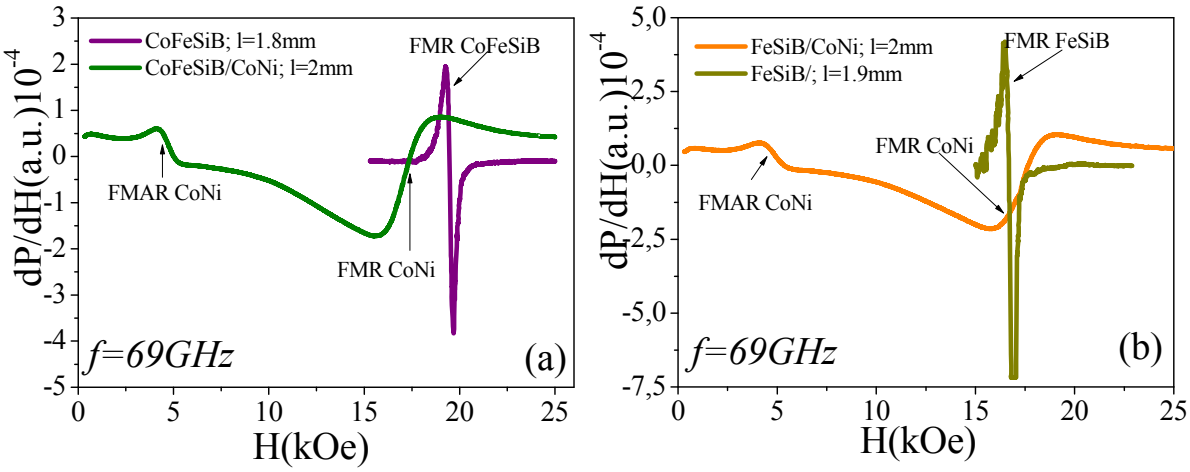

Figure 4.13 *Resonance spectra for single and biphase microwires measured in microwave frequency of 69GHz. (a) CoFeSiB and CoFe/CoNi; (b) FeSiB and Fe/CoNi.*

For such single and biphase microwires, the curves dP/dH are presented in *Fig. 4.13 (a, and b)* measured in microwave frequency of 69GHz. As can be seen, the anti-resonance FMAR peak is symmetric, while the experimental derivative FMR curves are distorted in both biphase microwires (*see Fig. 4.13 (a, and b*). This occurs most probably because the sample represents a large load to the microwave circuit [27].

The field derivative of the two resonance curves shows the ferromagnetic anti-resonance, FMAR, and the ferromagnetic resonance, FMR, for the hard external shell, CoNi, presented at low and high resonance field, respectively, which indicates that in electroplated wires, the amorphous wire is screened by CoNi. Instead we observe resonance and anti-resonance of CoNi.

This confirm the experimental results obtained by using the network analyzer techniques which presented in sections 4.2.1 and 4.2.2, that the presence of the external shell in biphase microwires gives rise to a second absorption peak ascribed to a capacitive effect. It is understood that CoNi shell is not sufficiently saturated magnetically so that it does not show properly ferromagnetic absorption.

The next objective of this chapter has been to obtain deeper knowledge on the microwave phenomena in multilayer microwires, through the low temperature dependence of their absorption peaks.

4.2.4. Temperature dependence study in CoFeSiB single and biphase microwires

The issue of this section has been to obtain deeper knowledge on the microwave phenomena in multilayer microwires through the low temperature dependence of their absorption peaks. To reach that goal, we have selected a single CoFe core and a soft/soft biphase microwire with different thickness of external FeNi microtube on a glass-coated CoFe based amorphous core with composition $(Co_{0.94}Fe_{0.06})_{72.5}Si_{12.5}B_{15}$ and diameter, d = 8 μm, covered by an 8 μm thick Pyrex coating so that, the total diameter is D = 24 μm. Such composition is typical for small negative magnetostriction, $\lambda_s \approx -1\times10^{-7}$, in amorphous alloys. However, magnetostriction in CoFe based amorphous systems is sensitive to various parameters as composition, quenching rate, structural relaxation state or applied stress [30]. In the present case, its actual value can be affected by the mechanical stress induced by the Pyrex coating and the external metallic shell.

a. Microwave behavior measured at room temperature

First study was performed in the Network analyzer facility. Fig. 4.12 shows the evolution of the impedance spectra (real component) of CoFeSiB/FeNi microwires with different thickness of FeNi microtube (t_{FeNi} = 0, 2, and 4μm) as a function of the AC frequency with the DC field as a parameter. For the single phase CoFeSiB microwire (Fig. 4.12.a), the single-peak absorption (labeled as FMR1) spectra evolves towards higher resonance frequency, fr, with increasing DC applied field. For biphase CoFeSiB/FeNi microwire with 2μm thick FeNi layer (Fig. 4.12.b) two absorption peaks are observed. The first absorption (labeled as FMR2 in Fig. 4.12.b) is observed at the lower frequency. The second absorption peak appears to be close to FMR1 of single phase CoFeSiB wire. Further analysis is presented below. In the case of CoFeSiB/FeNi microwire with 4μm thick FeNi layer (Fig. 4.12.c), an additional third peak (labeled as FMR3) is observed at higher frequency.

To analyze the evolution of the resonance frequency, we consider the Kittel's resonance condition for a tangentially magnetized planar film, which corresponds to the skin-depth layer at the wire surface [31, 32].

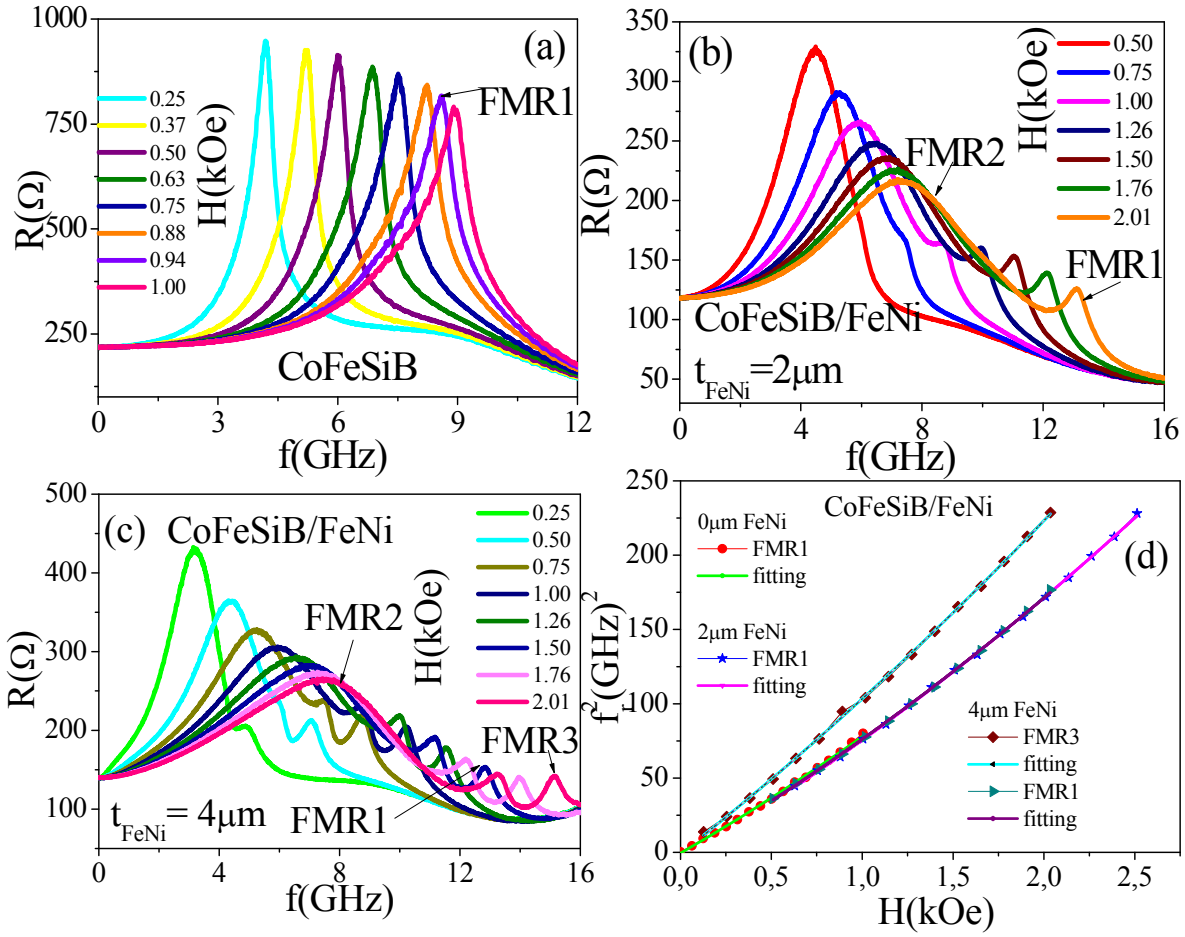

Figure 4.12 *Evolution of the FMR spectra (real part of impedance) with DC magnetic field of CoFe/FeNi microwires for different NiFe thickness: 0 (single phase)(a), 2 (b) and (c) 4μm. (d)* Square frequency of resonance, f_r, as a function of DC applied magnetic field for FMR2 and FMR3 absorption peaks at indicated microwires.

The experimental evolution of the frequency, f_r, with applied field at resonance, H_r, has been fitted according to eq. (4.1) for FMR1 and FMR3 absorptions in order to estimate the saturation magnetization, $4\pi M_s$, and anisotropy fields, H_K (see Figure 4.12. d). FMR1 is ascribed to CoFeSiB phase, while FMR3 is due to the presence of the FeNi external shell and appears only for the microwire with the higher thickness of FeNi shell. The fitted values are collected in Table I. The values of $4\pi M_s$ for FMR1 are relatively close, while it takes a significantly larger value for FMR3. The fitted anisotropy field, H_K, is negative in all the three samples showing an enhanced value for t_{NiFe} = 2 μm biphase microwire. Note particularly that fitted value H_K = -7.9 Oe for single phase microwire compares well with -6.2 Oe deduced from the hysteresis loop (see inset of Fig. 3.17 in chapter 3).

Table I.- Saturation magnetization, $4\pi M_s$, and anisotropy field, H_K, values fitted from eq. (4.1).

t_{FeNi} =	0		2 μm		4 μm	
	$4\pi M_s$ [kG]	H_k [Oe]	$4\pi M_s$ [kG]	H_k [Oe]	$4\pi M_s$ [kG]	H_k [Oe]
FMR1	9.02	-7.9	9.34	-63	9.21	-4.5
FMR3					12.30	-8.6

Finally, FMR2 absorptions observed at the lower frequency (in *Figs. 4.12.b* and *4.12.c*) for biphase microwires do not follow Kittel's resonance condition, as mentioned above.

Parallel FMR studies were performed by cavity-perturbation technique (DC-field dependence of microwave-absorption) at microwave X-band frequency (9.5 GHz).

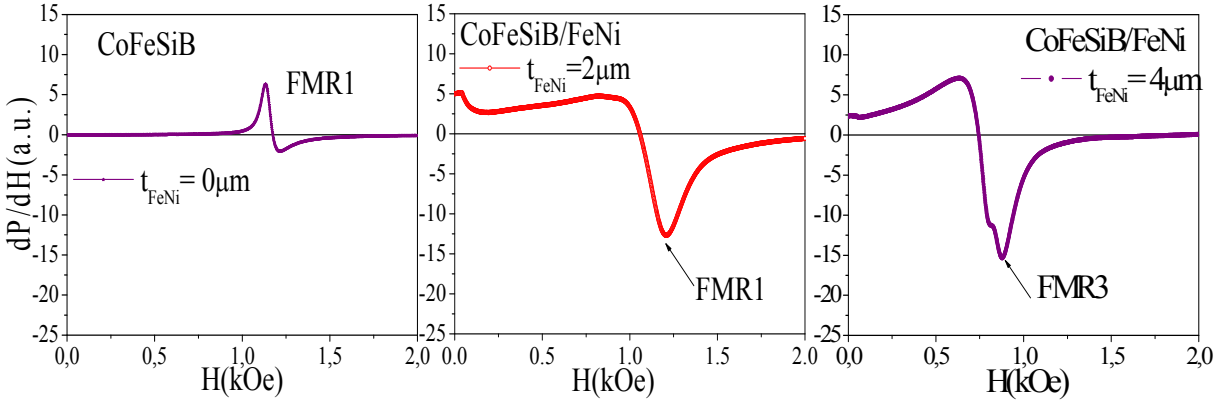

Figure 4.13 *the derivative resonance spectrum of single (CoFeSiB) and biphase microwires (CoFeSiB/FeNi) with different thickness of FeNi (0, 2 and 4 μm) measured at room temperature and at frequency 9.5GHz.*

The results corresponding to the single and biphase microwires are shown in *Fig. 4.13*, and they can be compared to data obtained with the network analyzer, NA, in *Fig. 4.12* for f_r = 9.5 GHz. The spectrum displays one resonant peak for single phase CoFeSiB microwire at 1.08 kOe which compares with 1.17 kOe of FMR1 as deduced from NA data. For t_{NiFe} = 2 μm biphase microwire, a main absorption is observed at 1.10 kOe which compares with 1.16 kOe from FMR1 in NA measurements which was ascribed to CoFeSiB metallic core. However, for biphase microwires we should expect in principle that the main absorption should be ascribed to the external FeNi phase. This is the case of t_{NiFe} = 4 μm, where the main absorption at 0.77 kOe corresponds to H_r =

0.87 kOe for FMR3 in NA measurements. Small additional absorptions at frequencies below the main peak can be hardly identified in Figures 4.13(b) and 4.13(c), which origin is not clear to ascribe.

b. *Temperature dependence on the Microwave properties*

The derivative of microwave absorption versus external magnetic field resonance spectra of single phase microwire measured at selected temperatures is shown in *Fig. 4.14.a*. A single absorption peak is observed which resonance field, H_r, and the total line width, ΔH, are plotted in *Fig. 4.14.b* as a function of temperature. Both parameters increase monotonically with temperature, although ΔH shows a small maximum at low temperature.

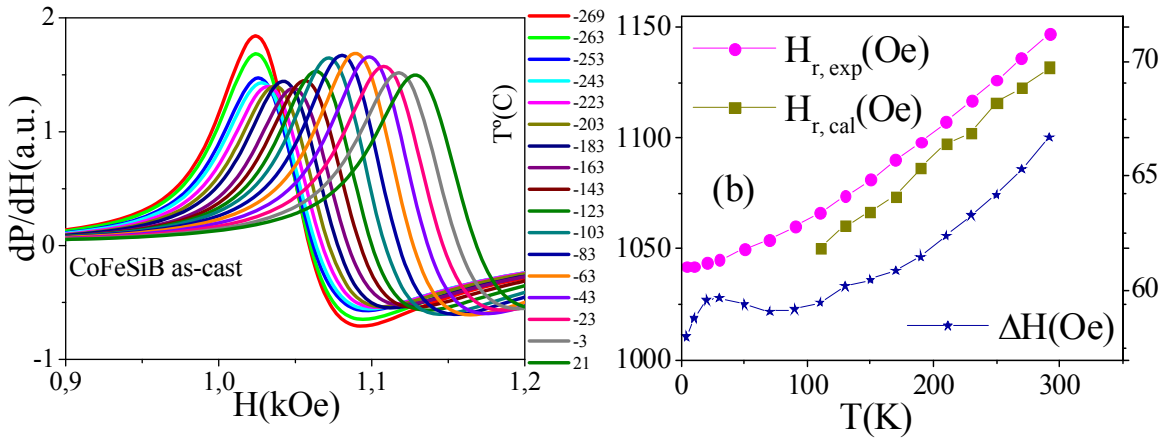

Figure 4.14 *Derivative resonance spectra of CoFeSiB single phase microwire at selected measuring temperatures (a), and temperature dependence of resonance field, H_r, (see text) and the total line width, ΔH (b).*

Considering eq. (4.1) and that $4\pi Ms >> H_r >> H_K$ in the first approximation, we derive the following expression for the temperature dependence of the resonance field, H_r:

$$H_r(T) \approx \frac{f_r^2}{\pi\gamma^2 M_S(T)} - H_K(T) \qquad (4.5)$$

where the two contributions to H_r on the right hand side of eq. (4.6) increase with increasing temperature (note the negative-circular anisotropy field value). *Fig. 4.14.b* shows the temperature dependence of $H_{r,exp}$ as deduced from data in *Fig. 4.14.a.* That is compared with $H_{r,cal}$ obtained using eq. (4.6) where we have introduced the values of $4\pi M_s(T)$ and anisotropy field, $H_K(T)$. The difference in both series of data is justified

when we realize that we are comparing experimental results obtained at very low frequency (hysteresis loops) with those from FMR absorption at the GHz frequency range.

The resonance spectra of biphase microwires with different thickness of external shell at selected temperatures are shown in *Fig. 4.15*. In the case of 2 μm thick FeNi microtube we observe a main absorption peak FMR1 whose resonance field, H_r, changes very noticeably at the low-temperature range and more moderately at higher temperatures. Also, a very little pronounced low-field peak can be observed. For the 4 μm thick FeNi microtube, the variation of the corresponding H_r is much more reduced, while the low-field absorption is detected clearly at low-temperatures. Inset in (b) depicts an enlarged view of the low-field peak.

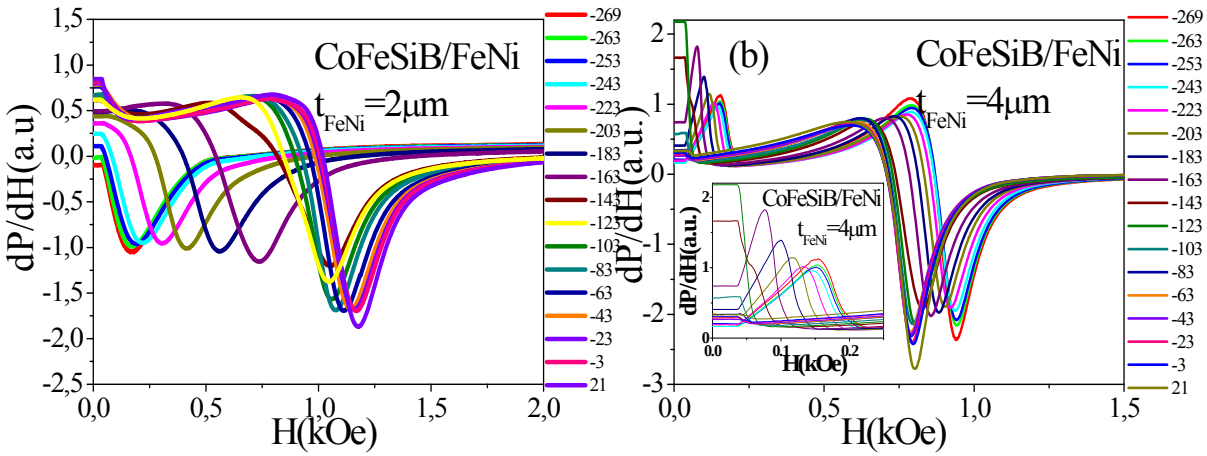

Figure 4.15 *Derivative resonance spectra of CoFeSiB/FeNi biphase microwires with 2μm (a) and 4 μm (b) thickness of the external shell at selected measuring temperatures. Inset in (b) depicts an enlarged view of the low-field peak.*

Fig. 4.16 collects the evolution of the main resonance field, H_r, as a function of temperature. It firstly includes the evolution for the single phase CoFeSiB microwire, for which a moderate monotonic increase of H_r with temperature is observed.

In the case of 2 μm thick NiFe microwire, at temperatures above -143ºC, we observe a similar behavior as that of CoFeSiB single phase microwire. This similarity, maybe accidental, could lead us to ascribe that absorption to the CoFeSiB core although we should consider as well that it corresponds to the external FeNi microtube. Note that a similar question arises in the interpretation of data obtained with the network analyzer at room temperature. Below -143ºC a pronounced reduction of H_r is observed. It could

be eventually interpreted if we assume a change of sign of anisotropy field in eq. (4.6). That is, assuming that the low-temperature axial anisotropy field ($H_K > 0$) evolves to circular anisotropy field ($H_K < 0$) at high temperatures.

An overall opposite evolution of H_r with temperature is observed in the case of the 4 μm thick FeNi microtube, including a change of trend at around -143ºC. Again, it can be ascribed to the change of sign of the anisotropy field. Now, it should be circular at low temperature ($H_K < 0$), and become axial ($H_K > 0$) at temperatures higher than around -143ºC.

The small-field absorption is observed at higher temperatures in the 2 μm thick FeNi biphase microwire, while it appears only at low temperatures in the 4 μm biphase microwire, where the circular anisotropy is expected. The origin of this phenomenon could be connected with the absorption in non-saturated samples. Note that its correlation with ferromagnetic antiresonance, FMAR, is in principle discarded since the antiresonance could be observed only above some critical frequency ($\omega/\gamma > 4\pi M_s$) which for FeNi lies in the order of 30 GHz.

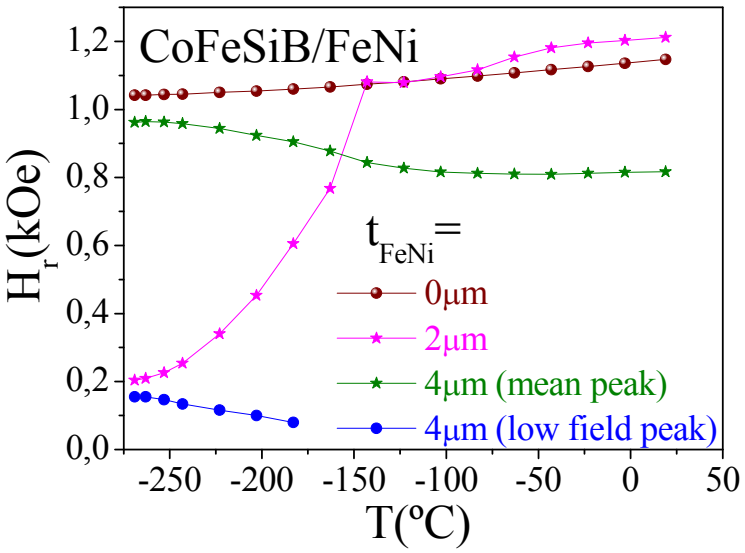

Figure 4.16 *Temperature dependence of resonant field, H_r, for the different microwires.*

The origin for the anomalous behavior observed in biphase microwires can be ascribed to the presence of strong induced anisotropy in FeNi layers at low temperatures, changing sign at about -143ºC. The substantial difference in the behavior

of the two biphase samples can be a consequence of the different magnetostriction constants, in both sign and magnitude, of the two FeNi layer (2 and 4 µm thick)).

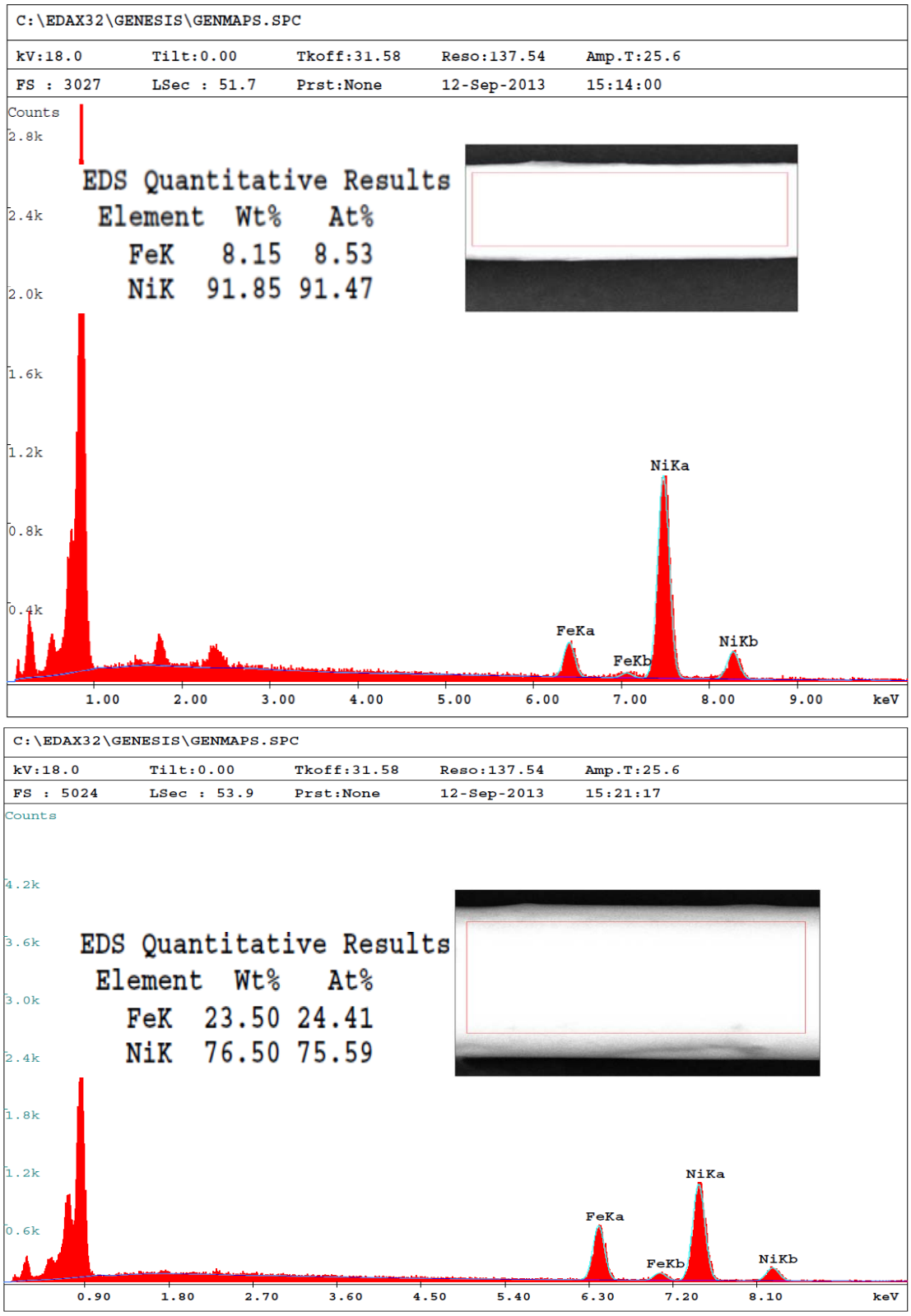

Figure 4.17 EDX microanalysis of external shell composition (FeNi). (Up) $Fe_{8.2}$ $Ni_{91.8}$ (with 2µm of thick), and (down) $Fe_{24.4}Ni_{75.6}$ (with 4 µm of thick).

In this concern, a final test of their compositions has been performed by SEM-EDX (FEI NOVA NANO 230 High Resolution Scanning Electron Microscope) as presented in *Fig. 4.17*. That analysis confirmed a different composition for the 2 and 4 μm thick external tubes namely, $Fe_{8.2}Ni_{91.8}$ and $Fe_{24.4}Ni_{75.6}$, respectively. For bulk FeNi alloys [35], the room temperature values of saturation magnetostriction are -16×10^{-6} and 8×10^{-6} for $Fe_{8.2}Ni_{91.8}$ and $Fe_{24.4}Ni_{75.6}$, respectively which supports our assumption.

Coming back to the ascription of FMR absorptions to given magnetic phases, FMR1 definitely corresponds to single phase CoFeSiB wire. In the case of 2 μm thick FeNi (positive magnetostriction) wire, FMR1 is hard to be ascribed clearly. Doubts arise trying to ascribe it to CoFeSiB core owing to the similar data for both network analyzer and cavity measurements (at room temperature) although we would expect that it comes from the FeNi shell. In the case of 4 μm thick FeNi (negative magnetostriction) shell microtube, the main peak in cavity measurement is associated to FMR3 in NA measurements from the FeNi shell because of the similarity of H_r fields (0.77 and 0.87 kOe) at 9.5 GHz.

We should recall that fittings to saturation magnetization in NA data are around 9 kG for FMR1 and 12 kG for FMR3 (see data in Table I). They could eventually be ascribed to saturation magnetization of $Fe_{8.2}Ni_{91.8}$ and $Fe_{24.4}Ni_{75.6}$, reported to be 8 kG and 13 kG, respectively in bulk material [34].

Finally, we should comment that a straightforward comparison of NA and classical FMR measurements on the biphase wires would require more rigorous theoretical analysis. In the cavity measurement, the microwave current passes through both the core and the FeNi tube. In contrast, in the Network Analyzer measurement, the microwave current passes mostly through the CoFeSiB core but also through the FeNi layer, because it is transmitted via the capacitance bridge between the core and the shell. However, it seems that in classical FMR the core is more effectively screened by the shell.

Once, the temperature dependence of microwave behavior has been established, as well the angular dependence has been taken account in this memory.

4.2.5. Angular dependence of microwave absorption in FeSiB and CoFeSiB microwires

Previously, the angular dependence of FMR, in amorphous ribbons has been widely investigated [36, 38], which allows the determination of different contributions to the total anisotropy field, H_k. Such angular dependence of microwave behavior has been also studied in multilayer thin films, and ferrites [36].

In this present work, we studied first the FMR behavior of CoFeSiB and FeSiB amorphous glass-coated microwires when subjected at high frequency of 9.5GHz, and measured at 0º as shown in the *Fig. 4.17*.

Moreover, the angular dependence of FMR behavior has been investigated in the frequency of 9.5GHz in the whole angular range between 0º (parallel to the wires) and 180º (perpendicular to the wires). Microwave absorption measurements on CoFe-based and Fe-based magnetic microwires were carried out at X-band spectrometer at room temperature. Additionally a comparison is made between the angular dependence of CoFe-based and Fe-based, exhibiting a good correlation.

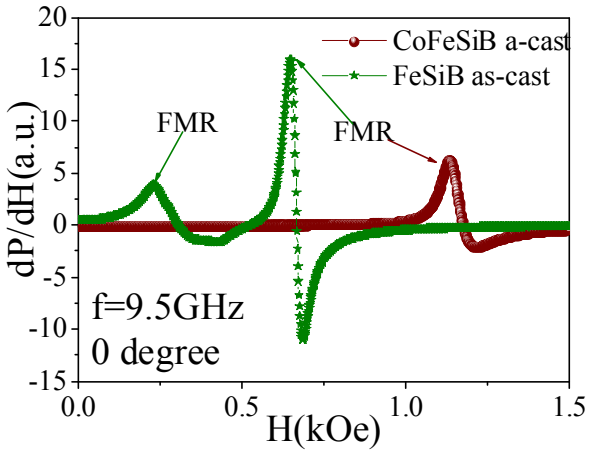

Figure 4.18 *the derivative resonance spectrum of two different single phase microwires FeSiB and CoFeSiB measured at room temperature and 9.5GHz.*

Fig. 4.18 presents the derivative resonance spectrum of the FeSiB and CoFeSiB microwires measured at 9.5GHz for field applied parallel to microwire. The spectrum displays two peaks in the case of FeSiB: a small one presented at low field, and a large one presented at high field. The small resonance peak originates in the FMR response of the inner core with axial anisotropy, while the large one is given by the response of the

outer shell with radial anisotropy [38]. In the case of CoFeSiB the spectrum displays just one peak, which correspond to the outer shell with circular anisotropy. Amorphous CoFeSiB microwires exhibit negative nearly zero magnetostriction leading to a transverse anisotropy.

Afterward, we investigated the angular dependence for the FMR behavior of CoFe-based and Fe-based glass-coated microwires. Fig.4.19 shows the angular dependence of FMR, which measured in the range from 0º to 180º for two selected microwires: FeSiB ($\lambda>0$) (Fig. 4.19(a)) and CoFeSiB ($\lambda\approx0$) (Fig. 4.19(b)). Fig.4.19 (a) presents variations of FMR spectra as function of angles from 0 to 180º. For 0º, the AC microwave field is parallel to the wire plan and dc field is parallel to the wire axis. While for 90º, the ac remains parallel to the plan, while the dc filed becomes normal to the wire plan. Measurements showed an increase in the resonant field as function of angles, which can be explained in the terms of a contribution of shape anisotropy field, SAF [36]. On the other hand, FMR spectra showed an increase in the width, ΔH_{FMR}, for angle variations of 0º to 90º, where ΔH_{FMR} is the separation between their maxima and minima. Moreover, the intensity of the signal decreases when increasing the angles up to 90º. For angles $90º<\theta<180º$, a symmetric decrease is observed for these angles as depicted in fig. 4.20.

Similarly, the angular behavior has been investigated in the case of Fe-based wire as presented in fig. 4.19(b). As can be observed, that resonant field, H_r, and the width, ΔH_{FMR}, increase with increasing the angles up to 90º, in both FMR spectra. As mentioned above, the spectrum of Fe-based microwires presented two FMR spectra: a small one presented at low field due to inner core, and a large one presented at high field corresponds to outer shell.

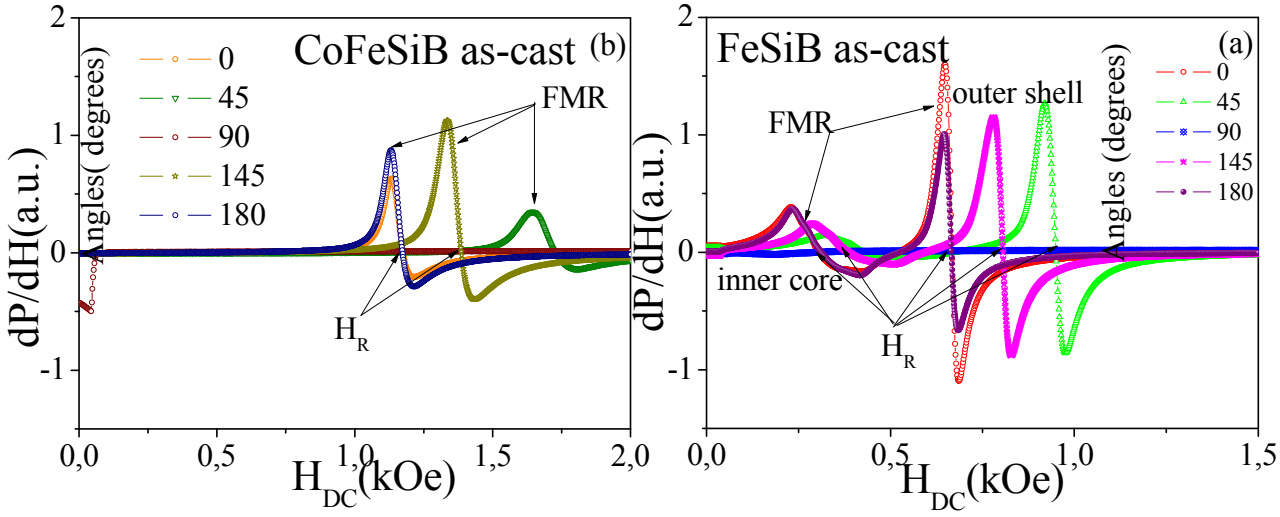

Figure 4.19 *Angle dependence of derivative resonance spectrum of two different single phase microwires CoFeSiB (a) and FeSiB (b) measured at 300K, and 9.5GHz.*

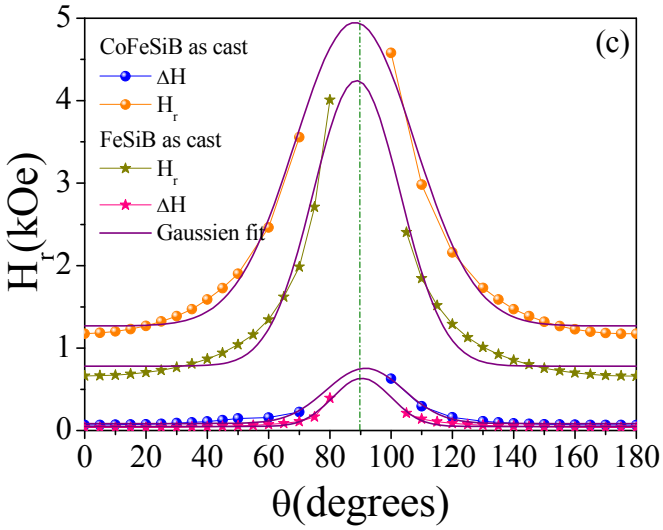

Figure 4.20 *Anglular dependence of resonant field, H_r, and absorption width, ΔH_{FMR}, in both selected samples CoFeSiB and FeSiB*

The *Fig. 4.20* shows the angular dependence of resonant field, H_r, and absorption width in both samples CoFeSiB and FeSiB. As can be observed, H_r shifted to larger values with maximum at 90º, which can be interpreted to originate in the shape anisotropy field [35, 39]. It corresponds to the energy needed to orientate the magnetic moments in the hardest direction, out of the plan. For 0º, SAF is a minimum because the magnetization remains within the plan, corresponding therefore to the smallest H_r values. This behavior was observed in both selected composition.

4.3. Conclusion

In conclusion, we demonstrated in this chapter the microwave behavior: FMR Spectra for selected single and biphase glass-coated microwires.

- In the first part, we investigated the influence of insulting glass Pyrex thicknesses in single and biphase wires, we found that: (i) for single-phase microwires the role of increasing the Pyrex thickness is reflected in the modification of the circular magnetoelastic anisotropy of the soft core. Increasing the Pyrex thickness results in a modest increase of that anisotropy; (ii) for both biphase investigated systems (CoFe/CoNi and CoFe/FeNi), a similar effect of the Pyrex thickness is observed, and (ii) biphase microwires show in addition the presence of an unexpected third absorption peak that is clearly of nonmagnetic origin.
- The aim of the second part is to understand the effect of annealing at higher temperatures, which deteriorates the magnetization process in two magnetic stages. FMR data indicate that for single phase microwires annealed up to 500 (below crystallization temperature), the absorption peaks are found in the range from 3 to 9 GHz for increasing applied fields from which we derive saturation magnetization value. After crystallization, the absorption peaks show much reduced dependence on applied field, and the FMR behavior cannot be fitted properly to the characteristics of the biphase material. In biphase microwires, the presence of the external shell gives rise to a second absorption peak ascribed to a capacitive effect. It is understood that CoNi shell is not sufficiently saturated magnetically so that it does not show properly ferromagnetic absorption.
- According to the first and second part, it should be emphasized the need of a deeper further study on the microwave behavior for hard external shell biphase wires. In order to gain a deeper knowledge about FMR behavior we investigated this kind of biphase wires (soft /hard) at high frequency by using a classical techniqueas presented in the third part.
- Also, a deeper study was performed on the temperature dependence and angular dependence. The following conclusions are outlined from the present study: (i) for single phase CoFeSiB microwire, a single absorption phenomenon is observed. At room temperature, the DC field dependence of resonance

frequency, f_r, fits to a Kittel law for in-plane tangentially magnetized thin film. The temperature dependence of the microwave behavior shows a monotonic increase of the resonant field, H_r, with temperature. This is interpreted considering the reduction of saturation magnetization and circular anisotropy field, H_K, as deduced from the temperature dependence of hysteresis loops. (ii) for biphase, CoFeSiB/FeNi, microwires, the resonance field, H_r, is equated to depend on the temperature dependent anisotropy field which evolves in a opposite manner for 2 and 4 μm thick FeNi shell microwires. For 2 μm thick sample, we assume an axial anisotropy at low temperatures ($H_K > 0$), which decreases with increasing temperature and changes sign at around 130 K to become circular ($H_K < 0$) at higher temperatures. For 4 μm thick sample, we have to consider a circular anisotropy at low temperature that becomes axial above 130K. Such opposite sign of the magnetoelastic anisotropy induced at low temperatures is interpreted considering the opposite sign of magnetostriction of corresponding FeNi layers. The strong stresses induced below room temperature are ascribed to the different thermal expansion coefficients of metallic layers and intermediate Pyrex glass layer.

4.4. References:

[1] Héctor García-Miquel; Caracterización de las propiedades magnéticas de vidrios metálicos en forma de microhilos de composición $(Fe_xCo_{100-x})_{72.5}Si_{12.5}B_{15}$, tesis doctoral española (1999).

[2] Mohammed Reda Brittel ; Létude expérimentale de la magnétoimpédance géante des fils ferromagnétiques doux en micro-ondas, tesis doctoral canadiense (2000).

[3] H. Garcia Miquel, J. M. Garcı´a, J. M. Garcı´a-Beneytez, and M. Vazquez, J. Magn. Magn. Mater. 231, 38 (2001).

[4] M. Ipatov, V. Zhukova, A. Zhukov, J. Gonzalez, and A. Zvezdin, J. Phys.: Conf. Ser. 200, 082009 (2010).

[5] J. Torrejon, G. A. Badini-Confalonieri, and M. Va´zquez, J. Phys. D: Appl. Phys. 43, 145001 (2010).

[6] R. El Kammouni, G. Infante, J. Torrejon, M.R. Britel, J. Brigui and M. Vazquez, Phys. Stat. Sol. A 208 ,(2011) 520.

[7] R. El Kammouni and M. Vazquez, IEEE Trans. Magn. 49, (2013) 34.

[8] D.S. Rodbell, J. Appl. Phys. 30, (1959) 1845.

[9] J. Torrejón, G. A. Badini-Confalonieri, M. Vázquez, J. Appl. Phys. 106 (2009) 023913.

[10] R. Valenzuela, A. Fessant, J. Gieraltwski, and C. Tannous, Sens. Actuators A 142, 533 (2008).

[11]H . Chiriac, T. A. Ovari, S. Corodeanu, and G. Ababei, Phys. Rev. B 76, 214433 2007).

[12] P. Ciureanu, M. Britel, D. Menard, C. Akeyl, A. Yelin, M. Rouabhi, and R. W. Cochrane, J. Magn. Magn. Mater. 196/197, 391 (1999).

[13] S. Vonsovskii."Ferromagnetic Resonance". Pergamon Press, NewYork. 35 (1966).

[14] H. Garcıa-Miquel, S. M. Bhagat, S. E. Lofland, G. V. Kurlyandskaya, and A. V. Svalov, J. Appl. Phys. 94, 1868 (2003).

[15] V. Raposo, M. Vázquez, A. G. Flores, M. Zazo, J. I. Íñiguez, Sens. Actuators A 106 (2003) 329-332.

[16] Z. M. Wu, Z. J. Zhao, L.P. Liu, H. Lin, J. K. Cheng, J. X. Yang, X. L. Yang, IEEE Trans. Magn. 43 (2007) 3146-3148-

[17] M. Vazquez, in: Handbook of Magnetism and Advanced Magnetic Materials, Vol. 4, edited by H. Kronmuller and S. Parkin (John Wiley and Sons, New York, 2007), p. 2193.

[18] A. Zhukov and V. Zhukova, *Magnetic Properties and Applications of Ferromagnetic Microwires With Amorphous and Nanocrystalline Structure*. Hauppauge, NY: Nova Science Publishers, Inc., 2009, vol. 162, p. 11788.

[19] H. Chiriac and T. A. Ovari, "Amorphous glass-covered magnetic wire: preparation, properties, application," *Prog. Mater. Sci.*, vol. 40, p. 333, 1996.

[20] L. Kraus, Phys. Letters 99A, (1983) 189.

[21] H. Garcia-Miquel, S.M. Bhagat, S.E. Lofland, G.V. Kurlyandskaya, A.V. Svalov, J. Appl. Phys. 94, (2003) 1868.

[22] S.E. Lofland, H. Garcia-Miquel, M. Vazquez and S.M. Bhagat, J. Appl. Phys. 92, (2002) 2058.

[23] D. Menard, M. Britel, P. Ciureanu, A. Yelon, V.P. Paramonov, A.S. Antonov, P. Rudkowski and J.O. Stroem-Olsen, J. Appl. Phys. 81, (1997) 4032.

[24] M. Ledieu, F. Schoenstein, S. Deprot, A.-L. Adenot, F. Bertin, and O. Acher, IEEE Trans. Magn. 39, (2003) 3046.

[25] A.N. Antonenko, S.A. Baranov, V.S. Larin and A.V. Torcunov, J. Mater. Sci. Eng. A 247, (1997) 248.

[26] D.P. Makhnovskiy and L.V. Panina, J. Appl. Phys. 93, (2003) 4120.

[27] L. Kraus, G. Infante, Z. Frait and M. Vazquez, Phys. Rev. B 83, (2011) 174438.

[28] H. García-Miquel and G.V. Kurlyandskaya, Chinese Phys. B, 17, (2008) 1430

[29] H. Montiel, G. Alvarez, I. Betancourt, R. Zamorano, and R. Valenzuela, Appl. Phys. Lett. 86, (2005) 072503.

[30]J.M. Barandiaran, A. Hernando, V. Madurga, O.V. Nielsen, and M. Vazquez, Phys. Rev. B 35, 5066 (1987).

[31] C. Kittel, Introduction to Solid State Physics (New York: Wiley, 1996), Chap. 16, p. 503.

[32] H. Chiriac, C.N. Coleniuc and T.A. Ovari, IEEE Trans Magn 35, (1999) 3841.

[33]Z. M. Wu, Z. J. Zhao, L. P. Liu, H. Lin, J. K. Cheng, J. X. Yang, and X. L. Yang 3146 IEEE Trans Magn. 43, (2007)3146.

[34] R.M. Bozorth, "Ferromagnetismus" (Van Nostrand, Prionceton, 1951).

[35] H. Montiel, G. Alvarez, R .Zamorano, R. Valenzuela, J. Non. Cryst. Solids, 353 (2007) 908.

[36]G. Alvarez, H. Montiel, D. de los, A. Garcia-Arribas, R .Zamorano, J. M. Barandiaran, and R. Valenzuela, J. Non. Cryst. Solids, 354 (2008) 5195-5197.

[37] V. A. Tulin, M. V. Astalov, A. C. Rodin, J. Magn, Magn, Mater. 258- 259 (2003) 201-203.

[38]Horia Chiriac, Corneliu Nicolai Colesniuc, and Tibor-Adrian, IEEE Trans. on Magn., Vol **15,** Nº **5,** Sept. 1999.

[39] R. Valenzuela, G. Alvarez, H.Montiel, M. P. Gutierrez, M. E. Mata-Zamora, F. Barron, A. Y. Sanchez, I. Betancourt, R. Zamorano, J. of Magn. Magn. Mater. 320 (2008) 1961-1965.

5.1. Conclusions

Along the description of the studies carried out in this work, we summarize the main conclusions reached:

- ✓ **On the fabrication samples: single and biphase microwires**

We have employed three fabrication methods to prepare multilayer magnetic microwires namely, quenching & drawing, sputtering and electroplating, all of them available at the ICMM/CSIC.

The precursor single phase glass-coated amorphous microwires were prepared by quenching and drawing technique. Two alloy compositions were selected, CoFe-based and Fe-based, because of their specific vanishing and high-positive magnetostriction values, respectively. The samples were prepared with tailored Pyrex thickness so that, we consider the following single phase soft magnetic microwires:

a) CoFe-based alloy with vanishing magneotstriction ($\lambda_s \approx -1x10^{-7}$) and different thickness of the Pyrex glass coating ($t_{Py} \approx 5$ to 10 μm)
b) Fe-base alloy with large magnetostriction ($\lambda_s \approx + 3x10^{-6}$) and different thickness of the Pyrex glass coating ($t_{Py} \approx 5$ to 10 μm)

In order to prepare biphase magnetic systems, a 30nm of thick Au nanolayer was sputtered onto the Pyrex of both CoFe and Fe-based glass-coated microwires. Then, an external magnetic microtube was electroplated onto the Au nanolayer with different thickness. Two alloy compositions were considered for the external shell: (i) CoNi (hard shell) and (ii) FeNi (soft shell). The external shell, with polycrystalline structure in both cases, was also tailored to different thickness.

That has allowed us to count on the following biphase magnetic systems:

c) Soft/soft, CoFe/FeNi and Fe/FeNi, biphase microwires with different thickness of the external phase ($t_{shell} \approx$ up to 6 μm)
d) Soft/hard, CoFe/CoNi and Fe/CoNi, biphase microwires with different thickness of the external phase ($t_{shell} \approx$ up to 6 μm)

- ✓ **On the low-frequency magnetic behavior**

Regarding the magnetic properties measured at low-frequency magnetic field, on single and biphase systems mentioned above, we have considered the following parameters:

a) Geometrical: Thickness of Pyrex glass-coating in single phase wires
b) Geometrical: Thickness of external shell (phase) in biphase wires.
c) Influence of thermal annealing
d) Measuring temperature

a) On the influence of insulting glass Pyrex and magnetization process:

The role of increasing the Pyrex thickness is reflected in modification of the mechanical stresses induced during the quenching & drawing fabrication process, and consequently in the intrinsic magnetoelastic anisotropy of the amorphous wires.

In the case of CoFe-based single phase wires, the magnetization process under axial magnetic field takes place by nearly reversible process of magnetization rotation from the transverse direction to the axial one.

We observe an increase of the circular magnetoelastic anisotropy, from which we conclude:

- Due to the small and negative value of the magnetostriction, the increase of anisotropy field is moderate.
- The stress induced by the increased Pyrex thickness is tensile in nature, since the circular magnetoelastic anisotropy increases, and considering the negative (small) magnetostriction.

In the case of Fe-based single phase wires, the magnetization process takes place mostly by a single large Barkhausen jump that gives rise to a square bistable hysteresis loop. That is interpreted to be due to the depinning and propagation of a single domain wall originated by the presence of strong tensile mechanical stresses from the fabrication.

The Pyrex thickness gives rise to enhanced axial magnetoelastic anisotropy and coercive field.

b) Magnetization process and Influence of thickness of magnetic external shell:

The hysteresis loops of biphase microwires contain two magnetization processes corresponding to each phase.

The presence of the external magnetic phase induces by itself significant mechanical stresses in the amorphous core.

In soft/soft Fe/FeNi microwires, we observe two large Barkhausen jumps corresponding to Permalloy and amorphous core respectively.

In soft/soft CoFe/FeNi system we observe one large Barkhausen jump corresponding to the Permalloy followed by a nearly non-hysteretic magnetization rotation process ascribed to the non-magnetostrictive core.

In addition to the induced magnetoelastic anisotropy, in soft/hard Fe/CoNi system, the presence of the external shell modifies significantly the coercive field of the bistable core which denotes the relevance of the magnetostatic field of the external shell.

In all the biphase Fe/CoNi and CoFe/CoNi soft/hard systems, the increase of thickness of the external shell enhances its magnetic fractional volume and the magnetization of the core reduces its contribution.

A final experience was performed for the CoFe/FeNi system where the alloy composition of the external shell FeNi was tailored by controlling the current density during its electroplating. Measurements were performed to reach Fe content between 12 and 26%. Later magnetic characterization has allowed to confirm a minimum coercivity for the alloy containing 19% Fe for which vanishing magnetostriction is expected for optimal Permalloy.

c) Effect of Annealing Treatments:

Thermal treatments are known to modify the metastable structure of amorphous samples. They result in modifications of the magnetic properties measured at room temperature after the treatments.

The objective was not to perform a detailed study on the influence of thermal treatments on the structure and the product of crystallization which has been extensively performed particularly in amorphous ribbons and less thoroughly in amorphous wires. Our aim was addressed to detect final influence in biphase systems, particularly at the microwave studies.

However, as for the low-frequency properties we can distinguish two main regimes for the annealing temperature:

- At moderate annealing temperature, roughly up to around 500ºC, the amorphous structure is kept, and as expected, only moderate softening is observed as a consequence of the partial release of internal stress quenched during the fabrication. In the case of Fe-base core, the bistable behavior is retained with small variation of the switching field. The variation of the Pyrex thickness also gives rise to reduced changes in that bistable behavior.

- Annealing above 500ºC results in continuous deterioration of the soft magnetic behavior as a result of the crystallization of the amorphous core. A huge enhancement of coercivity is observed after annealing at around 600-650ºC which is ascribed mainly to crystallized phases as Fe-Si and Fe-borides.

- Annealing at that range of temperatures do not give rise to significant changes in the magnetic properties of the external CoNi phase at room temperature.

d) Influence of Measuring Temperature:

We distinguish two main range of measuring temperatures, above and below room temperature. There is no previous systematic study on the temperature dependence of single phase microwires as is presented here, where we include also data for biphase systems. We have focused and analyzed main parameters as magnetic moment or coercivity.

- Above room temperature, up to 925ºC, the study has allowed us to determine high temperature magnetic characteristics as Curie temperature and evolution of coercivity.

We firstly paid attention particularly to the temperature evolution of the magnetic moment under applied field. That has allowed one to determine the Curie temperature of the amorphous core as well as the temperature of various crystallization processes.

Regarding CoFe single and CoFe/FeNi and CoFe/CoNi biphase systems, we conclude a Curie temperature of 380 ºC for the amorphous in the three systems. The Curie point for the FeNi alloy we deduce 604ºC, while for CoNi external shell, the measuring temperature is not high enough to allow for its determination.

In the case of Fe single and Fe/FeNi and Fe/CoNi bipha se systems, the Curie point of the amorphous core is 430ºC (from the 3 samples). We also estimate the temperature crystallization of Fe(Si) crystal phase at 530 ºC while it Curie temperature is estimated at 703ºC. All these values agree with Curie and crystallization temperatures reported for same or very similar alloys.

- Concerning the coercivity of the systems, we conclude that in the case of soft/hard biphase wires we identify two large irreversible processes corresponding to each phase up to the measuring temperature of around 340ºC. The coercivity of Fe and CoFe amorphous phases does not increase dramatically and changes remain in the range 0.05 to 0.5 Oe. As for the hard CoNi phase it decreases from around 90 Oe at room temperature down to about 10 Oe at 630ºC.
- Above around 360ºC up to 925ºC a new maximum of coercivity of around 40 Oe is measured which is connected to the crystallization of the amorphous phase. Then, coercivity decreases continuously until the maximum measuring temperature which is ascribed to some restructuration of the CoNi phase.

- At low temperature measurements have been performed in the temperature range from -173ºC up to room temperature.

First, we analyze the behavior for CoFe/FeNi soft/soft microwires. The coercivity of the soft CoFe core remains in the whole range between 0.2 Oe

(11.3 Oe circular anisotropy field) at -173ºC down to 0.1 Oe (9.8 Oe circular anisotropy field) at room temperature. The overlapping of the magnetization processes of CoFe core and soft FeNi shell determines that coercivity of the biphase microwires is given by that of FeNi shell that increases with the thickness of FeNi shell only up to 1.2 Oe at -175ºC for 4 μm thickness.

We have also analyzed the Fe/CoNi soft/hard system where magnetic bistability is observed in the whole range of measuring temperatures. Coercivity for the single phase wire decreases from 2.4 Oe at -175ºC down to 1.7 Oe at 25ºC. The coercivity of biphase system is given by that of the CoNi external shell which takes values in the order of 40 Oe.

- ✓ **On the Microwave behavior and FMR spectra:**

The study of microwave behavior and FMR spectra of single and biphase magnetic microwires have been performed paying attention to same parameters as for low-frequency properties. Some relevant conclusions are:

1) *Influence of insulating Pyrex and magnetic external shell*

The evolution of the ferromagnetic resonance frequency applied field allows us to determine intrinsic parameters as magnetic anisotropy field and saturation magnetization. Kittel equation was used to fit the evolution of the square frequency with the applied field.

The influence of the thickness of the insulting Pyrex layer and magnetic character of outer magnetic shell was investigated. In the case of CoFe single phase wires a single absorption peak is observed that evolves with the DC applied field. Saturation magnetization is estimated to 0.71 T coherent with reports on amorphous ribbons. The increase of Pyrex coat thickness gives rise to small variation of circular anisotropy field between 8 and 10 Oe for increase of 4 μm the Pyrex thickness.

The FMR spectrum of CoFe/CoNi (with hard external shell) biphase microwires present two peaks: one at high frequency corresponding to that of the core. The analysis of data for different thickness of Pyrex indicate a similar small variation of the fitting

parameters as for CoFe single phase as well as saturation magnetization (which confirms that both peaks for single and biphase wires correspond to the same phase).

An additional absorption is now observed at lower frequency. That has been ascribed to a capacitance effect caused by the intrinsic and geometrical nature of these multilayer structures.

However, no absorption peak has been found that can be ascribed to the magnetically hard CoNi phase. This is interpreted to be a consequence of the fact that the maximum applied field was not high enough to reach near saturation of that phase.

Consequently, we performed new measurements in soft/soft CoFe/FeNi microwires with different Pyrex thickness. In this case, similar variations are observed as a function of the Pyrex thickness. However, we now observe three absorption phenomena, the first two are coincident with the CoFe phase and the capacitance effect while a new one ascribed to the external shell phase is detected, with fitted saturation magnetization of 1.15 T, reasonable for FeNi.

2) *Effect of annealing treatment:*

The effect of annealing treatment of single and biphase microwires has been particularized to Fe/CoNi system, and it was found that:

- After annealing below crystallization temperature (up to 500ºC): FMR data indicate that for single phase microwires the absorption peaks are found in the range from 3 to 9 GHz for increasing applied fields from which we derive saturation magnetization value. In biphase microwires, the presence of the external shell gives rise to a second absorption peak ascribed to a capacitive effect. Again, it is understood that CoNi shell is not sufficiently saturated magnetically so that it does not show properly ferromagnetic absorption.
- Above crystallization temperature (up to 700ºC): The absorption peaks show much reduced dependence on applied field, and the FMR behavior cannot be fitted properly to the characteristics of the biphase material.

3) *Temperature dependence of microwave behavior*

Measurements were performed in a microwave cavity mostly at 9.5 GHz frequency applying higher magnetic fields.

- For single phase CoFeSiB microwire, a single absorption phenomenon is observed. At room temperature, the DC field dependence of resonance frequency fits to a Kittel-law for in-plane tangentially magnetized thin film. The temperature dependence of the microwave behavior shows a monotonic increase of the resonant field, with temperature. This is interpreted considering the reduction of saturation magnetization and circular anisotropy field, as deduced from the temperature dependence of hysteresis loops.
- For biphase, CoFeSiB/FeNi, microwires, the resonance field is adjustted to the temperature dependent anisotropy field which evolves in an opposite manner for 2 and 4 μm thick FeNi shell microwires. For a 2 μm thick sample, we assume an axial anisotropy at low temperatures which decreases with increasing temperature and changes sign at around -140ºC K to become circular at higher temperatures. For a 4 μm thick sample, we have to consider a circular anisotropy at a low temperature that becomes axial above -140ºC K. Such an opposite sign of the magnetoelastic anisotropy induced at low temperatures is interpreted considering the opposite sign of magnetostriction of corresponding FeNi layers. The strong stresses induced below room temperature are ascribed to the different thermal expansion coefficients of metallic layers and intermediate Pyrex glass layer.

5.2. Future work:

For further improvement of biphase microwires and understanding the origin of magnetic and microwave of external shell (hard (CoNi) and soft (FeNi)), we propose the following studies and work:

- A deeper study on the Hopkinson effect of single and biphase microwires as function of high temperature, in order to gain a deeper understanding about the temperature dependence under a low applied field with a comparison with a thin films and ribbons.
- A deeper study of preparation and the influence of magnetostriction of FeNi with different current density, in order to get an exact mutual percentage of Permalloy ($Fe_{20}Ni_{80}$). In this regards, a deeper knowledge of magnetic and microwave behavior of soft/soft systems will be taken account.
- An improvement of preparation of bilayer microwires with partially cover of magnetic external shell, in order to gain a deeper knowledge about the influence of electroplating effect on the core, and a comparison between fully and partially cover, in overall magnetic and microwave behavior.

5.3. Publications

Several contributions were made during these four years of work. The publications directly from this study are:

1. R. El Kammouni, G. Infante, J. Torrejón, M. Britel, J. Brigui, M. Vázquez. "*Microwave behaviour of CoFe-based single and two-phase microwires*" Phys. Status. Solidi A, 208, 3, (2011) 520-525.

2. R. El Kammouni and M. Vázquez. *"Effects of annealing treatment on low and high frequency magnetic properties of soft/hard biphase FeSiB/CoNi microwires*". IEEE Transactions on Mgnetics, 49, 1, (2013) 34-37.

3. R. El Kammouni, M. Vázquez, L. Lezama, G. Kurlyandskaya, and L. Kraus. "*Temperature dependence of microwave absorption phenomena in single and biphase soft magnetic microwires"*. J. Magn. Magn. Mater. 368, 126 (2014).

4. R. El Kammouni, I. Iglecias, K. Chichay, P.Svec, V. Rodionova, and M. Vazquez. *"High temperature magnetic behavior of soft/soft and soft/hard Fe and Co-based biphase microwires. J. Appl. Phys. 116, 093902 (2014).*

5. Iglesias, R. El Kammouni, K. Chichay, N. Perov, M. Vazquez, and V. Rodionova, "*Study of biphase microwires magnetic properties in temperature range from 295 to 1200K,"* accepted in Acta Physica Polonica A.

6. Iglesias I., El Kammouni R., Chichay K., Vazquez M. and Rodionova V. *"High temperature properties of CoFe/CoNi and Fe/CoNi biphase microwires"*, accepted in Solid State Phenomena.

Several collaborations and studies during these four years which are not related directly to this work were performed:

1. A.A. Chlenova, G.V. Kurlyandskaya, S.O. Volchkov, V.N. Lepalovskij, and R. El Kammouni." *Nanostructured magnetoimpedance multilayer with different thickness of FeNi components" Solid State Phenomena Vol. 215 (2014) pp 342-347.*
2. P. Klein, R. Varga, R. El Kammouni, and M. Vázquez. "*Magnetic properties of glass-coated FeWB microwires*", *Acta Physica Polonica, Vol. 126 (2014) DOI: 10.12693/A Phys. Pol. A.126.70*
3. P. Klein, R. Varga, I. Škorvánek, R. El Kammouni, and M. Vazquez. "*Magnetic properties of glass-coated amorphous and nanocrystalline FeMoBCu microwires*", *IEEE Tansactions on Magnetics, Vol. 50, No. 11, Nov. 2014, 2006303.*
4. M. Butta, M. Janosek, P. Ripka, L. Kraus, R. El Kammouni." *The influence of magnetostriction of NiFe electroplated film on the noise of fluxgate"*, *IEEE, Transactions on Magnetics Vol. 50, No. 11, Nov. 2014, 4006504.*

5. R. Hudak, R. Varga, J. Hudak, D. Prasticka, I. Poacek, P. Klein, R. El Kammouni, M. Vazquez. "*Influence on magnetic properties of glass-coated*

microwires by fixation for biomedical applications", submitted to IEEE, Transactions on Magnetics. ID: MAGCON 14-06-1390.

6. P. Klein, R. Varga, R. El kammouni, M. Vazquez. "*Temperature dependence of the switching field in amorphous bistable microwires*", submitted to IEEE, Transactions on Magnetics. ID: MAGCON 14-06-1403.

7. **V**. Kolesar, R. El Kammouni, M. Kubliha, V. Labas, and M. Vazquez. **"***Mechanical oscillations of multilayer microwires induced by thermal expansion during d.c. joule heating***", (TO BE SUBMITTED).**

Participation on international scientific conferences

- I. Iglesias, R. El Kammouni, K. Chichay, N. Perov, V.Rodionova, M. Vazquez. *"High temperature magnetic properties of single and biphase magnetic microwires",* INTERMAG Europe Conf. Dresden, Germany, 4th – 8th May 2014 (Oral).
- P. Klein, R. Varga, R. El Kammouni, M. Vazquez. *"Magnetic properties of glass-coated amorphous and nanocrystalline FeMoBCu microwires",* INTERMAG Europe Conf. Dresden, Germany, 4th – 8th May 2014 (Oral).
- R. El kammouni, G. Badini-Confalonieri and M. Vázquez. "*Effects of annealing treatment on microwave properties of amorphous FeSiB-base microwires"*. EMSA 2012, 9th European conference on magnetic sensors and actuators, Prague July 1-4, 2012 (Oral).
- M. Vazquez, R. El Kammouni, and S.K. Pal. *"Ferromagnetic Resonance Studies in Single and Bi-phase Magnetic Microwires"*. AES 2012, Advenced Electromagnetics Symposium. 16-19 April 2012, Paris-France (invited).
- G. Infante, V. Raposo, R. El Kammouni and M. Vazquez, "*On the origin of multiple microwave absorptions in bimagnetic microwires",* INTERMAG Conf. Taipei, April 2011 (Oral).
- G**.** Infante, L. Kraus, V. Raposo, R. El Kammouni, and M. Vazquez. "*Ferromagnetic resonances in single and two-phase magnetic microwires*", ((55th annuel conference on magnetism and magnetic materials (MMM): Atlanta, GA, USA, 14th-18th Nov. 201 (Oral).
- L. G. Vivas, R. Pérez, O. de Abril, M. Vázquez, R. El Kammouni y M. R. Brittel "*Magnetic nanodot andnanowire arrays: Magnetization and microwave properties*". ANM 2010- 3rd International Conference on Advanced Nano Materials. Agadir (Morocco), 12th-15th Sept.2010 (Oral).
- R. El Kammouni, G. Infante, J. Torrejón, M. Britel, J. Brigui, M. Vázquez. *Microwave behavior of CoFe based single and multilayer magnetic microwire*", 2010 (IWMW) International Workshop on Magnetic Wires, 8th -9th July 2010 Bodrum- Turkey (Oral).

- R. El Kammouni, Luis Lezama, Galina Kurlyandskaya, Manuel Vázquez, "*Temperature dependence of ferromagnetic resonance in single and biphase magnetic microwires*". JEMS, 25-30 August 2013 in Rhodes, Grees (Poster).
- Iglesias, R. El Kammouni, K. Chichay, N. Perov, M. Vazquez, and V. Rodionova, "*Study of biphase microwires magnetic properties in temperature range from 295 to 1200K,"* The European conference physics of magnetism 2014 (PM'14) 23-27 June Poznan, Poland (Poster).
- Iglesias I., El Kammouni R., Chichay K., Vazquez M. and Rodionova V. *"High temperature properties of CoFe/CoNi and Fe/CoNi biphase microwires",* MISM 29 June-3 July 2014 Moscow, Russia (Poster).
- R. Hudak, R. Varga, J. Hudak, D. Prasticka, I. Poacek, P. Klein, R. El kammouni, M. Vazquez. "Influence on magnetic properties of glass-coated microwires by fixation for biomedical applications", EMSA, 6-9 July 2014 in Vienna, Austria (Poster).
- P. Klein, R. Varga, R. El Kammouni, M. Vazquez. "Temperature dependence of the switching field in amorphous bistable microwires", EMSA, 6-9 July 2014 in Vienna, Austria (Poster).